



**Screening, Purification and Characterisation of
anti-*Pseudomonas aeruginosa* Compounds Produced by
Endophytic Fungi from *Kigelia africana***

by

Mamokoena Quali

(211512973)

Submitted in fulfilment of the academic requirements for the degree of Master of Science (MSc) in the Discipline of Microbiology, School of Life Sciences, College of Agriculture, Engineering and Science at University of KwaZulu-Natal (Westville Campus)

As the candidate's supervisors, we have approved this dissertation for submission.

Signed: Name: R. Govinden

Date:

Signed: Name: R. Moodley

Date:

ABSTRACT

The emergence of new diseases and drug resistant pathogens coupled with the side effects presented by conventional or synthetic drug use calls for the discovery of new antibiotics and chemotherapeutics. *Pseudomonas aeruginosa* is a multifaceted Gram-negative opportunistic pathogen which is responsible for ten percent of all hospital infections. This, therefore, directed the search for novel bioactive molecules with new targets from previously understudied sources.

Plants have bioactive compounds that have been used for traditional healthcare for thousands of years. In the interest of plant preservation, the focus has shifted to include the plant microbiome; interestingly, not only were the plants themselves producing the bioactive metabolites but also their associated microbiome. The focus of this study was to screen and determine the optimum time to produce anti-*Pseudomonas aeruginosa* metabolites, to purify the compounds of interest and characterise them. Forty-five endophytic fungi were grown in solid substrate fermentation on rice to produce extracts of varying ages (one week to four weeks).

Thin layer chromatography (TLC) coupled with bio-autography revealed that the anti-*P. aeruginosa* compound was produced after three weeks. Average zones of inhibition of 40.33, 20.33 and 22 mm were obtained using the Kirby-Bauer disc diffusion assay. All rows A, B, C and D show very strong activity as the MICs of the extracts were 156.5 µg/mL, 39.06 µg/mL, 78.73 µg/mL and 19.53 µg/mL for T1, T2, T3 and T4, respectively. Thin layer chromatography was conducted, and optimum separation was observed using hexane: ethyl acetate (60:40, v/v). Fractionation was carried out using a silica gel column with six different ratios of a hexane: ethyl acetate solvent system. The first round of purification resulted in twenty-seven fractions with five fractions having similar TLC profiles. These fractions were combined and subjected

to a second round of purification that gave three fractions. One fraction was observed to have good anti-*P. aeruginosa* activity and acceptable purity levels after nuclear magnetic resonance spectroscopy. Compound one, a dilactone (3a,10b-dimethyl-1,2,3,3a,5a,7,10b,10c-octahydro-5,8-dioxa-acephenanthrylene-4,9-dione, molecular formula C₁₆H₁₈O₄) was isolated as a white solid from the extract of the fungus *Neofusicoccum luteum*. This compound was previously isolated from the fungus *Oidiodendron griseum*. The relative configuration of the compound was confirmed by X-ray crystallography. Although the isolated compound is not novel, its ability to inhibit the growth of *P. aeruginosa* is new. This suggests that known compounds need to be screened across a wide range of pathogens and organisms to determine potential activity.

PREFACE

The experimental work described in this dissertation was carried out in the School of Life Sciences and School of Chemistry & Physics, University of KwaZulu-Natal (Westville Campus), Durban, South African from February 2016 to November 2018, under the supervision of Dr. R. Govinden and the co-supervision of Dr. R. Moodley, respectively. These studies represent original work by the author and have not otherwise been submitted in any form for any degree or diploma to any tertiary institution. Where use has been named of the work of others it is duly acknowledged in the text.

COLLEGE OF AGRICULTURE, ENGINEERING AND SCIENCE

DECLARATION 1- PLAGIARISM

I,.....Mamokoena Quali.....declare that

1. The research reported in this thesis, except where otherwise indicated, is my original research.
2. This thesis has not been submitted for any degree or any examination at any other university.
3. This thesis does not contain other persons' data, pictures, graphs or other information, unless specifically acknowledged as being sourced from other persons.
4. This thesis does not contain other persons' writing, unless specifically acknowledged as being sourced from other researchers.

LIST OF ABBREVIATIONS

AA- Amino acid

ADPRT- ADP ribosyltransferase

BCGs- Biosynthetic gene clusters

BLAST- Basic local alignment search tool

CF- Cystic fibrosis

CHCl₃- Chloroform

DEPT- Distortionless enhancement by polarization transfer

DNA- deoxyribonucleic acid

EPS- extracellular polymeric substances

ESBL- extended spectrum beta lactamase-producing

EtOAc- Ethyl acetate

HMBC- Heteronuclear Multiple Bond Correlation

HPLC- High performance liquid chromatography

ITS- Internal transcribed spacer

MDR- Multi-drug resistant

MeOH- Methanol

MIC- Minimum inhibitory concentration

MRSA- multidrug resistant *Staphylococcus aureus*

MTT- 3-(4,5-dimethylthiazol-2-yl)-2,5-diphenyl tetrazolium bromide

NA- Nutrient agar

NCBI- National Center for Biotechnology Information

NMR- Nuclear magnetic resonance

NRPs- Non-ribosomal peptide synthases

P. aeruginosa- *Pseudomonas aeruginosa*

PCR- Polymerase chain reaction

PDA- Potato dextrose agar

PKs- Polyketide synthases

PPP- Pentose phosphate pathway

Rf- Retention factor

SSF- Solid substrate fermentation

TCA- Tricarboxylic acid

TLC- Thin layer chromatography

UV- Ultraviolet

VRE- vancomycin resistant *Enterococcus* sp.

VREF- vancomycin resistant *Enterococcus faecium*

TABLE OF CONTENTS

ABSTRACT	II
PREFACE	IV
DECLARATION 1- PLAGIARISM	V
LIST OF ABBREVIATIONS	VI
LIST OF FIGURES	X
LIST OF TABLES	XIV
ACKNOWLEDGEMENTS	XV
CHAPTER 1: INTRODUCTION AND LITERATURE REVIEW	1
1.1 INTRODUCTION	1
1.2. <i>Pseudomonas aeruginosa</i>	2
1.3 MEDICINAL PLANTS	9
1.4 ENDOPHYTES	14
1.5 SEPARATION, PURIFICATION AND CHARACTERISATION OF FUNGAL BIOACTIVE EXTRACTS	19
1.6 CHARACTERISATION OF ANTIMICROBIAL COMPOUNDS	26
1.7 TOXICITY ASSAYS AND <i>in vivo</i> EVALUATION	27
1.8 <i>In vitro</i> EVALUATION OF CITRUS FLAVONOIDS	28
1.9 RATIONALE FOR THE STUDY	28
1.10 HYPOTHESIS TESTED	29
1.11 AIMS AND OBJECTIVES	29
1.12 REFERENCES	30
CHAPTER 2: SCREENING EXTRACTS FOR ANTI- <i>P. AERUGINOSA</i> ACTIVITY	39
2.1 INTRODUCTION	39
2.2 MATERIALS AND METHODS	41
2.3 RESULTS	46
2.4 DISCUSSION	54
2.5 CONCLUSION	57
2.6 REFERENCES	59
CHAPTER 3: PURIFICATION AND CHARACTERISATION OF THE <i>NEOFUSICOCCUM LUTEUM</i> ANTI-<i>P. AERUGINOSA</i> COMPOUND FROM THE ETHYL ACETATE CRUDE EXTRACT	63
3.1 INTRODUCTION	63
3.2 MATERIALS AND METHODS	65
3.3 RESULTS	66
3.4 DISCUSSION	71
3.5 CONCLUSION	73
3.6 REFERENCES	74
4.1 SUMMARY OF FINDINGS	77

4.2 CONCLUSIONS-----	78
4.3 RECOMMENDATIONS FOR FUTURE WORK-----	78
4.4 REFERENCES-----	80
APPENDIX A -----	81
APPENDIX B-----	90
APPENDIX C-----	93
APPENDIX D -----	96
APPENDIX E-----	98
APPENDIX F-----	99
APPENDIX G -----	106

LIST OF FIGURES

Figure 1.1: Biofilm lifestyle cycle of <i>P. aeruginosa</i> PAO1 grown in glucose minimal media. In stage I, planktonic bacteria initiate attachment to an abiotic surface, which becomes irreversible in stage II. Stage III corresponds to microcolony formation. Stage IV corresponds to biofilm maturation and growth of the three-dimensional community. Dispersion occurs in stage V and planktonic bacteria that are released from the biofilm colonise other sites (Rasamiravaka <i>et al.</i> , 2015).	4
Figure 1.2: Mechanisms of resistance in multidrug resistant <i>P. aeruginosa</i> (Sherrard <i>et al.</i> , 2014).	5
Figure 1.3: Three mechanisms of antibiotic resistance in biofilms (Stewart and Costerton, 2001).	6
Figure 1.4: Virulence factors produced by <i>P. aeruginosa</i> (Gelattly and Hancock, 2013).	8
Figure 1.5: <i>Kigelia africana</i> . A, B, C, D showing the tree, leaves, flower and fruits, respectively (Saini, 2009).	11
Figure 1.6: Structure of kigelin (Idris <i>et al.</i> , 2013).	12
Figure 1.7: Interactions between endophyte, parasites and host plants (Kusari <i>et al.</i> , 2012).	14
Figure 1.8: Strategies employed by endophytic fungi to protect plants against insects (Kusari <i>et al.</i> , 2013).	15
Figure 1.9: Biosynthesis of secondary metabolites from precursors of the central carbon metabolism. PPP: Pentose Phosphate Pathway. ETC: Electron Transport Chain. TCA: Tricarboxylic acid. AAs: amino acids (Nielsen and Nielsen, 2017).	17
Figure 1.10: General approaches in extraction, isolation and characterisation of bioactive metabolites (Sasidharan <i>et al.</i> , 2011).	19
Figure 1.11: Thin layer chromatography (Kumar <i>et al.</i> , 2013).	21

Figure 1.12: Thin layer chromatography (TLC) and TLC bioautography for antimicrobial activity in <i>Acacia</i> sp. (Samrot <i>et al.</i> , 2016).....	22
Figure 1.13: Schematic diagram indicates the direct bioautographic process (Dewanjee <i>et al.</i> , 2015).	23
Figure 1.14: Schematic diagram of agar overlay bioautography (Dewanjee <i>et al.</i> , 2015).	24
Figure 1. 15: High performance liquid chromatography system (Czaplicki, 2013).	25
Figure 2.1: Growth of endophytic fungi on potato dextrose agar media for 4 days. A and B: show ZF 52 and ZF 53 fungal isolates (top and bottom); C and D: show KZ 81 and ZF KZ 44.	46
Figure 2.2: Development of mycelial mat growth during the SSF. A: ZF 52, B: ZF 53.....	47
Figure 2. 3: Endophytic fungi extracts obtained following solvent extraction.....	48
Figure 2.4: Kirby Bauer disc diffusion assay demonstrating anti- <i>P. aeruginosa</i> activity of ethyl acetate extracts of endophytic fungi; A: ZF 34 and B: KZ 81, KZ 43, KZ 31 and KZ 78.	49
Figure 2.5: Kirby Bauer disc diffusion assay demonstrating anti- <i>P. aeruginosa</i> activity of ZF 52 extracts after varying fermentation periods. A1 indicates ZF 52 extract produced after one (T1) and two (T2) weeks and A2 indicates ZF 52 extracts produced after three (T3) and four (T4) weeks.	49
Figure 2.6: Resazurin colour reaction for minimum inhibitory concentration ($\mu\text{g/mL}$) determination of extracts against <i>P. aeruginosa</i> . Row A: 1 week ZF 52 extract 156.3; row B: 2 week ZF 52 extract 39.06; row C: 3 week old ZF 52 extract 78.13 and row D is a 4 week old ZF 52 extract 19.53.	50
Figure 2. 7: TLC analysis of ZF 52 crude ethyl acetate extracts; separated using (A) $\text{CDCl}_3\text{:EtOAc}$ (60:40). A - ZF 52 at four week ethyl acetate extract viewed with staining; (B)	

- ZF 52 separation using chloroform:ethyl acetate (Rf: 0.22, 0.30, 0.34, 0.43, 0.57 and 0.78) without staining (60:40).....	51
Figure 2.8: TLC analysis ZF 52 crude ethyl acetate extracts of varying ages separated using hexane:EtOAc and viewed under UV. T1- one week old; T2- two week old; T3- three week old and T4 is a four week old ZF 52 ethyl acetate extract.	51
Figure 2. 9: Bio-autogram of <i>P. aeruginosa</i> treated ZF 52 extract. Live cells appear pink and dead cells are presented by a halo. A - bio-autogram; B - TLC plate.....	52
Figure 2. 10: Genomic DNA isolated from ZF 52 on agarose gel. L1: 100 bp plus marker, L2 and L3: ZF52 DNA.....	52
Figure 2.11: Agarose gel image of the ITS2 region of 18S rRNA gene after PCR amplification. L1: 100 bp Gene ruler, L2: PCR amplification product, L3: negative control.	53
Figure 3. 2: Thin layer chromatography of fractions A, B, C and D.	66
Figure 3. 3: Broth microtitre serial dilution assay ($\mu\text{g/mL}$) for MIC determination of partially purified pooled fractions. Wells 1-10 contain cells, Muller Hinton broth and sample; Well 11 contains 8% DMSO in water and Well 12 contains more media as a replacement for extract.	66
Figure 3. 4: Broth microtitre serial dilution assay ($\mu\text{g/mL}$) for MIC determination for purified compound 1. Wells 1-10 contain cells, Muller Hinton broth and sample; Well 11 contains 8% DMSO in water and Well 12 contains more media as a replacement for extract.	67
Figure 3.5: ^1H NMR spectrum of compound 1 in CDCl_3	68
Figure 3.6: Expanded ^1H NMR spectrum of compound 1 in CDCl_3 (A and B).....	69
Figure 3.7: ^{13}C NMR spectrum of compound 1 in CDCl_3	69
Figure 3.8: DEPT spectra of compound 1.	70
Figure 3.9: HMBC spectrum of compound 1.	70

Figure 3.10: Major HMBC correlations observed in compound 1.	71
---	----

LIST OF TABLES

Table 1.1: <i>Pseudomonas aeruginosa</i> resistance mechanisms towards antibiotics (Hancock and Speert, 2000)	9
Table 1.2: Pharmacological activities of different phytoconstituents of <i>Kigelia africana</i>	13
Table 2.1: Scoring of activity of extracts (mm) (Chenia, 2013)	43
Table 2. 2: Interpretation of the resazurin microtitre assay	50
Table 2.3: BLAST analysis of ZF 52	53
Table 3.1: Interpretation of the resazurin microtitre assay for Fraction C	67
Table 3.2: Interpretation of the resazurin microtitre assay for compound 1	67

ACKNOWLEDGEMENTS

The author wishes to extend her sincere gratitude to the following person(s) and organizations:

God, for the gift of life

Dr. R. Govinden, Discipline of Microbiology, UKZN (Westville campus) for her supervision, support and encouragement during the course of the study;

Dr. R. Moodley, Discipline of Chemistry, UKZN (Westville campus) for her understanding, project design and supervision;

Dr. O. Bodede, Discipline of Chemistry, UKZN (Westville campus) for his general assistance with the project;

National Research Foundation for financial support;

Her family (Ms. N. Mfobo, Ms. M Qwayi, Mr. M.T. Kuali and Mr. T. Kuali) for their support, love and encouragement;

The postgraduate students and staff at the Discipline of Microbiology in particular Ms R. Paul, Mr. J.E. Naicker, Ms. N. Singh, Ms. S. Singh and Ms. U. Vencatasu for the endless laughter and joy in the lab.

CHAPTER 1: INTRODUCTION AND LITERATURE REVIEW

1.1 INTRODUCTION

In the world today, modern medicine is being used to treat the range of diseases and infections of individuals, with varying rates of success. In addition, preventative measures such as improved sanitation, better living conditions and clean water practises are being implemented to reduce the risk of such infections. Despite these improvements, numerous disease-causing pathogenic microbes are becoming more resistant to antimicrobial chemicals. The drug development rate is slower than the rate of microbial resistance, which is proving to be challenging (Gabriel and Olubunmi, 2009). The most encountered problem when treating microbial infections is antimicrobial resistance (Zankari *et al.*, 2017).

The appearance of new diseases and drug tolerant pathogens, together with the side effects caused by conventional drug use demands that new drugs be discovered. Over the past decade, increasing outbreaks caused by methicillin resistant *Staphylococcus aureus* (MRSA), *Enterococcus* sp. that are vancomycin resistant (VRE), extended spectrum beta lactamase-producing (ESBL) *Escherichia coli* and *Pseudomonas aeruginosa* have been reported (Hancock and Speert, 2000; Hirsch and Tam 2010). There is thus, an urgent need for novel antibiotics with new targets that may prove efficacious in treating infections caused by these resistant microbes. Several candidate drugs, namely, quinupristin/dalfopristin and the oxazolidinone linezolid, have been tested and are reputed to be effective in treating vancomycin resistant *Enterococcus faecium* (VREF) and skin infections caused by MRSA, *Streptococcus pyogenes* and other Gram-positive bacteria (Kraft *et al.*, 2014). However, these new antibiotics fail or have little activity against Gram-negative bacteria (Wright *et al.*, 2017). This is the main hurdle that needs to be overcome in order to combat the growing resistance of *P. aeruginosa*.

1.2. *Pseudomonas aeruginosa*

Pseudomonas aeruginosa is aerobic, Gram-negative and rod shaped. Due to its ability to cause diseases in immuno-compromised patients, it is referred to as an opportunistic pathogen. It is a versatile microbe able to tolerate low oxygen conditions, survive in nutrient deficient environments and tolerates a temperature range from 4-42°C. It is a multifaceted pathogen which is able to cause a wide range of infections and is the main cause of opportunistic nosocomial infections, causing approximately 10% of hospital infections. Chronic lung infections which lead to the death of patients with cystic fibrosis are mainly caused by this pathogen (Lutz and Lee, 2011).

The National Nosocomial Infection Surveillance done in South African hospitals over three decades showed *P. aeruginosa* to be the eighth most isolated pathogen from blood (3.4%) and the third most common cause of urinary tract infections (16.3%) (Hancock and Speert, 2000; Hirsch and Tam, 2010). The general prevalence of *P. aeruginosa* infections remained constant from 1986 to 2003. However, the incidence of resistant strains increased drastically in 2003. The rate of resistance of *P. aeruginosa* to imipemen increased by 15.9% in 2003 and by 20% to quinolones and third generation cephalosporins (Hirsch and Tam, 2010). Likewise, a study on Intensive Care Unit patients in South African hospitals reported a notable increase in *P. aeruginosa* strains resistant to at least three out of four antibiotics (multidrug resistant, MDR) (Nathwani *et al.*, 2008).

Pseudomonas aeruginosa is highly adaptive and this quality is proved by its ability to survive in the highly stressful and hostile environment found within a lung with cystic fibrosis (CF) (Minstanley *et al.*, 2016). Nitrosative, osmotic and oxidative stresses are some examples of stresses found within CF infected lungs (Silva *et al.*, 2010). Phenotypic analysis of isolates found within these infected lungs show an accumulation of auxotrophic mutations, conversion

of isolates from motile to sessile and the formation of mucoid colonies. The above-mentioned adaptations all provide protection to *P. aeruginosa* from antibiotics and host responses. Other adaptations the emergence of hypermutators (Minstanely *et al.*, 2016). Since CF patients are usually under long treatment with antimicrobials, the fast emergence of antimicrobial resistance is frequently encountered. Therefore, screening, purifying and characterising bioactive products with anti-*P. aeruginosa* activity is important, especially in South Africa where there is a high number of immuno-compromised patients.

1.2.1 *Pseudomonas aeruginosa* biofilms

Pseudomonas aeruginosa is considered an important plant and human pathogen due to its ability to produce various virulence factors (Epps and Walker, 2006). Apart from this, the ability of *P. aeruginosa* to form biofilms on many surfaces makes antibiotic treatments ineffective and thus promotes chronic infectious diseases. Biofilm formation is a continuous cycle, where organised bacterial communities are enclosed in a matrix of extracellular polymeric substances (EPS) which holds microbial cells together and allows adherence to surfaces (Rasamiravaka *et al.*, 2015). Extracellular polymeric substances are composed mainly of exopolysaccharides, extracellular DNA (eDNA), biomolecules and polypeptides that form a highly hydrated mixture that is implicated in the overall structure and architectural strength of the biofilm (Ding *et al.*, 2016).

Varying biofilm phenotypes can be expressed, depending on the strain of *P. aeruginosa* and the nutritional conditions. For example, in glucose limiting conditions, the *P. aeruginosa* PAO1 biofilm life cycle can be divided into five phenotypic stages (Figure 1.1). The reversible attachment of planktonic bacterial cells onto a growth surface begins this cycle (Figure 1.1 a, Stage I), irreversible attachment of bacteria which form microcolonies in the EPS matrix

continues this process (Figure 1.1 b, Stage II). Gradually, bacterial microcolonies expand and their individual contributions lead to a more structured phenotype with noncolonised space (Figure 1.1 c, Stage III). Later, free spaces within the biofilm become filled with bacteria and covers the whole surface (Figure 1.1 d, Stage IV). Three-dimensional communities grow as observed in Figure 1.1, Stages III and IV. Figure 1.1 e, Stage V, shows the last stage which is bacterial conversion from non-motile to planktonic form, in order to spread and inhabit other surfaces (Nikolaev and Plakunov, 2007; Flemming and Wingener, 2010; Rasamiravaka *et al.*, 2015).

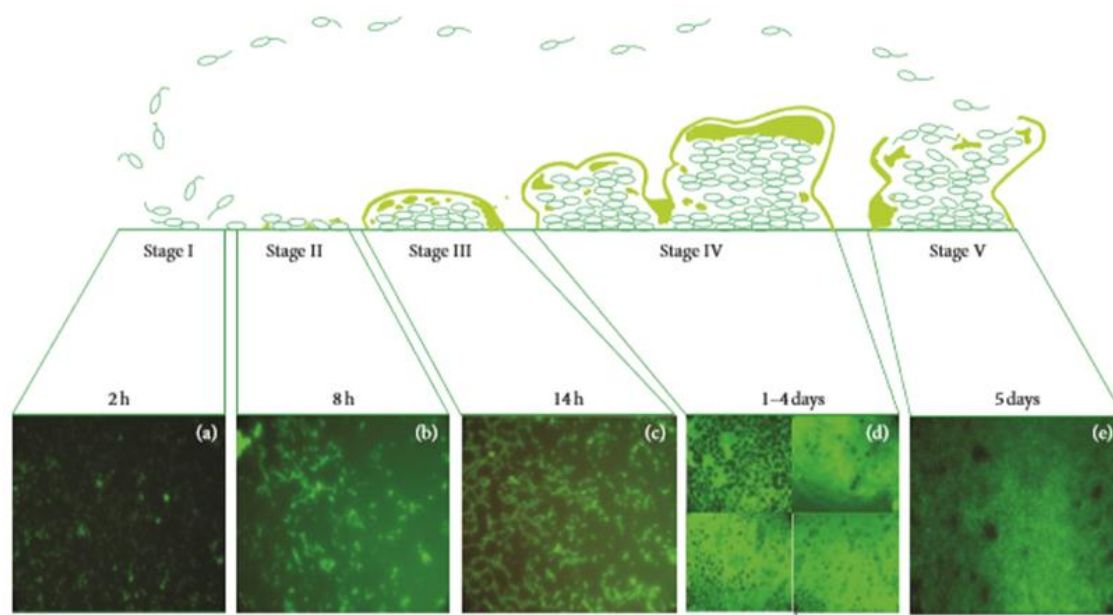


Figure 1.1: Biofilm lifestyle cycle of *P. aeruginosa* PAO1 grown in glucose minimal media. In stage I, planktonic bacteria initiate attachment to an abiotic surface, which becomes irreversible in stage II. Stage III corresponds to microcolony formation. Stage IV corresponds to biofilm maturation and growth of the three-dimensional community. Dispersion occurs in stage V and planktonic bacteria that are released from the biofilm colonise other sites (Rasamiravaka *et al.*, 2015).

1.2.2 *Pseudomonas aeruginosa* biofilm formation as a resistance mechanism

Antimicrobial resistance is the natural response of bacteria to antibiotic exposure. It can come about by spontaneous genetic mutations, be intrinsic to a bacterium, or be linked to horizontal

gene transfer (Sherrard *et al.*, 2014). *Pseudomonas aeruginosa* displays resistance to numerous antibiotics due to its ability to form biofilms. Figure 1.2 depicts the mechanisms of resistance to antibiotics which is largely due to a reduced activity of antibiotics inside the biofilm (Sherrard *et al.*, 2014). It is hypothesised that antibiotics do not penetrate the biofilm (Gomes *et al.*, 2012). This could be because it acts as a physical barrier which keeps antibacterial agents out of the biofilm (e.g. aminoglycosides) preventing their diffusion (Figure 1.2) (Sherrard *et al.*, 2012; Gupta *et al.*, 2015). This interaction also prevents the passage of antibiotics into the biofilm base, for example, in cystic fibrosis patients, steep oxygen slopes and oxygen deprived cavities form inside the cystic fibrosis mucus layer due to increased oxygen utilisation together with poor oxygen diffusion within the mucus.

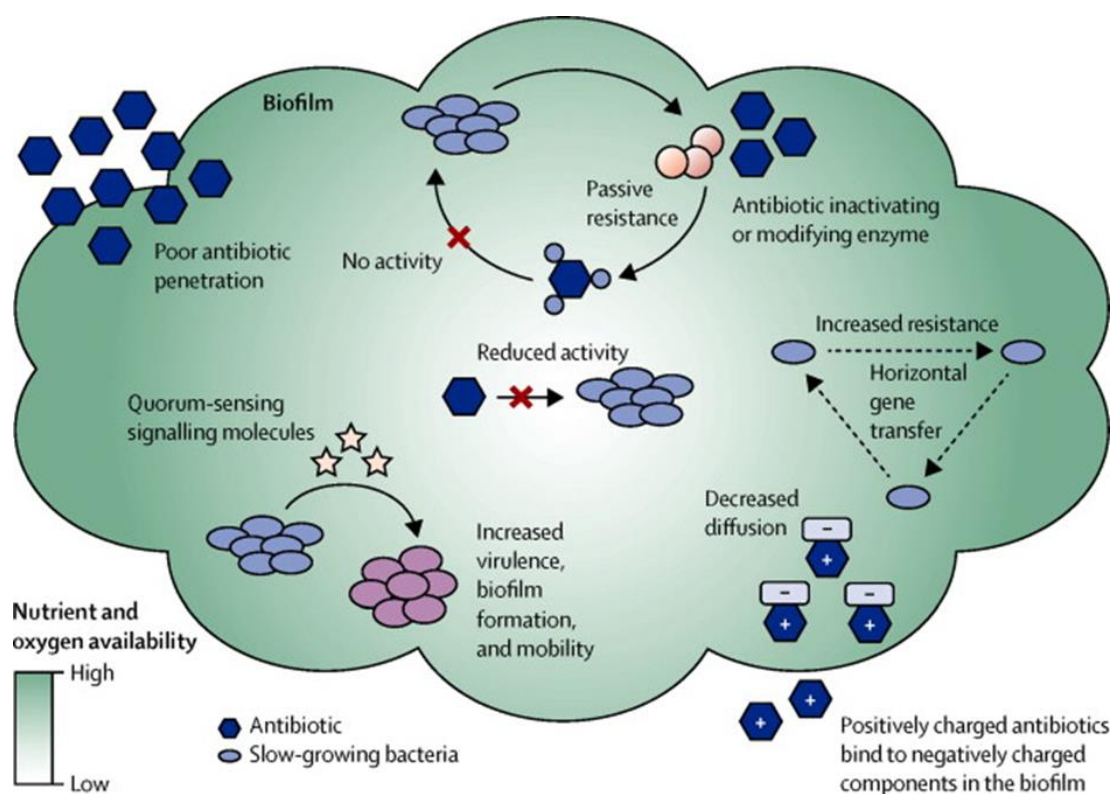


Figure 1.2: Mechanisms of resistance in multidrug resistant *P. aeruginosa* (Sherrard *et al.*, 2014).

Hill and co-workers (2005) revealed aerobically grown *P. aeruginosa* to be more susceptible to β -lactam, aminoglycoside and colistin antibacterial agents than anaerobically grown *P. aeruginosa* (Hill *et al.*, 2005). Furthermore, since aminoglycoside antibiotics need oxidative phosphorylation in order to enter bacterial cells, a low oxygen concentration inactivates these antibiotics (Schaible *et al.*, 2012). In addition, hypoxia is reported to increase efflux pump expression in *P. aeruginosa* and this causes increased resistance to cephalosporin and penicillin antimicrobials (Schaible *et al.*, 2012). Biofilm formation in cystic fibrosis is a symptom of chronic airway infection. Bacteria growing in biofilms are buried in an exopolymeric matrix (which includes exopolysaccharide, protein and DNA) that have been shown to be more resistant when compared to planktonic cells (Lutz and Lee, 2011; Sherrard *et al.*, 2014). A sub population of bacteria in the biofilm may adapt a protective phenotype and become persister cells. Figure 1.3 summarises the different types of cells found within a biofilm.

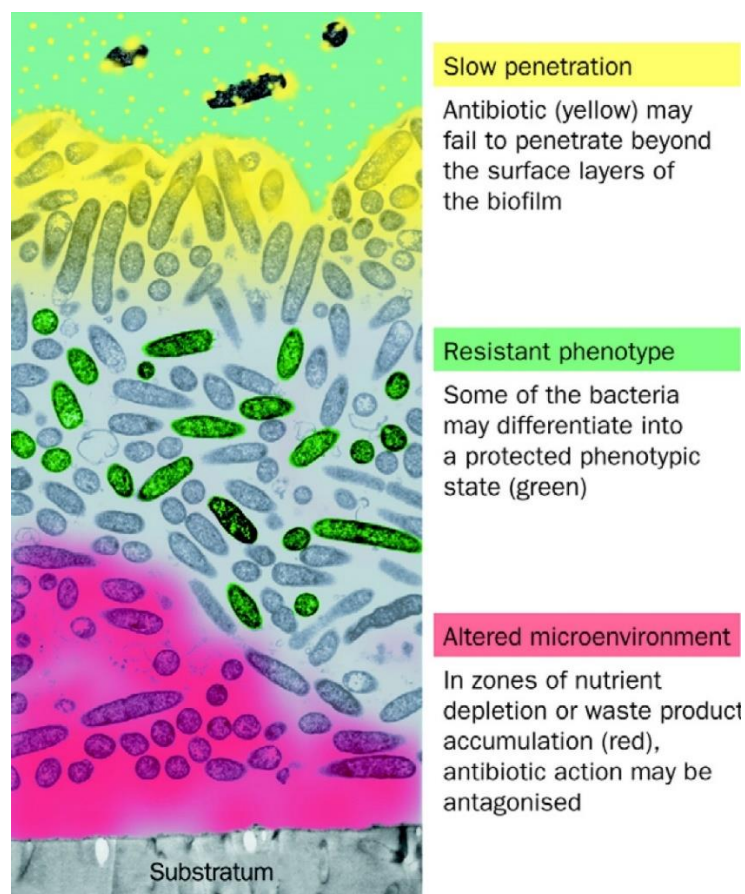


Figure 1.3: Three mechanisms of antibiotic resistance in biofilms (Stewart and Costerton, 2001).

1.2.3 *Pseudomonas aeruginosa* virulence factors

Pseudomonas aeruginosa has five known virulence factors: (i) flagella and type 4 pili, (ii) type 3 secretion system, (iii) quorum sensing and biofilm formation, (iv) lipopolysaccharides and (v) proteases (Figure 1.4). Each *P. aeruginosa* cell possesses several type 4 pili and a single polar flagellum that can initiate an inflammatory response. During infection, the bacterium can attach to host epithelial cells by binding its flagellum to the asialylated glycolipid asialoGM1 which can elicit a strong NF κ B-mediated inflammatory response via signalling through TLR5 and a caspase-1-mediated response through the Nod-like receptor, Ipa (Mena *et al.*, 2008). Mutants which don't have flagella cannot elicit an inflammatory response. Thus, flagella are believed to be required to establish an infection. Type 4 pili are the most important attachment apparatus. Pili can also facilitate aggregation, causing the bacteria to form microcolonies on host target tissues, effectively forming a dense packing of bacteria in one location. They protect the bacteria from antibiotics and the host immune system (Williams *et al.*, 2010).

Pseudomonas aeruginosa microcolonies are highly implicated in chronic cystic fibrosis. Pilin-deficient mutants and those that do not display twitching motility, show reduced virulence in various models (Mena *et al.*, 2008). Type 3 secretion systems (T3SS) are common among several pathogenic Gram-negative bacteria as a way of injecting toxins directly into host cells. The T3SS in *P. aeruginosa* has four effectors which were identified as – ExoY, ExoS, ExoT, and ExoU – far fewer than many other well-characterised T3SS (e.g. *Salmonella enterica* SPI-1 has 13, *Shigella* sp. have 25) (Hauser, 2009). The T3SS of *P. aeruginosa* is encoded by 36 genes on five operons. The entire system is transcriptionally controlled by ExsA, a member of the AraC family of transcriptional activators (Yahr and Wolfgang, 2006). Nearly all strains express one of the two major exotoxins, exoU or exoS, but very rarely both.

ExoS is bifunctional, including both N-terminal GTPase-activating protein activity and C-terminal ADP ribosyltransferase (ADPRT) activity (Otter *et al.*, 2011). Both activities are linked to the actin cytoskeletal organisation, although the ADPRT activity is understood to play a larger part in pathogenesis. ExoU is a phospholipase and is estimated to be 100 times more potent a cytotoxin than ExoS and causes rapid death of host eukaryotic cells due to loss of plasma membrane integrity consistent with necrosis (Mena *et al.*, 2008). Lipid A can be sequentially bound by host cell coreceptors MD2 and CD14 leading to activation of the TLR4 to NF κ B signalling pathway and triggering the production of pro-inflammatory cytokines and chemokines, inflammation, and over time endotoxic shock (Bardoel *et al.*, 2011). Alkaline protease is a type 1 secreted zinc metalloprotease that is known for its degradation of host complement proteins and host fibronectin. In addition, alkaline protease has been shown to interfere with flagellin signalling through host TLR5 by degrading free flagellin monomers and thereby helping *P. aeruginosa* to avoid immune detection (Gellatly and Hancock, 2013).

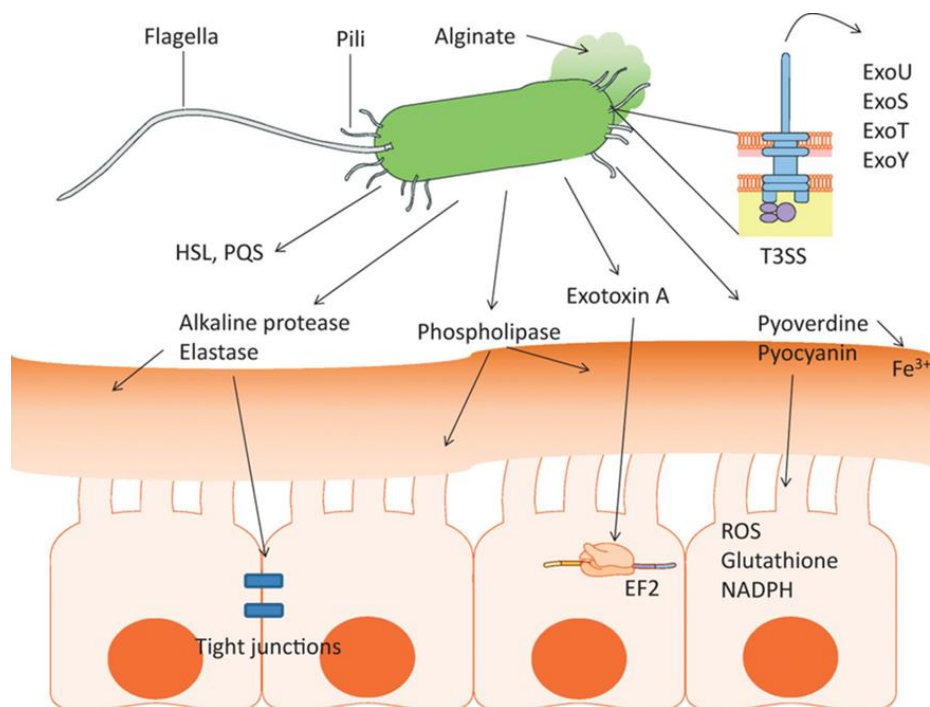


Figure 1.4: Virulence factors produced by *P. aeruginosa* (Gelattly and Hancock, 2013).

The prominence of *P. aeruginosa* as a pathogen is due to its high intrinsic resistance to antibiotics (Table 1.1), to the point that the efficacy of even the newest antibiotics is significantly altered (Lutz and Lee, 2011). This, therefore, directed the search for novel bioactive molecules from previously unexplored sources.

Table 1.1: *Pseudomonas aeruginosa* resistance mechanisms towards antibiotics (Hancock and Speert, 2000)

Class	Agents	Mechanism of action
Penicillin	Ticarcillin, Carbenicillin, Piperacillin	Depression of chromosomal β -lactam. Overexpression of the MexAB-OprM multidrug efflux pump due to a NalB mutation. Specific plasmid-mediated β -lactamases.
Cephalosporin	Ceftazidime Cefoperazone Cefepime Cefpirome	Depression of chromosomal β -lactam. Overexpression of the MexAB-OprM multidrug efflux pump due to a NalB mutation. For the fourth generation cephalosporins cefepime and cefpirome, overexpression of the MexCD-OprJ multidrug efflux pump due to an NfxB mutation.
Aminoglycoside	Gentamicin Tobramycin Amikacin	Overexpression of the MexXY efflux pump in impermeability type-resistance due to a mutation in the regulatory gene MexZ. Plasmid-mediated production of modifying enzymes.
Quinolones	Ciprofloxacin	Target site mutations in the GyrA (or sometimes the GyrB) topoisomerase subunit; Overexpression of multidrug efflux pumps due to NalB, NfxB or NfxC mutations.
Polymixin	Colistin	Outer membrane LPS changes due to PhoP/PhoQ regulatory mutations. No evidence this occurs in the clinic.
Carbapenem	Imipenem Meropenem	Loss of specific outer membrane porin channel, OprD; Reduction in levels of OprD due to an NfxC mutation that also upregulates multidrug resistance due to MexEF-OprN. For meropenem overexpression of the MexAB-OprM multidrug efflux pump due to a NalB mutation.

1.3 MEDICINAL PLANTS

Plants contain bioactive compounds which have been used for traditional healthcare for thousands of years. The ethno-pharmaceutical knowledge of Traditional Chinese medicine includes over 5000 species (Miller *et al.*, 2012). Plants play a significant role in drug development and discovery, worldwide. From 1981 to 2010, 26% of new drugs were natural products and this peaked to 50% in 2010 (Newman and Cragg, 2012). Plants with antibacterial properties are of central importance as biological sources of novel active metabolites that may

provide a solution to the alarming incidence of antibiotic resistance in clinical strains. Medicinal plants offer a promising source for such drugs. These plants are reservoirs of compounds that can be used in drug development (Hassan, 2012).

Cassia fistula is a medicinal plant that produces bioactive secondary compounds, which are currently being used as dietary supplements, medicines and other useful commercial products (Kadhim *et al.*, 2016). Investigations into this plant were prompted by their use in traditional medicine which has been passed down from generation to generation (Mishra and Behal, 2010). *Cassia fistula* has been reported to contain flavonoids, alkaloids, tannins, terpenes, and glucosides (Ali, 2014). These compounds are responsible for the antibacterial activity of the plant and form the basis for its use in the manufacture of antibiotics.

The combined effects of the secondary metabolites of papaya impart medicinal properties that prevent heart disease, colon cancer and strokes (Aravind *et al.*, 2013). Recently, the aloe plant was discovered to possess antiseptic properties along with other properties including laxative and anti-inflammatory skin agent which clears acne and soothes eczema (Mavintha and Bidya, 2014). Plants with anti-inflammatory properties have been reported to display antimicrobial activity too.

Plant essential oils are a very diverse group of secondary metabolites that are potentially useful sources of antimicrobial compounds. Many studies have reported on the antimicrobial activity of essential oils (Soković *et al.*, 2010; Moussaoui and Alaoui, 2016). According to Moreti (2004), essential oils, unlike antibiotics, consist of numerous molecules that bacteria cannot gain resistance towards. These essential oils they are known for their potent antiviral, anti-fungal, anti-inflammatory and antibacterial effects. The combination of essential oils with antibiotics may lead to new ways to treat infectious diseases. Many researchers have studied the synergistic effects resulting from the combination of antibiotics with different plant extracts

which reduced bacterial resistance to drugs (Ghaleb and Mhanna, 2008; Stefanovic and Comic, 2012; Moussaoui and Alaoui, 2016).

1.3.1 *Kigelia africana*

Taking all medicinal plants in Africa into consideration, the most widely distributed is *Kigelia africana* (Figure 1.5). *K. africana* is found in tropical regions including Central, South and West Africa (Saini *et al.*, 2009; Oyedeji and Bankole-Oje, 2012). It is referred to as the sausage tree due to the big fruit that it bears (0.6 m in length and 4 kg weight) (Saini *et al.*, 2009; Azu *et al.*, 2010).

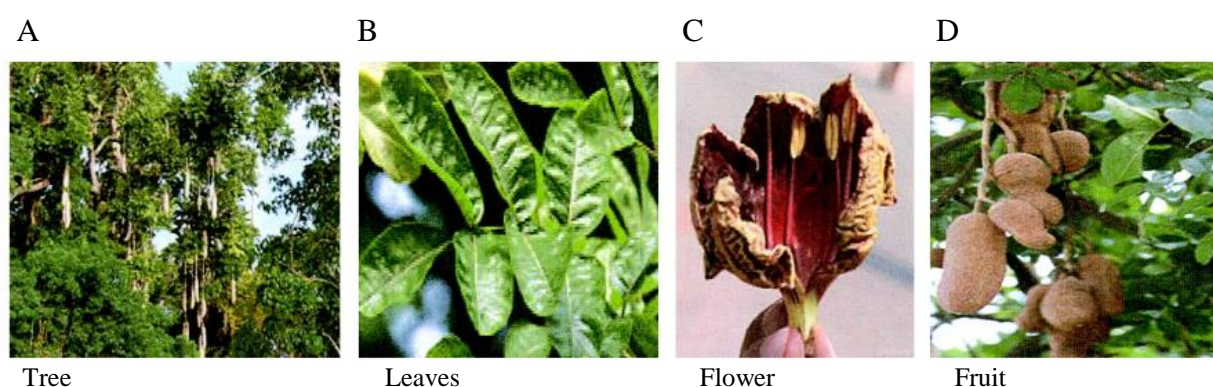


Figure 1.5: *Kigelia africana*. A, B, C, D showing the tree, leaves, flower and fruits, respectively (Saini, 2009).

All parts of the plant have been reportedly used to treat illnesses (Idris *et al.*, 2013). In rural regions of Africa, various forms of the plant are believed to cure a large number of illnesses. These include topical applications for fungal infections, psoriasis, eczema and boils (Atawodi *et al.*, 2017). This plant has also been administered internally for the treatment of malaria, toothache, pneumonia, ringworm, tapeworm and diabetes (Azu *et al.*, 2010). During famine in Malawi, the seeds were roasted and eaten (Azu, 2013). In the Zambezi Valley, the Tonga women apply cosmetic creams of *K. africana* to their faces to maintain and ensure blemish-free faces (Saini *et al.*, 2009). Other applications of *K. africana* include a preparation of the

flowers for application on breasts of lactating females to increase the flow of milk (Atawodi *et al.*, 2017). *K. africana* extracts are used to treat toothaches and sores associated with diabetes; this prompted the study of this plant for its potential to produce antibacterial compounds (Siani *et al.*, 2009).

1.3.2 *Kigelia africana* metabolites

Several metabolites have been extracted from various parts of this plant. These include the furanone derivative 3-(2-hydroxyethyl)-5-(2-hydroxypropyl)-dihydrofuran-2-(3H)-one and four irridiods (7-hydroxy viteoid II, 7-hydroxy eucommic acid, hydroxy-10-deoxyeucommiol and 10-deoxyeucommol) (Akanni *et al.*, 2017). A novel phenylpropanoid derivative was isolated from the fruit and identified as 6-*p*-coumaroyl sucrose, as well as ten known phenylpropanoids and phenylethanoids and a flavonoid glucoside. Kigelin (Figure 1.6), the major constituent in *K. africana* was also isolated in 1971 by Govindchari *et al.* (1971).

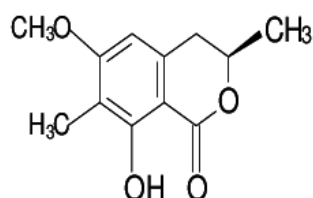


Figure 1.6: Structure of kigelin (Idris *et al.*, 2013).

Kigelin is a 8-hydroxy-6,7-dimethoxy-3-methyl-3,4-dihydroisocoumarin. Other compounds such as 6-methoxymethymellein, stigmasterol, lapachol, β -sitosterol, 3-dimethyl kigelin, kigelinone, naphthaquinones, dehydro- α -lalachone and isopinnatal, isolated from various parts of the plant were found to impart antibacterial and antifungal activity (Grace *et al.*, 2002; Gabriel and Olubumni 2009; Idris *et al.*, 2013). Other properties of the plant include antiprotozoal and anti-amoebic activity (Oyedepi and Brankole-Oje 2012). Table 1.2 depicts

some classes of secondary metabolites isolated from *K. africana* and their biological activities based on studies by Akunyili *et al.* (1991), Kwo and Cracker (1996), Grace *et al.* (2002) and Saini *et al.* (2009).

Table 1.2: Pharmacological activities of different phytoconstituents of *Kigelia africana*

Activity	Irridiods	Naphthoquinone	Meroterpenoid naphthoquinones	Coumarin derivatives	Lignans	Sterols	Flavonoids
Anticancer	+	+	+	+	+	+	+
Anti-mollusidal	+	-	-	-	-	-	+
Against syphilis and gonorrhea	+	+	-	-	-	+	+
Antidiarrheal	+	-	-	-	-	-	+
Antiulcer	+	-	-	-	-	-	+
Antifungal	-	-	+	-	+	+	+
Antimalarial	-	-	+	-	+	-	-
Anti-inflammatory	+	+	+	-	-	+	+
Antibacterial	+	+	+	-	+	+	-
Against postpartum haemorrhage	+	-	-	+	-	+	-
Anti-Pneumonia	+	-	-	-	-	+	+

Keys: -Not active; + active

In the interest of plant preservation, the focus has shifted to include the plant microbiome. Studies have surprisingly shown that not only were the plants themselves producing the bioactive metabolites, but their associated microbiomes were as well (Jalgaonwala *et al.*, 2011).

1.4 ENDOPHYTES

Investigations on the same plant species located in different geographical regions/countries have shown that they carried different active metabolites suggesting that the bioactive secondary metabolites are produced by endophytic microorganisms. Endophytes are microorganisms (including Actinomycetes, fungi and bacteria) which colonise plants without any symptoms (De Bary, 1886 cited by Sadrati *et al.*, 2013; Kusari *et al.*, 2013). Mutualism or asymptomatic colonisation has been attributed to a balance of antagonism between the host defence responses and the virulence factors of the endophytic microorganism by Kusari and co-workers (2013) (Figure 1.7). Figure 1.7 also shows that the presence of certain environmental factors may cause a shift from mutualism to pathogenesis.

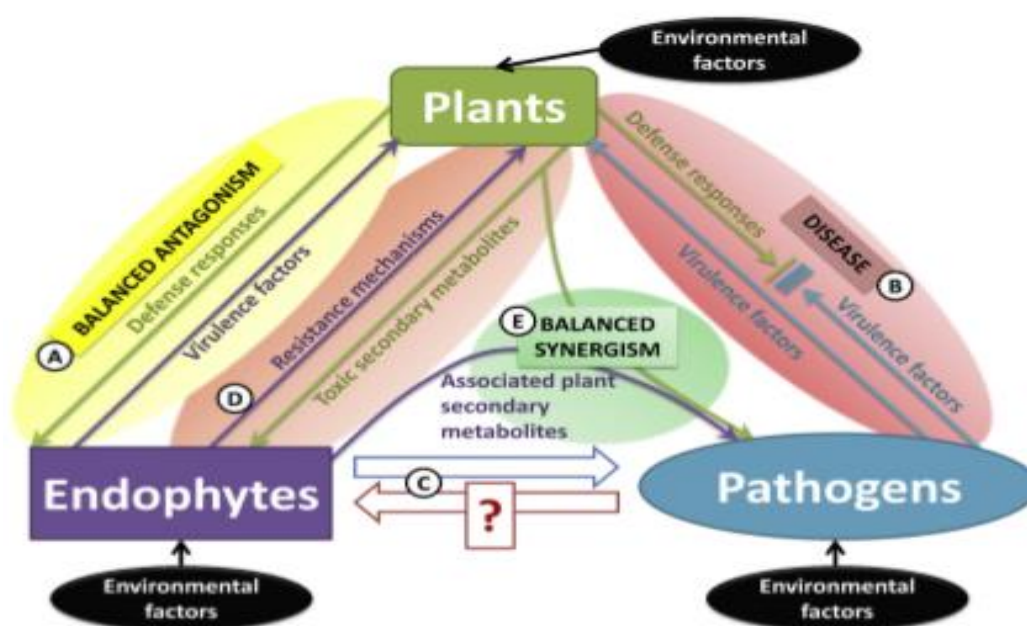


Figure 1.7: Interactions between endophyte, parasites and host plants (Kusari *et al.*, 2012).

Endophytes and plants produce similar metabolites, probably due to the endophyte and plants coevolving over several millennia (Kusari *et al.*, 2012). The plant provides shelter and nutrients and in return the endophytes protect the plant from biotic and abiotic stresses. An

early report of this by Webber (1981), showed that the endophytic fungus, *Phomopsis oblonga*, provided protection to elm trees against the beetle, *Physosnenum brevilineum*. This endophytic fungus reduced the spread of the causal agent of Dutch elm disease by producing toxic repellents against *P. brevilineum* (Kusari *et al.*, 2013). Figure 1.8 depicts this protection by endophytic fungi. It was later proven that endophytic fungi belonging to the family *Xylariaceae* could synthesise toxic secondary metabolites that affect beetle larvae (Claydon *et al.*, 1985; Suryanarayanan, 2017).

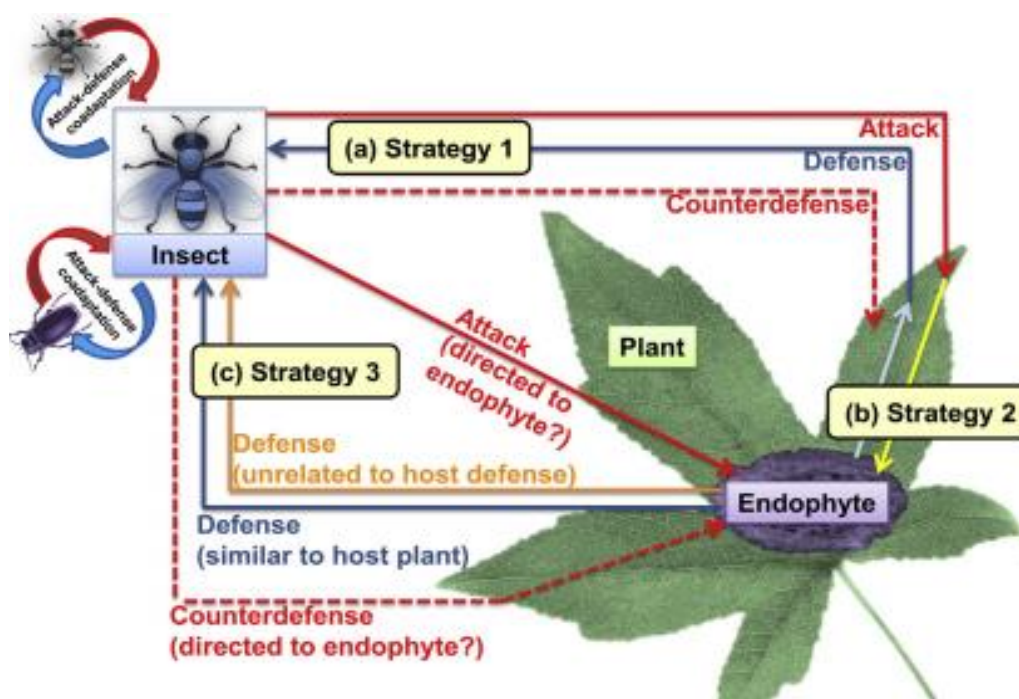


Figure 1.8: Strategies employed by endophytic fungi to protect plants against insects (Kusari *et al.*, 2013).

Due to the emergence of drug resistant superbugs, there is an ever-increasing need for obtaining new compounds which are aimed at alleviating illnesses caused by pathogens (Sadrati *et al.*, 2013). The ability of older types of antimicrobial agents to cure diseases continues to decrease. In addition, synthetic drugs threaten the environment and have serious side effects (Clay,

2014). Removal of these agents creates a gap which needs to be filled by new compounds with the ability to control human pathogens. There is an immediate need to find and produce environmentally safe drugs (Sadrati *et al.*, 2013).

Research conducted by Stierle *et al.* (1993; 1995) reporting on the discovery of the endophytic fungus, *Taxomyces andreane*, which produces Taxol®, an anticancer drug, directed intense attention towards endophytic fungi (Das *et al.*, 2017). This formed the basis and major motivating factor towards the study of fungal endophytic bioactive molecules. They are considered excellent reservoirs of therapeutically active compounds due to their genetic diversity (Darsih *et al.*, 2017). Endophytic fungi have been found to be present in all plants studied to date and are thought to be ubiquitous in plants (Huang *et al.*, 2001; Kirk *et al.*, 2001; Strobel and Daisy 2003; Jalgaonwala *et al.*, 2011).

It is estimated that 1.5 million endophytic fungi live within plants and lichens (Huang *et al.*, 2008). The incidence of endophytes within plant tissue appears to be environmentally influenced. Arnold and Lutzoni (2007) showed that the incidence of infection by endophytes approached 100% in plants situated in tropical regions; this incidence is exponentially higher than in plants found in polar regions. Rosa *et al.* (2009) later confirmed these findings.

Most endophytic fungi belong to the phylum Ascomycota, while some belong to the phyla Basidiomycota and Zycomycota (Huang *et al.*, 2001). It was shown that the presence or absence of endophytic fungi can affect plant structures and communities. Arbuscular mycorrhizal fungi grow deep into the soil facilitating better uptake of nutrients from the soil, especially the roots (Cosme *et al.*, 2018). This improves plant growth and survival allowing taller and stronger plants. The presence of root endophytes. Thus, plants that grow near plants with root endophytic fungi also reap the benefits of more nutrient availability (Allen *et al.*,

2018). The whole plant community benefits. These fungi also change the internal morphology of plant tissue by forming arbuscules within the plant tissue.

Investigations into the genomes of plants and associated endophytes have revealed that they contain conserved gene clusters that have co-evolved during their long association reportedly dating back 400 million years (Chagas *et al.*, 2018). These gene clusters encode novel secondary metabolites that may have potential medicinal applications (Lahn *et al.*, 2017). Much work has been conducted to elucidate the genomes of several endophytic fungi. Wang and co-workers (2001) sequenced the *Pestalotiopsis fici* genome and found that it harboured numerous secondary metabolite synthesis genes: 27 polyketide synthases (PKS), 12 non-ribosomal peptide synthases (NRPS), 5 dimethylallyl tryptophan synthases, 4 putative PKS-like enzymes, 15 putative NRPS-like enzymes and 15 terpenoid synthases. These core enzymes are distributed into 74 different secondary metabolite clusters. Secondary metabolites are synthesised when precursor metabolites are limited during primary metabolism (Figure 1.9) (Nielsen and Nielsen, 2017).

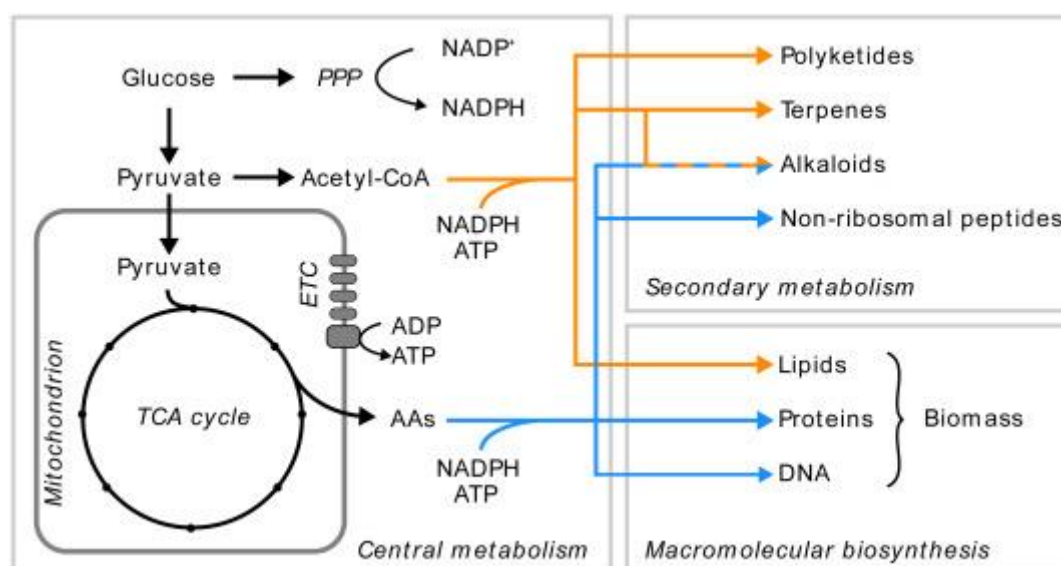


Figure 1.9: Biosynthesis of secondary metabolites from precursors of the central carbon metabolism. PPP: Pentose Phosphate Pathway. ETC: Electron Transport Chain. TCA: Tricarboxylic acid. AAs: amino acids (Nielsen and Nielsen, 2017).

These precursors are predominantly amino acids or short chain carboxylic acids, backbone enzymes like PKSs, DMATs, NRPSs or TCs link them together. The resulting oligomers are chemically modified by enzymes which are controlled by the usual transcriptional regulators as the backbone enzymes. The characteristic trait of genes involved in the secondary metabolite pathways is that they cluster in the chromosome in biosynthetic gene clusters (BCGs) (Nielsen and Nielsen, 2017). The ability to produce secondary metabolites is common to most living organisms but it is unevenly distributed. In known antimicrobial compounds (about 22 500 in total), 45% are produced by actinomycetes, 38% by fungi and 17% are from bacteria. In addition, even with this abundance of compounds, it is estimated that only 100 are used for human therapy, with most of these being produced by actinomycetes. However, it must be acknowledged that aside from penicillin, other fungal secondary metabolites have been of pharmaceutical use; these include, but are not limited to, griseofulvin, statins and mycophenolic acid.

Natural products produced by endophytic microbes are observed to inhibit and kill a variety of harmful pathogens, including bacteria, fungi and protozoans (Darsih *et al.*, 2017). These products are also known to deter herbivores (Jalgoanwala *et al.*, 2011, Das *et al.*, 2017). *Cryptosporiopsis quercina* is a fungus from which a unique antifungal compound named cryptocandin was extracted. This compound contains known amino acids and one new amino acid (3-hydroxy-4-hydroxy methyl proline) (Nandini *et al.*, 2018). Cryptocandin has shown very efficient activity against human fungal pathogens, namely, *Trycophyton* spp. and *Candida albicans*. Antifungal activity by cryptocandin was also observed against *Botrytis cineria* and *Sclerotinia sclerontiorum* which are plant pathogens.

The study into endophytic fungi is only just beginning as only a tenth of fungal species have been isolated out of the approximately 1.5 million thought to exist. The study of the endophytes

of *K. africana* are still in the developmental stages as little is known about them. Idris *et al.* (2013) isolated endophytic fungi from *K. africana* and screened extracts produced by these fungi for antibacterial activity. The seven endophytic fungi isolated were identified to be *Aspergillus* sp., *Aspergillus flavus*, *Cladosporium* sp., *Curvularia lunata* and three unknown fungi. The *Aspergillus* sp., *Cladosporium* sp. and two of the unknown fungi displayed antibacterial activity. These results, therefore, suggest that endophytic fungi from *K. africana* have the potential to produce useful bioactive compounds with antimicrobial activity.

1.5 SEPARATION, PURIFICATION AND CHARACTERISATION OF FUNGAL BIOACTIVE EXTRACTS

Natural products, such as plant extracts, either as pure compounds or as standardized crude extracts, provide unlimited opportunities for new drug discovery because of the unmatched availability of chemical diversity (Mahmoudvand *et al.*, 2015). According to the World Health Organization (WHO), more than 80% of the world's population relies on traditional medicine for their primary healthcare needs (Oyebode *et al.*, 2016). A summary of the general approaches in extraction, isolation and characterisation of bioactive compound from plant extracts can be found in Figure 1.10 (Sasidharan *et al.*, 2011).

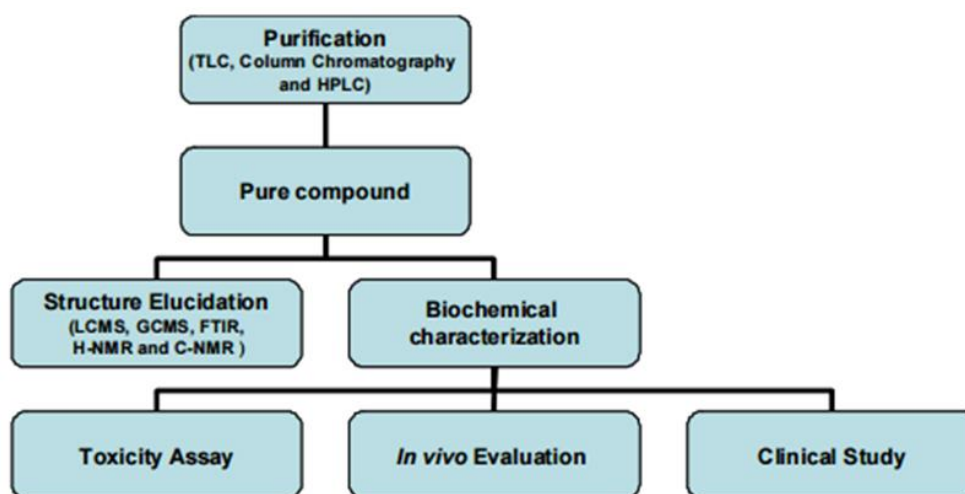


Figure 1.10: General approaches in extraction, isolation and characterisation of bioactive metabolites (Sasidharan *et al.*, 2011).

1.5.1 Thin layer chromatography (TLC)

Thin layer chromatography (TLC) is a method mainly used in forensic drug chemistry, which separates compounds of a drug mixture (Harper *et al.*, 2017). Forensic laboratories use TLC to examine unknown drug mixtures. In TLC, the mobile phase is a solvent (liquid), and the stationary phase is a thin aluminium sheet coated with a thin layer of adsorbent material, usually silica gel, aluminium oxide (alumina), or cellulose. The mobile phase transports the solute through the stationary phase (Sasidharan *et al.*, 2011). The speed at which the solute move on the TLC plate depends on the strength of the mobile phase as it dissolves the solute and migrates it up the plate (Klimek-Turek *et al.*, 2016), together with the sorbent as it pulls the solute out of solution and back into the sorbent. The molecules move *via* a stop and go motion due to the solute being absorbed and desorbed repeatedly (Santiago and Strobel, 2013). A small fraction of the solute moves at a given time with each spot travelling a certain distance.

Substances that are strongly attracted to the solid layer move slowly because they spend more time in the sorbent and fast-moving compounds have a low affinity for the stationary phase and a high affinity for the mobile phase and thus spend more time in the mobile phase. Therefore, separation of compounds with varying properties is achieved by exploiting the interactions of the solutes with the mobile and stationary phases. Analysis of this assay entails calculating the R_f value and that is the distance migrated by the compound divided by the distance migrated by solvent (Kumar *et al.*, 2013) (Figure 1.11). This value gives meaning to TLC as it can be compared to the R_f values of known standards.

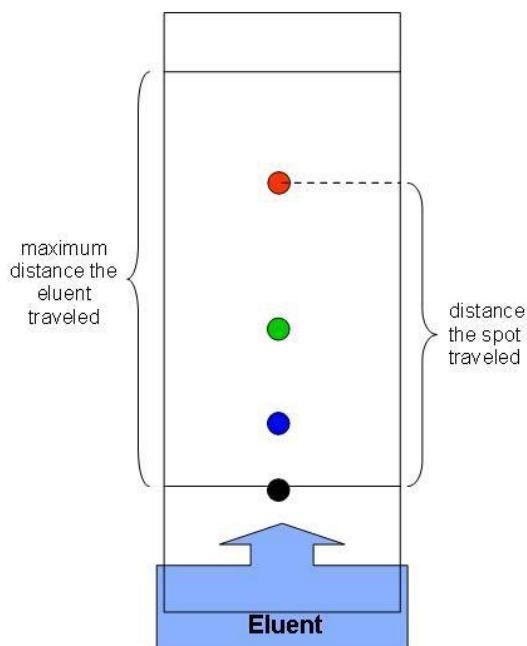


Figure 1.11: Thin layer chromatography (Kumar *et al.*, 2013).

A study by Abok and Manulu in 2017, was conducted to identify phytochemical constituents of *Syzygium guineense* leaf extract. The bark and leaves of *S. guineense* are used to treat dysentery, wounds, ulcers, tuberculosis and chronic diarrhea. TLC analysis was conducted using hexane and ethyl acetate as solvents. Hundred % hexane, hexane: ethyl acetate (2:1) and hexane: ethyl acetate (3:1) were used. It was observed that 100% hexane did not resolve the contents, while hexane:ethyl acetate (2:1) and hexane: ethyl acetate (3:1) yielded three and seven bands with R_f values 0.13, 0.23, 0.84 and 0.007, 0.13, 0.23, 0.32, 0.40, 0.54, 0.81 respectively (Abok and Manulu, 2017).

1.5.2 Bio-autography

Bio-autography enables the localising of antimicrobial activities of an extract on the chromatogram, thus it supports the search for new antimicrobial agents through bioassay-guided isolation (Swapna *et al.*, 2015). The advantages of the bio-autography agar overlay method includes use of small amounts of sample extract and the ability to identify the exact

component with antimicrobial activity from the crude sample (Rahalison *et al.*, 1991). There are various methods to TLC bio-autography (direct, contact and agar overlay). Figure 1.12 represents direct bio-autography which entails the spraying of a 24-hour culture on a dried TLC plate, incubating at 37°C for 24 hours and spraying with 3-(4,5-dimethylthiazol-2-yl)-2,5-diphenyl tetrazolium bromide (MTT) as conducted by Samrot *et al.*, 2016. The resultant spots (compounds) with antibacterial activity appear clear while the compounds with no antimicrobial activity appear green. The most commonly used dyes are MTT and tetrazolium dye.

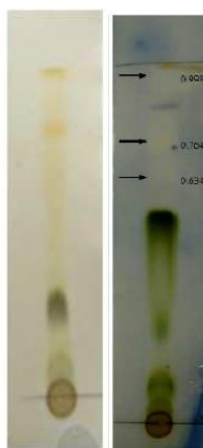


Figure 1.12: Thin layer chromatography (TLC) and TLC bioautography for antimicrobial activity in *Acacia* sp. (Samrot *et al.*, 2016).

In contact bio-autography, antimicrobial compounds diffuse from a developed TLC plate to an agar plate inoculated with the test strains (Sherma, 2008; Dewanjee *et al.*, 2015). The chromatogram is placed face down onto the inoculated agar layer for a specific period to enable diffusion of the compounds from the TLC plate to the agar plate. The chromatogram is removed, and the agar layer is incubated. The zones of inhibition on the agar surface, corresponding to the spots in chromatographic plates, are indicative of the antimicrobial agents. An overall view of contact bio-autography is shown in Figure 1.13. Incubation time for the

growth ranges between 16 and 24 hours but it can be reduced to 5–6 hours by 2,3,5-tetrazolium chloride (Dewanjee *et al.*, 2015).

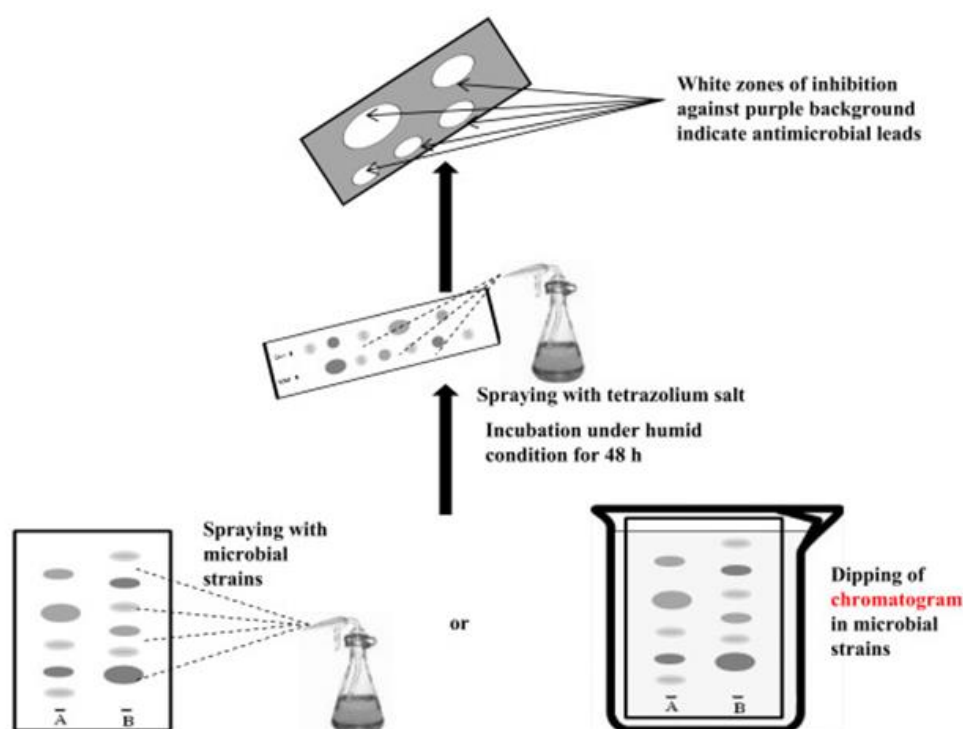


Figure 1.13: Schematic diagram indicates the direct bioautographic process (Dewanjee *et al.*, 2015).

Agar overlay is a combination of contact and direct bio-autography. In this method, the chromatogram is covered in a molten, seeded agar medium. After solidification, incubation and staining (usually with tetrazolium dye), the inhibition or growth bands can be seen (Figure 1.14).

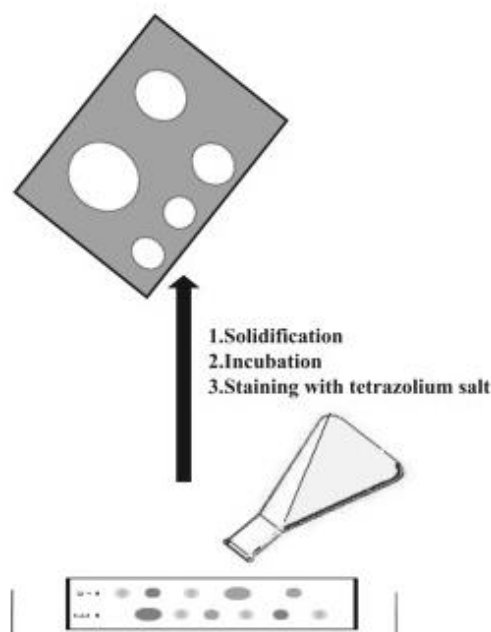


Figure 1.14: Schematic diagram of agar overlay bioautography (Dewanjee *et al.*, 2015).

1.5.3 High performance liquid chromatography (HPLC)

High performance liquid chromatography (HPLC) is a widely used technique for the isolation of natural products (Capone *et al.*, 2015). In order to fully characterise the active entity, natural products are often isolated following the biological evaluation of a relatively crude extract. The bioactive component is often present only as a minor component in the extract and the resolving power of HPLC is well suited to rapidly process multicomponent samples on both an analytical and preparative scale (Hayes *et al.*, 2014).

Gradient elution in which the proportion of organic solvent to water is altered with time may be desirable if more than one sample component is being studied and significantly differ from each other in retention under the conditions employed (Sasidharan *et al.*, 2011). Purification of the compound of interest using HPLC is the process of separating or extracting the target compound from other (possibly structurally related) compounds or contaminants. Each compound should have a characteristic peak under certain chromatographic conditions. Identification of compounds by HPLC is a crucial part of any HPLC assay. In order to identify

any compound by HPLC, a detector must first be selected (Hayes *et al.*, 2014). Once the detector is selected and is set to optimal detection settings, a separation assay must be developed. The parameters of this assay should be such that a clean peak of the known sample is observed from the chromatograph. The identifying peak should have a reasonable retention time and should be well separated from extraneous peaks at the detection levels which the assay will be performed. UV detectors are popular among all the detectors because they offer high sensitivity) and also because majority of naturally occurring compounds encountered have some UV absorbance at low wavelengths (Capone *et al.*, 2015) (190-210 nm). Figure 1.15 shows a summarised illustration of how HPLC components.

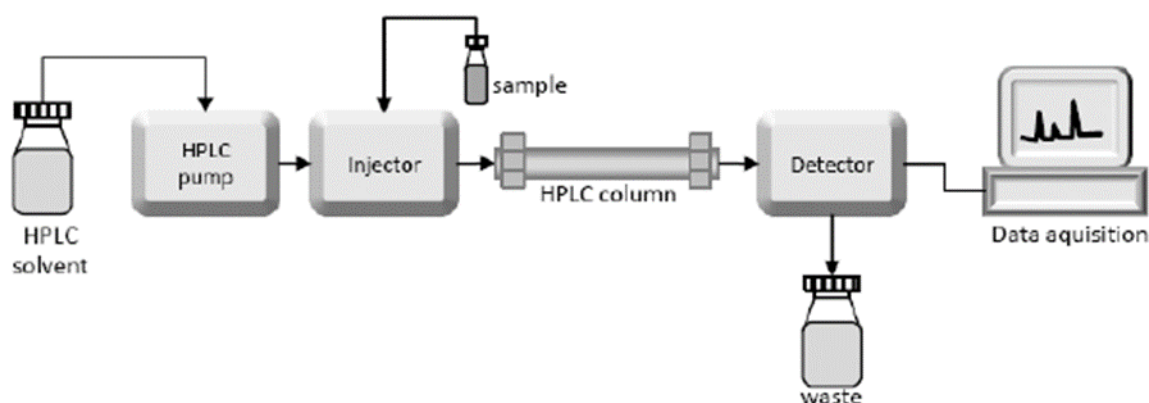


Figure 1. 15: High performance liquid chromatography system (Czaplicki, 2013).

Phenolic acids were extracted from the three date varieties and identified by high-performance liquid chromatography (HPLC) as described by Mansouri *et al.* (2005). One hundred grams of sample was mixed with 300 mL methanol/water (4:1, v/v) for 5 h at room temperature and with continuous agitation. The mixture was then centrifuged for 5 minutes at 6000g and the supernatant was evaporated under vacuum at 40 °C. The residue from the evaporation was treated with 200 mL of water (pH 2 with HCl) and left to rest for 5 min. The resulting mixture was then passed through a glass column (4.6 cm × 15 cm) packed with Amberlite XAD-2 resin (Fluka Chemie; pore size 9 nm, particle size 0.3–1.2 mm). Gallic acid, vanillic acid, coumaric

acid and ferulic acid to name a few and the acids were later tested for antioxidant activity Kchaou *et al.*, 2016).

1.6 CHARACTERISATION OF ANTIMICROBIAL COMPOUNDS

Structural determination of compounds uses information from a vast range of spectroscopic techniques (Zhang *et al.*, 2018). These include infrared (IR) spectroscopy, nuclear magnetic resonance (NMR) spectroscopy, mass spectroscopy (MS) and UV- visible spectroscopy (UV-Vis) (Altermimi *et al.*, 2017). Passing electromagnetic radiation through an organic molecule that absorbs some of the radiation is the basic principle of spectroscopy. Measuring the quantity of absorbed electromagnetic radiation produces a spectrum (Zhang *et al.*, 2018). The spectrum is bond specific and depending on the spectra, the structure of the molecule can be elucidated. For structural clarification, scientists use spectra produced from three or four regions, namely visible, ultraviolet, infrared and electrical beam (DeVijlder *et al.*, 2018).

1.6.1 Nuclear Magnetic Resonance (NMR) spectroscopy

Magnetic properties of selected atomic nuclei are what NMR is based on, namely, the nuclei of the carbon atom, the hydrogen atom, the proton and an isotope carbon (Vioglio *et al.*, 2018). NMR allows researchers to study molecules by noting variances between various magnetic nuclei and giving the positions at which, these differences are found within the nuclei of these molecules (Hansen *et al.*, 2016). In addition, it shows the kinds of atoms found in neighbouring groups. In essence, it is able to conclude on the number and type of atoms present in each of these environments.

1.6.2 Fourier-transform infrared spectroscopy (FTIR)

When infrared light passes through an organic compound, some of the frequencies will be absorbed; however, some are transmitted through the sample without absorption happening. IR absorption is related to the vibrational changes that occur inside a molecule when it is exposed to infrared radiation. Essentially infrared spectroscopy can be described as vibrational spectroscopy. Different bonds (C–O, C–C, N–H, C≡C, C=C, C=O and O–H) have different vibrational frequencies (Jeffrey *et al.*, 2015; Altermimi *et al.*, 2017). The presence of these bonds in a molecule means that its identification is possible by detecting their unique frequency absorption bands in an IR spectrum. Fourier transform infrared spectroscopy (FTIR) is a high-resolution analytical tool to identify the functional groups present in a compound (Karimi and Taherzadeh, 2016). FTIR offers a rapid and non-destructive investigation to fingerprint herbal extracts or powders.

Samples for FTIR can be prepared in a number of ways. For liquid samples, the simplest way is to place one drop of sample between two plates of sodium chloride. The drop forms a thin film between the plates. Solid samples can be milled with potassium bromide (KBr) and then compressed into a thin pellet which can be analysed. Otherwise, solid samples can be dissolved in a solvent such as methylene chloride, and the solution then placed onto a single salt plate. The solvent is then evaporated off, leaving a thin film of the original material on the plate.

1.7 TOXICITY ASSAYS AND *in vivo* EVALUATION

Opoponax essential oil, a chemical component; β -bisabolene and an alcoholic analogue, α -bisabolol, were tested for selectively kill breast cancer cells by Yeo and co-workers in 2016. It was observed that only β -bisabolene, a sesquiterpene constituting 5% of the essential oil, exhibited selective cytotoxic activity for mouse cells (IC₅₀) and human breast cancer cells

(IC50). This loss of viability was because of the induction of apoptosis. β -bisabolene was also effective in reducing the growth of transplanted 4T1 mammary tumours by 37.5% (Yeo *et al.*, 2016).

1.8 *In vitro* EVALUATION OF CITRUS FLAVONOIDS

Meiynanto and co-workers (2012) tested citrus flavonoids for the potential to treat cancer. The flavonoids worked either alone or as combination with chemo-preventive agents. The mechanisms of action involved but were not limited to cell cycle modulation, apoptosis induction and antiangiogenic effects. Naturally occurring compounds were also shown to reduce the incidence of resistance and thus increase the efficacy of chemotherapeutics. Oestrogen plays a crucial role in the development and differentiation of breast and endometrial cells, thus may have certain effects in the growth of cancer. *Citrus reticulata* ethanolic extract was potential to be developed as phytoestrogen as its presence in animal trials shows its ability to mimic oestrogens function of strengthening bones and lowering cholesterol levels (Meiynanto and Anindyajati, 2012).

1.9 RATIONALE FOR THE STUDY

The emergence of diseases and drug resistant pathogens coupled with the side effects presented by conventional or synthetic drugs necessitates the discovery of new antibiotics, agrochemicals and chemotherapeutics. *Kigelia africana* fungal endophytes are not well known and thus they offer untapped potential for drug discovery. In 2014, forty endofungal extracts from the Lab 2 culture collection were previously screened for antimicrobial and antioxidant activity with two, namely, ZF 52 and ZF 91, displaying excellent antibacterial activity (minimum inhibitory concentrations of 25 and 0.1953 $\mu\text{g/mL}$, respectively) against a resistant *P. aeruginosa* strain.

The active anti-*P. aeruginosa* compounds produced by ZF 52 and ZF 91 needed to be purified and more *K. africana* endophytic fungi should be screened for anti-*P. aeruginosa* activity.

1.10 HYPOTHESIS TESTED

It was hypothesized that *K. africana* ZF 52, ZF 91 and other endofungal extracts will display antimicrobial activity against *P. aeruginosa*. It was further hypothesized that the extracts with anti-*P. aeruginosa* activity could be purified and characterised.

1.11 AIMS AND OBJECTIVES

The aim of the study was to perform a phytochemical analysis on the medicinal plant species, and to test *K. africana* ZF 52, ZF 91 and other endofungal extracts for antimicrobial activity against *P. aeruginosa*.

The following objectives were set to test the above hypothesis and achieve the aims of the study:

- To extract biomolecules from endophytic fungal strains, ZF 52, ZF 91 and to screen Lab 2 endophytic fungi culture collections for anti-*P. aeruginosa* activity
- To induce secondary metabolite production in solid substrate fermentation
- To obtain concentrated extracts of secondary metabolites in various solvent systems
- To purify extracts produced by ZF 52, ZF 91 and Lab 2 culture collection using preparative thin layer chromatography, bio-autography and column chromatography
- To characterise the purified anti- *P. aeruginosa* compound

To identify the purified compound by Fourier transform infrared spectroscopy (FTIR) and nuclear magnetic resonance (NMR) spectroscopy.

1.12 REFERENCES

- Abok JI, Manulu C. 2017. TLC analysis and GCMS profiling of hexane extracts of *Syzygium guineense* leaf. *Journal of Medicinal Plants Studies*, 5: 261-265.
- Akanni EO, Olaniran IO, Akinbo BD, Iyiola M, Ogunlade A, Sanni B, Adejumo T. 2017. *Kigelia africana* stem bark, fruit and leaf extracts alleviate benzene-induced leukaemia in rats. *Journal of Pharmaceutical Research International*, 18: 1-10.
- Akunyili DN, Houghton PJ and Raman A. 1991. Antimicrobial activities of the stem bark of *Kigelia pinnata*. *Journal of Ethnopharmacology*, 35: 173-177.
- Allen MF, O'Neill MR, Crisafulli CM, MacMahon JA. 2018. Succession and Mycorrhizae on Mount St. Helens. In: Crisafulli C., Dale V. (eds) *Ecological Responses at Mount St. Helens: Revisited 35 years after the 1980 Eruption*. Springer, New York, NY
- Ali A. 2014. *Cassia fistula* Linn: A review of phytochemicals and pharmacological studies. *International Journal of Pharmaceutical Sciences and Research*, 5: 2125-2130.
- Altemimi A, Lakhssassi N, Baharlouei A, Watson DG, Lightfoot DA. 2017. Phytochemicals: Extraction, isolation, and identification of bioactive compounds from plant extracts. *Plants*, 6: 42-65.
- Alvin A, Miller KI, Neilan BA. 2014. Exploring the potential of endophytes from medicinal plants as source of anti-mycobacterial compounds. *Microbiology Research*, 169: 483-495.
- Aravind G, Bhowmik D, Duraivel S, Harish G. 2013. Traditional and medicinal uses of *Carica papaya*. *Journal of Medicinal Plants Studies*, 1: 7-15.
- Arnold AE, Lutzoni F. 2007. Diversity and host range of foliar fungal endophytes: are tropical leaves biodiversity hotspots? *Ecology*, 88: 541-549.
- Atawodi SE, Olowoniyi OD, Adejo GO, Liman ML. 2017. Phytochemical, pharmacological and therapeutic potentials of some wild Nigerian medicinal trees. *Medicinal and Aromatic Plants of the World – Africa*, 3: 283-309.
- Azu OO. 2013. The sausage tree (*Kigelia africana*): Have we finally discovered a male sperm booster? *Journal of Medical Plant Research*, 7: 903-910.
- Azu OO, Duru FIO, Osinubi AA, Noronha CC, Elehsa SO, Okanlawon AO. 2010. Protective agent *Kigelia africana* fruit extract, against cisplatin induced kidney oxidant injury in Spurge-Dawley rats. *Asian Journal of Pharmaceutical and Clinical Research*, 3: 84-88.

- Bacon CW, Porter JK, Robbins JD, Luttrell ES. 1977. *Epichloe typhina* from toxic tall fescue grasses. *Applied and Environmental Microbiology*, 324: 576-581.
- Bardoel BW, van der Ent S, Pel MJ, Tommassen J, Pieterse CM, van Kessel KP, van Strijp JA. 2011. *Pseudomonas* evades immune recognition of flagellin in both mammals and plants. *PLoS Pathogens*, 7: e1002206.
- Hirsch EB, Tam VH. 2010. Impact of multidrug-resistant *Pseudomonas aeruginosa* infection on patient outcomes. *Expert Review of Pharmacoeconomics and Outcomes Research*, 10: 441-451.
- Chagas FO, de Cassia Pessotti R, Caraballo-Rodríguez AM, Pupo MT. 2018. Chemical signalling involved in plant–microbe interactions. *Chemical Society Reviews*, 47: 1652-1704.
- Capone DL, Ristic R, Pardon KH, Jeffery DW. 2015. Simple quantitative Determination of potent thiols at ultratrace levels in wine by derivatization and high-performance liquid chromatography–tandem mass spectrometry (HPLC-MS/MS) analysis. *Analytical Chemistry*, 287: 1226-1231.
- Clay K. 2014. Defensive symbiosis: a microbial perspective. *Functional Ecology*, 28: 293-298.
- Claydon N, Grove JF, Pople M. 1985. Elm bark-beetle boring and feeding deterrents from *Phomopsis oblonga*. *Phytochemistry*, 24: 937-943.
- Cosme M, Fernandez I, van der Hiejden MGA, Pietse CMJ. 2018. Non-mycorrhizal plants: The exceptions that prove the rule. *Trends in Plant Science*, 23(7): 577-587.
- Czaplicki S. 2013. Column chromatography, chapter: Chromatography in Bioactivity. *Analysis of Compounds*, 99-122.
- Darsih C, Prachyawarakorn V, Mahidol C, Ruchirawat S, Kittakoop P. 2017. A new polyketide from the endophytic fungus *Penicillium chermesinum*. *Indonesian Journal of Chemistry*, 17: 360-364.
- Das A, Rahman MI, Ferdous AS, Amin A, Rahman MM, Nahar N, Uddin MA, Islam MR, Khan H. 2017. An endophytic Basidiomycete, *Grammothele lineata*, isolated from *Corchorus olitorius*, produces paclitaxel that shows cytotoxicity. *PLoS ONE*, 12: e0178612.
- Das K, Tiwari RKS, Shrivastava DK. 2010. Techniques for evaluation of medicinal plant products as antimicrobial agents: current methods and future trends. *Journal of Medicinal Plants Research* 4: 104-111.

- Dewanjee S, Gangopadhyay M, Bhattacharya N, Khanra R, Dua TK. 2015. Bioautography and its scope in the field of natural product chemistry. *Journal of Pharmaceutical Analysis*, 5: 75-84.
- Ding Y, Zhou Y, Yao J, Szymanski C, Fredrickson J, Shi L, Cao B, Zhu Z, Yu X. 2016. In situ molecular imaging of the biofilm and its matrix. *Analytical Chemistry*, 88: 11244-11252.
- Epps LC, Walker PD. 2006. Fluoroquinolone consumption and emerging resistance. *US Pharmacology*, 10: 47–54.
- Flemming HC, Wingender J. 2010. The biofilm matrix. *Nature Reviews Microbiology*, 8: 623–633.
- Gabriel OA, Olubunmi A. 2009. Comprehensive scientific demystification of *Kigelia africana*: A review. *African Journal of Pure and Applied Chemistry*, 3: 158-164.
- Gellatly SL, Hancock REW. 2013. *Pseudomonas aeruginosa*: new insights into pathogenesis and host defences. *Pathogens and Disease*, 67: 159–173.
- Ghaleb A, Mhanna M. 2008. Synergistic effects of plant extracts and antibiotics on *Staphylococcus aureus* strains isolated from clinical specimens. *Middle East Journal of Scientific Research*, 3: 134-139.
- Gomes F, Leite B, Teixeira P, Azeredo J, Oliveira R. 2012. Farnesol in combination with N-acetylcysteine against *Staphylococcus epidermidis* planktonic and biofilm cells. *Brazilian Journal of Microbiology*, 235-242.
- Govindchari TR, Patankar SJ, Visanathan N. 1971. Isolation and structure of 2 new dihydroisocoumarins from *Kigelia pinnata*. *Phytochemistry*, 10: 1603-1606.
- Grace OM, Light ME, Lindsey KL, Mulholland DA, van Staden J, Jaker AK. 2002. Antibacterial activity and isolation of active compounds from fruits of the traditional African medicinal tree *Kigelia africana*. *South African Journal of Botany*, 68: 220-222.
- Gupta S, Maclean M, Anderson JG, MacGregor SJ, Meek RM, Grant MH. 2015. Inactivation of microorganisms isolated from infected lower limb arthroplasties using high-intensity narrow-spectrum (HINS) light. *The Bone and Joint Journal*, 97: 283-288.
- Hancock REW, Speert DP. 2000. Antibiotic resistance in *Pseudomonas aeruginosa*: mechanisms and impact on treatment. *Drug resistance updates*, 3: 247-255.
- Hansen MR, Graf R, Spiess HW. 2016. Interplay of structure and dynamics in functional macromolecular and supramolecular systems as revealed by Magnetic Resonance Spectroscopy. *Chemical Reviews*, 116: 1272-1308.

- Harper L, Powell J, Pijl EM. 2017. An overview of forensic drug testing methods and their suitability for harm reduction point-of-care services. *Harm Reduction Journal*, 14: 52-65.
- Hassan R. 2012. Medicinal Plants (Importance and Uses). *Pharmaceutica Analytica Acta*, 3: 10.
- Hauser AR. 2009. The type 3 secretion system of *Pseudomonas aeruginosa*: infection by injection. *Nature Reviews Microbiology*, 7: 654–665.
- Hayes R, Ahmed A, Edge T, Zhang H. 2014. Core-shell particles: Preparation, fundamentals and applications in high performance liquid chromatography. *Journal of Chromatography A*, 1357: 36-52.
- Hill D, Rose B, Pajkos A, Robinson M, Bye P, Bell S, Elkins M, Thompson B, Macleod C, Aaron SD, Harbour C. 2005. Antibiotic susceptibilities of *Pseudomonas aeruginosa* isolates derived from patients with cystic fibrosis under aerobic, anaerobic, and biofilm conditions. *Journal of Clinical Microbiology*, 43: 5085–5090.
- Hirsch EB, Tam VH. 2010. Impact of multidrug-resistant *Pseudomonas aeruginosa* infection on patient outcomes. *Expert Review of Pharmacoeconomics and Outcomes Research*, 10: 441-451.
- Huang WY, Cai YZ, Surveswaran S, Hyde KD, Corke H, Sun M. 2008. Molecular phylogenetic identification of endophytic fungi isolated from tree *Artemisia* species. *Fungal Diversity*, 36: 69-88.
- Huang Y, Wang J, Li G, Zheng Z, Su W. 2001. Anti-tumour and antifungal activities in endophytic fungi isolated from pharmaceutical plants. *FEMS Immunology and Medical Microbiology*, 31: 163-167.
- Idris A, Al-tahir I, Idris E. 2013. Antibacterial activity of endophytic fungi extracts from the medicinal plant *Kigelia africana*. *Egyptian Academic Journal of Biological Sciences*, 5: 1-9.
- Jalgaonwala RE, Mohite BV, Mahajan RT. 2011. A review: Natural products from plant associated endophytic fungi. *Journal of Microbiology and Biotechnology Research*, 1: 21-32.
- Jeffrey JL, Terrett JA, MacMillan DD. 2015. O–H hydrogen bonding promotes H-atom transfer from α C–H bonds for C-alkylation of alcohols. *Science*, 349: 1532-1536.
- Kadhim MJ, Mohammed GJ, Hameed IH. 2016. *In-vitro* antibacterial, antifungal and phytochemical analysis of methanolic extract of fruit *Cassia fistula*. *Oriental Journal of Chemistry*, 32: 1329-1346.

- Karimi K, Taherzadeh MJ. 2016. A critical review of analytical methods in pre-treatment of lignocelluloses: Composition, imaging and crystallinity. *Bioresource Technology*, 200: 1000-1018.
- Kchaou W, Abbes F, Mansour RB, Blecker C, Attia H, Besbes S. 2016. Phenolic profile, antibacterial and cytotoxic properties of second grade dates extract from Tunisian cultivars (*Pheonix dactylifera* L.). *Food Chemistry*, 194: 1048-1055.
- Kirk PM, Cannon PF, David JC, Staplers JA. 2001. Ainsworth and Bisby dictionary of the fungi. CAB International, Oxon, UK.
- Kraft R, Herndon DN, Mlcak RP, Finnerty CC, Cox RA, Williams FN, Jeschke MG. 2014. Bacterial respiratory tract infections are promoted by systemic hyperglycemia after severe burn injury in pediatric patients. *Burns*, 40: 428-435.
- Kumar A, Patil D, Rajamohanam PR, Ahmad A. 2013. Isolation, purification and characterization of vinblastine and vincristine from endophytic fungus *Fusarium oxysporum* isolated from *Catharanthus roseus*. *PLoS ONE*, 8: 1-10.
- Kumar S, Jyotirmayee K, Sarangi M. 2013. Thin layer chromatography: A tool of biotechnology for isolation of bioactive compounds from medicinal plants. *International Journal of Pharmaceutical Sciences Reviews and Research*, 18: 126-132.
- Kusari S, Pandley SP, Spiteller M. 2013. Untapped mutualistic paradigms linking host plant and endophytic fungal production of similar bioactive metabolites. *Phytochemistry*, 91: 81-87.
- Kusari S, Verma VC, Lamshoeft M, Spiteller M. 2012. An endophytic fungus from *Azadirachta indica* A. Juss. that produces azadirachtin. *World Journal of Microbiology and Biotechnology*, 28: 1287-1294.
- Kwo VT, Craker LE. 1996. Screening Cameroon medicinal plant extracts for antimicrobial activity. *Acta Horticulture*, 426: 147-155.
- Lahn L, Schafhauser T, Wibberg D, Rückert C, Winkler A, Kulik A, Weber T, Flor L, Karl-Heinz van Pée, Kalinowski J, Ludwig-Müller J, Wohlleben W. 2017. Linking secondary metabolites to biosynthesis genes in the fungal endophyte *Cyanoderma asteris*: The anti-cancer bisanthraquinone skyrin. *Journal of Biotechnology*, 257, 233–239.
- Lakshmi Naga Nandini M, Rajesh Naik SM, Ruth CH, Gopal K. 2018. Biodiversity and antimicrobial activity of endophytes. *International Journal of Pure Applied Bioscience*, 6(5): 1176-1190.

- Lutz JK, Lee J. 2011. Prevalence and antimicrobial-resistance of *Pseudomonas aeruginosa* in swimming pools and hot tubs. *International Journal of Environmental Research and Public Health*, 8: 554-564.
- Mahmoudvand H, Ezzatkhah F, Sharififar F, Sharifi I, Dezaki ES. 2015. Antileishmanial and cytotoxic effects of essential oil and methanolic extract of *Myrtus communis* L. *The Korean Journal of Parasitology*, 531 :21-27.
- Mansouri A, Embarek G, Kokalou E, Kefalas P. 2005. Phenolic profile and antioxidant activity of the Algerian ripe date palm fruit (*Phoenix dactylifera*). *Food Chemistry*, 89: 411-420.
- Manvitha K, Bidya B. 2014. Aloe Vera: a wonder plant, its history, cultivation and medicinal uses. *Journal of Pharmacognosy and Phytochemistry*, 2: 85-88.
- Mena A, Smith EE, Burns JL, Speert DP, Moskowitz SM, Perez JL and Oliver A. 2008. Genetic adaptation of *Pseudomonas aeruginosa* to the airways of cystic fibrosis patients is catalysed by hypermutation. *Journal of Bacteriology*, 190: 7910–7917.
- Meiyanto E; Hermawan Adam, Anindyajati A. 2012. Natural Products for cancer-targeted therapy: Citrus flavonoids as potent chemopreventive agents. *Asian Pacific Journal of Cancer Prevention*, 13: 427-436.
- Miller KI, Qing C, Sze YDM, Neilan BA. 2012. Investigation of the biosynthetic potential of endophytes in Traditional Chinese anticancer herbs. *PLOS ONE*.
- Minstanely C, O'Brien S, Brockhurst MA. 2016. *Pseudomonas aeruginosa* evolutionary adaptation and diversification in cystic fibrosis chronic lung infections. *Trends in Microbiology*, 24: 327-337.
- Mishra N, Behal KK. 2010. Antimicrobial activity of some spices against selected microbes. *International Journal of Pharmaceutical Sciences*, 2: 187-196.
- Moretti E. 2004. "Workers' education, spill overs, and productivity: Evidence from plant-level production functions." *American Economic Review*, 94: 656-690.
- Moussaoui F, Alaoui T. 2016. Evaluation of antibacterial activity and synergistic effect between antibiotic and the essential oils of some medicinal plants. *Asian Pacific Journal of Tropical Biomedicine*, 6: 132-37.
- Nathwani D, Morgan M, Masterton RG, Dryden M, Cooksen BD, French G. 2008. Guidelines for UK practice for the diagnosis and management of methicillin-resistant *Staphylococcus aureus* (MRSA) infections presenting in the community. *Journal of Antimicrobial Chemotherapy*, 61: 976-994.

- Newman DJ, Cragg GM. 2012. Natural products as sources of new drugs over the 30 years from 1981 to 2010. *Journal of Natural Products*, 75: 311-335.
- Nielsen JC, Nielsen J. 2017. Development of fungal cell factories for the production of secondary metabolites: Linking genomics and metabolism. *Synthetic and Systems Biotechnology*, 2: 5-12.
- Nikolaev IA, Plakunov VK. 2007. Biofilm: “City of microbes” or an analogue of multicellular organisms? *Mikrobiologiya*, 76: 149-163.
- Otter JA, Yezli S, French GL. 2011. The role played by contaminated surfaces in the transmission of nosocomial pathogens. *Infection Control and Hospital Epidemiology*, 32: 687-699.
- Oyebode O, Kandala NB, Chilton PJ, Lilford RJ. 2016. Use of traditional medicine in middle-income countries: a WHO-SAGE study. *Health Policy and Planning*, 31: 984-991.
- Oyediji FO, Bankole-Oje OS. 2012. Quantitative evaluation of the antipsoriatic activity of sausage tree (*Kigelia africana*). *Journal of Pure and Applied Chemistry*, 6: 214-218.
- Klimek-Turek, A, Sikora M, Rybicki M, Dzido TH. 2016. Frontally eluted components procedure with thin layer chromatography as a mode of sample preparation for high performance liquid chromatography quantitation of acetaminophen in biological matrix. *Journal of Chromatography A*, 1436: 19-27.
- Rasamiravaka T, Labtani Q, Duez P, El Jaziri M. 2015. The formation of biofilms by *Pseudomonas aeruginosa*: A review of the natural and synthetic compounds interfering with control mechanisms. *BioMed Research International*, 759348: 1-17.
- Rosa H, Vaz ABM, Caligorne RB, Campolina S, Rose CA. 2009. Endophytic fungi associated with the Antarctic grass *Deschampsia antarctica*. *Polar Biology*, 32: 161-167.
- Sadrati N, Daoud N, Zerroug A, Dahamna S, Bouharati S. 2013. Screening of antimicrobial and antioxidant secondary metabolites from endophytic fungi isolated from wheat (*Triticum durum*). *Journal of Plant Protection Research*, 53: 128-136.
- Saini S, Kaur H, Verma B, Singh R, Singh SK. 2009. *Kigelia africana* - An overview. *Natural Product Radiance*, 8: 190-197.
- Samrot AV, Sahiti K, Raji P, Rohan B, Kumar D, Sharma K. 2016. TLC Bio-autography guided identification of antioxidant and antibacterial activity of *Acacia Senegal*. *Der Pharmacia Lettre*, 8:41-47.
- Santiago M, Strobel S. 2013. Chapter twenty-four - thin layer chromatography. *Methods in Enzymology*, 533: 303-324.

- Sasidharan S, Chen Y, Saravanan D, Sundram KM, Latha LY. 2011. Extraction, isolation and characterisation of bioactive compounds from plants' extracts. *African Journal of Complementary and Alternative Medicine*, 8: 1-10.
- Schaible B, Taylor CT, Schaffer K. 2012. Hypoxia increases antibiotic resistance in *Pseudomonas aeruginosa* through altering the composition of multidrug efflux pumps. *Antimicrobial Agents Chemotherapy*, 56: 2114-2118.
- Sherma J. 2008. Planar chromatography. *Analytical Chemistry*, 80:4253–4267.
- Sherrard LJ, Tunney TM, Elborn JS. 2014. Antimicrobial resistance in the respiratory microbiota of people with cystic fibrosis. *Lancet*, 384: 703-13.
- Silva IN, Pessoa FD, Ramirez MJ, Santos MR, Becker JD, Cooper VS, Moreira LM.
- Soković M, Glamočlija J, Marin PD, Brkić D, Griensven LJ. 2010. Antibacterial effects of the essential oils of commonly consumed medicinal herbs using an *in-vitro* model. *Molecules*, 15: 7532-7546.
- Stefanovic O, Comic L. 2012. Synergistic antibacterial interaction between *Melissa officinalis* extracts and antibiotics. *Journal of Applied Pharmaceutical Science*, 2: 1-5.
- Stewart PJ, Costerton JW. 2001. Antibiotic resistance of bacteria in biofilms. *Lancet*, 358: 135–138.
- Stierle A, Strobel GA, Stierle D. 1993. Taxol and taxane production by *Taxomyces andreanae*, an endophytic fungus of Pacific yew. *Science*, 260: 214-216.
- Strobel G, Daisy B. 2003. Bioprospecting for microbial endophytes and their natural products. *Microbiology and Molecular Biology Reviews*, 67: 491-502.
- Suryanarayanan TS. 2017. Fungal endophytes: An eclectic review. *KAVAKA*, 4: 1-9.
- Swapna G, Jyothirmai T, Lavanya V, Swapnakumari S, Sri Lakshmi Prasanna A. 2015. Extraction, and characterization of bioactive compounds from plant extracts a review. *European Journal of Pharmaceutical Science and Research*, 2 :1-6.
- Vioglio PC, Chierotti MR, Gobetto R. 2016. Solid-state nuclear magnetic resonance as a tool for investigating the halogen bond. *CrystEngComm*, 18: 9173-9184.
- Wang X, Liu R, Yang Y, Zhang M. 2015. Isolation, purification and identification of antioxidants in an aqueous aged garlic extract. *Food Chemistry*, 187: 37-43.
- Webber J. 1981. A natural control of Dutch elm disease. *Nature*, 292: 449-451.
- Williams BJ, Dehnbostel J, Blackwell TS. 2010. *Pseudomonas aeruginosa*: host defence in lung diseases. *Respirology*, 15: 1037–1056.

- Wright H, Bonomo RA, Paterson DL. 2017. New agents for the treatment of infections with Gram- negative bacteria: restoring the miracle or false dawn? *Clinical Microbiology and Infection*, 23: 704-712.
- Yahr TL, Wolfgang MC. 2006. Transcriptional regulation of the *Pseudomonas aeruginosa* type III secretion system. *Molecular Biology*, 62: 631-640.
- Zankari EA, Allesøe R, Joensen KG, Cavaco LM, Lund O, Aarestrup FM. 2017. Point Finder: a novel web tool for WGS-based detection of antimicrobial resistance associated with chromosomal point mutations in bacterial pathogens. *Journal Antimicrobial Chemotherapy* 72: 2764-2768.
- Zhang QW, Lin LG, Ye WC. 2018. Techniques for extraction and isolation of natural products: a comprehensive review. *Chinese Medicine*, 13 (20): 1-26.

CHAPTER 2: SCREENING EXTRACTS FOR ANTI- *P. aeruginosa* ACTIVITY

2.1 INTRODUCTION

The rise of microbial resistance to antibiotics and the scarcity of new drugs has long been the subject of discussion (Theuretzbacher and Mouton, 2011). The lack of new drug development, misuse and overuse has been attributed to the antibiotic resistance crisis (Ventola, 2015). Alexander Fleming stated in 1945 that the drug penicillin would be in great demand which would lead to an era of antibiotic abuse (Ventola, 2015). The emergence of resistance is driven by three main mechanisms, namely: the rapid increase of antibiotic resistant bacteria due to overexposure to antimicrobial compounds or other contaminants (heavy metals and biocides), horizontal gene transfer of antibiotic resistance genes and recombination and genetic mutation (Berendock *et al.*, 2015). Acquiring effective, affordable and novel drugs to treat microbial infections is a global healthcare challenge but mainly in third world countries where more than half of the deaths are due to infectious diseases (Awouafack *et al.*, 2012; Srivastava *et al.*, 2013; Elisha *et al.*, 2017).

It is estimated that 80% of the world's population relies on herb-based medicine. Except for homeopathy, the healing properties of these plants are evaluated by their chemical composition (Ventola, 2015). Many plants are used in medicine with Indian Ayurveda and the Chinese system using roughly 2000 and 5757 plants, respectively (Ventola, 2015). Similar to Asia, Africa is known for its ancient traditional practices and vast number of traditional healers. Due to this, scientists have focused their attention on these plants that have the capacity to heal. Plants have the ability to produce a variety of secondary metabolites, for example, tannins, alkaloids, flavonoids, glycosides, terpenoids, steroids, quinones, coumarins and saponins (Das *et al.*, 2010), which have been the source of antimicrobial substances (Fernebrot, 2011; Elisha *et al.*, 2017).

In the Southern African tropical regions, a commonly encountered medicinal plant is *K. africana*. All parts of this plant have been used in traditional medicine; the fruit is used to treat ulcers, syphilis, abscesses, wounds and rheumatism (Bello *et al.*, 2016). The bark and roots are used to treat pneumonia. In West Africa, the fruit is used to treat haemorrhoids, dysentery and gynaecological disorders. The traditional medicinal uses of *K. africana* point to the plants potential as a source of antibacterial compounds. However, there is no scientific research to validate its ethnomedicinal use. There have been studies which examined the plant chemistry, but these were not been linked with bioactivity studies (Das *et al.*, 2010; Arkhipov *et al.*, 2014; Cook and van Vuuren, 2014). Some studies using the bark extracts showed cytotoxicity and good results in treating renal carcinoma and melanoma (Saini *et al.*, 2009; Arkhipov *et al.*, 2014). Different parts of this plant showed growth inhibition against *Klebsiella pneumonia*, *Proteus vulgaris*, *S. aureus*, *Escherichia coli* and *P. aeruginosa* (Hussain *et al.*, 2016).

In recent years, focus has shifted to conservation of medicinal plants which has led to the search for alternative sources of secondary metabolites (Kusari *et al.*, 2013). Studies on plant microbiomes indicated that the plant along with its associated microbiome produces bioactive molecules. Investigations of the same plant species located in different geographical regions showed that they produced different bioactive metabolites, which suggested that the endophytic microorganisms produce the bioactive metabolites and not the plants (Idris *et al.*, 2013; Kusari *et al.*, 2013). Endophytes are bacteria, actinomycetes and fungi that inhabit healthy plants without causing them any harm (Das *et al.*, 2017).

Pseudomonas aeruginosa is the leading cause of infection in hospitalised patients. It is resistant to many antimicrobial agents due to its various resistance mechanisms (Joo *et al.*, 2011; Nyasulu *et al.*, 2012; Holmes *et al.*, 2016). The ability of the organism to develop additional resistance during treatment further limits treatment (Hancock and Speert, 2000;

Mudau *et al.*, 2013). Risk factors for *P. aeruginosa* infections include presence of previous antibiotic use, admission to an intensive care unit, indwelling devices, prolonged hospital stay, pre-existing diseases and an immuno-compromised status (Harris *et al.*, 2002; Joo *et al.*, 2011; Mudau *et al.*, 2013).

A study conducted by Nyasulu *et al.* (2017) followed the trend of increased *P. aeruginosa* resistance in South African hospitals between 2005 to 2009 and observed a moderate rise in resistance for aminoglycosides (gentamicin 21.7% to 53.7%, tobramycin 38.7% to 60.2% and 25.7% to 39.1% for amikacin), carbapenems (a rise from 45% to 55% for meropenem and imipenem), cephalosporins (cefepime 36.6% to 43.6% and 17.1% to 24.6% for ceftazidime) and ciprofloxacin (25.9% to 53.7%) (Nyasulu *et al.*, 2017). The increasing resistance of *P. aeruginosa* to most classes of antibiotics warrants the screening of previously untapped sources for anti-*P. aeruginosa* activity.

2.2 MATERIALS AND METHODS

2.2.1 Growth and maintenance of cultures

Endophytic fungal isolates (previously isolated from leaves of *K. africana*) were obtained from the Lab 2 culture collection and sub cultured onto potato dextrose agar (PDA). The isolates were grown for four days at room temperature (RT), stored at 4°C and used as working stocks (Strobel and Daisy, 2003). *Pseudomonas aeruginosa* ATCC 27853 was sub-cultured from stock culture (Dr Chenia, Microbiology Department in UKZN) and grown on Nutrient agar (NA) at 37°C for 24 h. Long-term endofungal stocks were prepared by inoculating spores from aged plates into 1.5 mL Eppendorf tubes containing 1 mL of 40% glycerol. Bacterial stocks were prepared by growing a loopful of a 24 h plate culture of *P. aeruginosa* into 3 mL nutrient

broth and transferring 0.5 mL of broth culture and 0.5 mL of 40% glycerol into a 1.5 mL Eppendorf tube. Both fungal and bacterial stocks were kept at -80°C.

2.2.2 Production of biomolecules

To induce production of biomolecules, standardised inocula (8 mm blue pipette tip back) from PDA plates were inoculated into rice medium (10 g of rice supplemented with 20 mL peptone water (0.5% peptone and 0.3% sodium chloride)). Solid substrate fermentation (SSF) was performed at room temperature for 30 days (Talonsi *et al.*, 2012). In addition, to determine optimum time of bioactive molecule production, aliquots of biomass were extracted weekly, for four weeks.

2.2.3 Extraction of bioactive molecules

Bioactive biomolecules were extracted from mycelial mats using ethyl acetate (EtOAc) (Prabavathy and Nachiyar, 2014). To halt the fermentation process, 10 g of the rice medium containing the biomass was soaked in 50 mL of EtOAc for 24 h under gentle agitation (100 rpm, RT). The biomass and the EtOAc extract were separated by vacuum filtration through Whatman No.1 filter paper. The EtOAc extract containing bioactive compounds was washed with 50 mL demineralized water to remove traces of starch. The organic layers were collected and evaporated using a rotary evaporator. The extract was weighed and resuspended in EtOAc to a final concentration of 10 mg/mL and stored in the refrigerator at 4°C until required.

2.2.4 Assessing anti-*P. aeruginosa* activity

2.2.4.1 Disc diffusion assay

The test strain used was a multidrug resistant *P. aeruginosa* ATCC 27853, which is resistant to β -lactams, aminoglycosides and fluoroquinolones. The test bacteria were inoculated onto nutrient agar (NA) plates and incubated for 24 h at 37°C. For a standardised inoculum for the disc diffusion assay, culture was inoculated in 500 μ L of demineralised water and the cell density was standardised to 0.5 McFarland standard using a spectrophotometer (UV 1800). The standardised bacterial cells were spread onto Mueller-Hinton (Merck, Germany) plates using sterile cotton swabs and left to dry. Extracts (100 μ L) were saturated on sterile filter paper discs and used as antibiotic discs. The plates were incubated at 37°C for 24 h and the resultant zones of inhibition were measured and scored according to Table 2.1. The experiment was done in triplicate.

Table 2.1: Scoring of activity of extracts (mm) (Chenia, 2013)

0-6	7-9	10-15	16-17	≥ 18
No activity	No significant activity	Poor activity	Good activity	Significant activity

2.2.4.2 Minimum inhibitory concentration (MIC) determination

The broth dilution microtitre assay was carried out as described by Kwon *et al.* (2007) to determine the minimum inhibitory concentration (MIC). The lowest dilution or concentration which inhibits growth is the MIC (Kwon *et al.*, 2007; Zin *et al.*, 2007). The standardised test culture inoculum was prepared as described in 2.2.4.1. The bacterial cells were harvested and

standardised to 0.5 McFarland standard in sterile distilled H₂O. A 1:140 dilution of cells was made in Muller Hinton (MH) broth (71 µL of standardised cells and 9.929 mL of MH broth).

Microtitre plates were loaded with the different components as follows: 100 µL of MH broth was added into all the wells, an aliquot of 100 µL of extract was added into well one, mixed and 100 µL was transferred to well two, and so on until well nine. The final 100 µL from well nine was discarded. After addition of extracts, 100 µL of the 1:140 diluted cells were added to all the wells. Plates were incubated at 37°C for 24 h. Thereafter 30 µL resazurin dye was added and further incubated at 37°C for 4 h. Results were read as follows: live cells were pink and dead cells were blue. The highest dilution displaying the blue colour was regarded as the MIC.

2.2.5 Thin layer chromatography

Crude extract (1 µL) was spotted onto thin layer chromatography (TLC) plates (Merck silica gel 60, 20 x 20 cm F254 aluminium sheets: Merck, Germany) and left to develop in various solvent systems (Yu *et al.*, 2010). A solvent system of chloroform (CHCl₃):methanol (MeOH) and hexane:EtOAc (using 100% CHCl₃ or hexane that was increased stepwise by 10% to 100% MeOH or EtOAc, respectively) was screened to assess their separation efficiency (Selvameenal *et al.*, 2009). The TLC plates were spotted with the sample using capillary tubes, the plates were placed in the solvent mixture in a developing tank and left to run till the solvent front reached approximately half a centimetre from the top of the plate. TLC plates were viewed under an ultraviolet lamp (254 nm) and developed using 10% H₂SO₄ in MeOH (Selvameenal *et al.*, 2009).

2.2.6 Bio-autography

Agar overlay bio-autography was performed by pouring 10 mL of molten agar seeded with 1 mL of *P. aeruginosa* bacterial suspension (0.5 McFarland standard) over the developed

chromatogram and incubating at 37°C for 24 h. After incubation, all plates were sprayed with a 2% (w/v) 2,3,5–triphenyltetrazolium salt stain which stains live cells red (Dewajee *et al.*, 2015). Clear zones were taken to represent inhibition of growth by anti-*P. aeruginosa* compounds.

2.2.7 Identification of fungal isolates that produce active compounds of interest

2.2.7.1. Genomic deoxyribonucleic acid isolation

Genomic deoxyribonucleic acid (DNA) isolation was conducted using the ZR Soil Microbe DNA MiniprepTM (Zymo Research, USA) according to the manufacturer's instructions. After extraction, the DNA was analysed by agarose gel electrophoresis. DNA samples were stored at -20°C.

2.2.7.2 Amplification of internal transcribed spacer two region

The universal primers for the fungal internal transcribed spacer two (ITS2) region of the 18S ribonucleic acid (rRNA) gene were used in the PCR reaction (White *et al.*, 1990; Ristaino *et al.*, 1998). The ITS primer pair sequences were as follows:

Forward: ITS 5 (5' – GGAAGTAAAAGTCGTAACAAGG – 3')

Reverse: ITS 4 (5' – TCCTCCGCTTATTGATATGC – 3')

The PCR reaction mixture (50 µL) consisted of template DNA, 2.5 µM of each of the forward and reverse primers, 25 mM MgCl₂, 10 mM dNTPs, *Taq* DNA polymerase, 10 mM buffer (Thermo Scientific). The reaction mixture was brought to 50 µL using double distilled water. Amplification of the reaction mixture was conducted under the following thermal cycling conditions: initial denaturation at 94°C for 5 min, 30 cycles of denaturation at 94°C for 30 s, annealing at 55°C for 30 s and extension at 72°C for 30 s (Anderson *et al.*, 2003).

2.2.7.3. Sequencing of ITS2 region

The PCR products were visualised using electrophoretic analysis on a 1% agarose gel stained with ethidium bromide. After confirmation that the amplification was successful, amplicons were sequenced using Sanger sequencing at Stellenbosch University, South Africa. The identity of the isolates was determined using the basic local alignment search tool (BLAST) analysis, using the NCBI database (Anderson *et al.*, 2003).

2.3 RESULTS

2.3.1 Growth and maintenance of cultures

Potato dextrose agar plates were used to successfully resuscitate thirty-three endophytic fungi as the grown fungi matched the original isolates in terms of varying characteristics and pigmentation. The pigmentation of the mycelia intensified with age from lightly pigmented as the mycelia grew into fresh media (Fig 2.1). This was observed for all fungi growing on PDA.

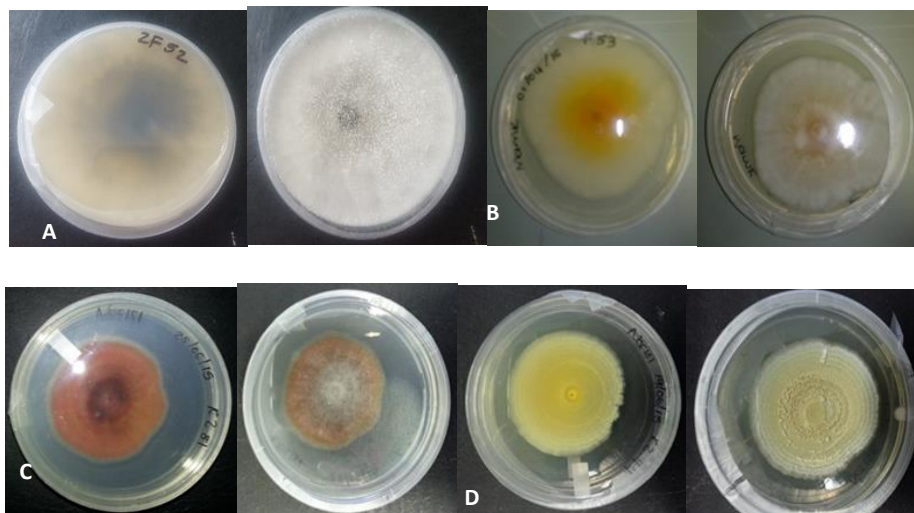


Figure 2.1: Growth of endophytic fungi on potato dextrose agar media for 4 days. A and B: show ZF 52 and ZF 53 fungal isolates (top and bottom); C and D: show KZ 81 and ZF KZ 44.

2.3.2 Production of biomolecules

The solid substrate fermentation reaction contents showed varying pigmentation where initial growth was observed on day four of the 30-day period for fast growing fungi and as delayed as day 15 for slow growing fungi. The presence of white fluffy growths on the surface of the solid substrate was common in all the fermentation vessels. Pigmentation developed with time as observed in Figure 2.2. A characteristic of most of the fermenting biomass was that it matched the pigment observed on PDA plates, with one exception namely ZF 52, which was black and yellow on PDA and black in SSF.

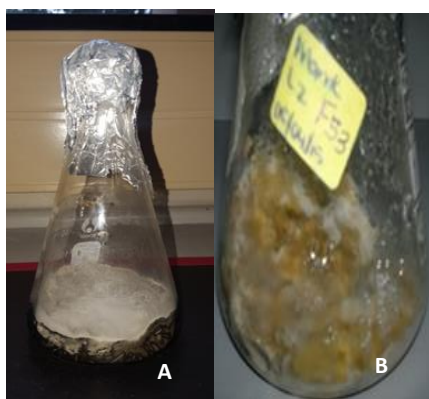


Figure 2.2: Development of mycelial mat growth during the SSF. A: ZF 52, B: ZF 53.

2.3.3 Extraction of bioactive molecules

An assortment of pigments was observed after solvent extraction. The pigmentation of the extracts mostly matched the pigments of the biomass on the PDA plates and SSF reaction vessels, with the exception of ZF 52 whose extract matched only the growth on PDA and not during SSF (Fig 2.3).



Figure 2. 3: Endophytic fungi extracts obtained following solvent extraction.

2.3.4 Assessing anti-*P. aeruginosa* activity

2.3.4.1 Disc diffusion assay

Variable results were obtained using the disc diffusion assay for the 45 extracts. Most extracts did not inhibit *P. aeruginosa*, while a few (three) had significant activity (Figure 2.4 A and B). The size of the zones of inhibition depicted good activity of the extracts. ZF 52 displayed the largest zone of inhibition (40 mm) for T4. Zones of inhibition obtained differed from extract to extract and these ranged from 0-40 mm. ZF 52, ZF 91 and ZF 34 had very good activity, however, due to difficulties encountered in resuscitating long-term cultures from storage, ZF 91 and ZF 34 were not tested further resulting in ZF 52 being the only fungal extract tested further. A time course was conducted in order to observe the difference in activity from week one to week four. The bioactive compounds are produced as early as week as seen in Fig 2.4 C.

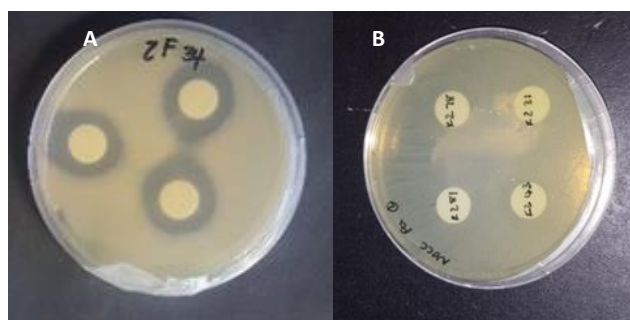


Figure 2.4: Kirby Bauer disc diffusion assay demonstrating anti-*P. aeruginosa* activity of ethyl acetate extracts of endophytic fungi; A: ZF 34 and B: KZ 81, KZ 43, KZ 31 and KZ 78.

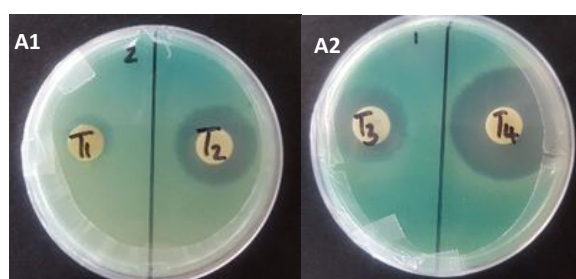


Figure 2.5: Kirby Bauer disc diffusion assay demonstrating anti-*P. aeruginosa* activity of ZF 52 extracts after varying fermentation periods. A1 indicates ZF 52 extract produced after one (T1) and two (T2) weeks and A2 indicates ZF 52 extracts produced after three (T3) and four (T4) weeks.

2.3.4.2 MIC determination

Minimum inhibitory concentrations were determined for those extracts with large inhibition zones, namely, the ZF 52 extracts produced after varying periods of solid substrate fermentation (T1 to T4) (Figure 2.6). All rows A, B, C and D show very strong activity. Extract T4 displayed the strongest activity (lowest MIC) against *P. aeruginosa* while the one with the weakest activity (highest MIC) was T1. The crude extracts developed greater antimicrobial activity over time; the MICs of the extracts were 156.5 $\mu\text{g/mL}$, 39.06 $\mu\text{g/mL}$, 78.73 $\mu\text{g/mL}$ and 19.53 $\mu\text{g/mL}$ for T1, T2, T3 and T4, respectively.

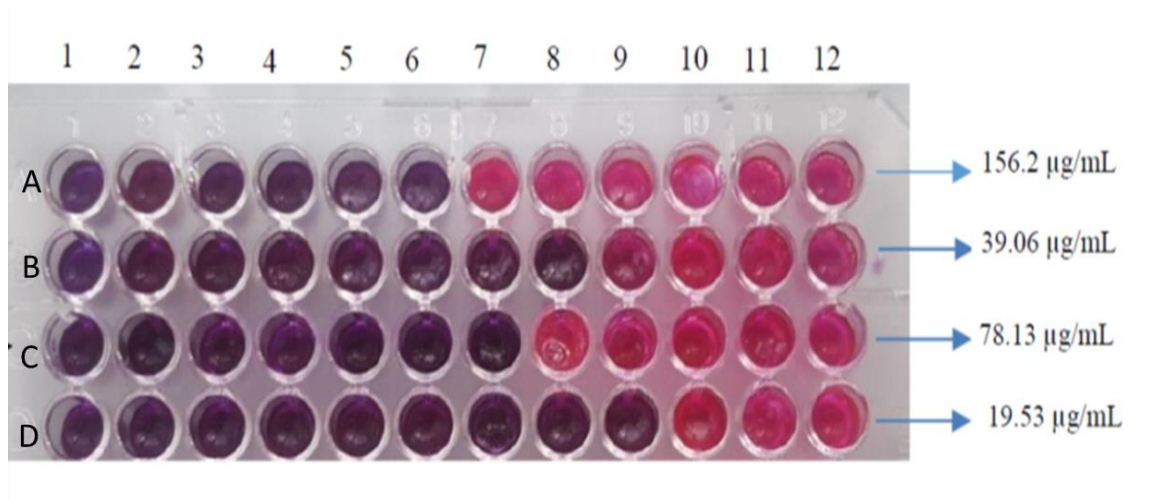


Figure 2.6: Resazurin colour reaction for minimum inhibitory concentration ($\mu\text{g/mL}$) determination of extracts against *P. aeruginosa*. Row A: 1 week ZF 52 extract 156.3; row B: 2 week ZF 52 extract 39.06; row C: 3 week old ZF 52 extract 78.13 and row D is a 4 week old ZF 52 extract 19.53.

Table 2. 2: Interpretation of the resazurin microtitre assay

Extract	Concentration ($\mu\text{g/mL}$)											
	1	2	3	4	5	6	7	8	9	10	11	12
	5000	2500	1250	625	312.5	156.3	78.13	39.06	19.53	9.766	4.883	2.441
T1	-	-	-	-	-	-	+	+	+	+	+	+
T2	-	-	-	-	-	-	-	-	+	+	+	+
T3	-	-	-	-	-	-	-	+	+	+	+	+
T4	-	-	-	-	-	-	-	-	-	+	+	+

Keys: +: growth; -: no growth

2.3.5 Thin layer chromatography

All the solvents tested resulted in separation of the different compounds in the crude extract. CHCl_3 and EtOAc resulted in little separation of the different compounds in the extract (Figure 2.7 A), with smears being observed. Figure 2.7 B shows better separation resulting from TLC using hexane and EtOAc. Figure 2.8 C showed the separating of the time-course extracts when viewed under UV light. The compound with R_f values around 0.78 was produced from the first week. On the second week the band begins to separate, and the band is seen slightly higher

than the one at T1. Better separation and more compounds are observed from week three while the four-week-old extract shows that the compounds become more concentrated. The compounds within ZF 52 crude extract are really produced from the first week of SSF, this corroborates Figure 2.5.



Figure 2. 7: TLC analysis of ZF 52 crude ethyl acetate extracts; separated using (A) CDCl_3 :EtOAc (60:40). A - ZF 52 at four week ethyl acetate extract viewed with staining; (B) - ZF 52 separation using chloroform:ethyl acetate (R_f : 0.22, 0.30, 0.34, 0.43, 0.57 and 0.78) without staining (60:40).

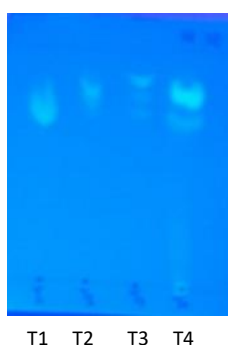


Figure 2.8: TLC analysis ZF 52 crude ethyl acetate extracts of varying ages separated using hexane:EtOAc and viewed under UV. T1- one week old; T2- two week old; T3- three week old and T4 is a four week old ZF 52 ethyl acetate extract.

2.3.6 Bio-autography

Bio-autography revealed that the majority of the compounds resolved on the TLC plates contained bactericidal activity as three (R_f : 0.22, 0.30 and 0.78) bands produced halos after the

dye was sprayed (Figure 2.9). However, the bands close to the origin had no bactericidal activity because these bands appeared pink.



Figure 2. 9: Bio-autogram of *P. aeruginosa* treated ZF 52 extract. Live cells appear pink and dead cells are presented by a halo. A - bio-autogram; B - TLC plate.

2.3.7 Identification

2.3.7.1 Genomic DNA isolation

It was extremely difficult to lyse the mycelia of ZF 52. Poor yields of genomic DNA were obtained after several attempts of using aged mycelia. In the final attempt, a 24 h culture was manually disrupted using forceps. The resultant small mycelia were then subjected to bead bashing as per kit instruction manual but the vortexing time was increased from 30 s to 60 s. A barely visible yield of genomic DNA was obtained visualised on an agarose gel which was stained with ethidium bromide (Figure 2.10).

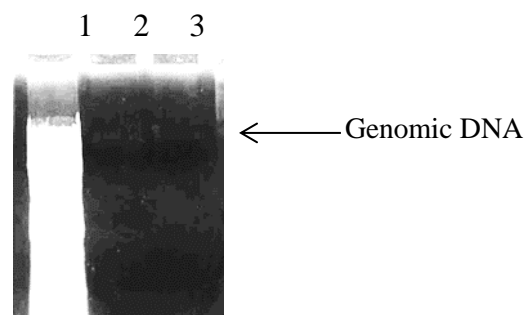


Figure 2. 10: Genomic DNA isolated from ZF 52 on agarose gel. L1: 100 bp plus marker, L2 and L3: ZF52 DNA.

2.3.7.2 PCR amplification

Figure 2.11 shows the gel image of the PCR product obtained after amplification of the ITS2 region of the 18S rRNA gene. The PCR amplification was successful as the expected amplicon size of 600 bp was obtained.

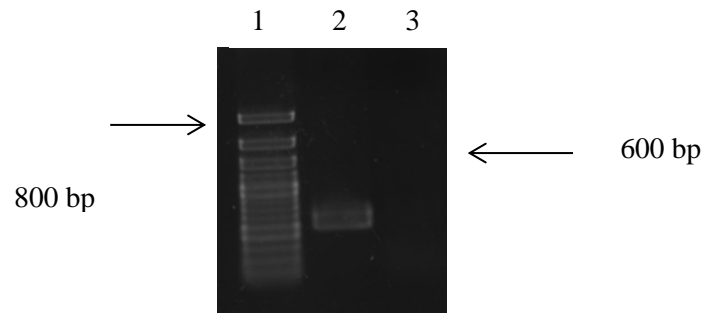


Figure 2.11: Agarose gel image of the ITS2 region of 18S rRNA gene after PCR amplification. L1: 100 bp Gene ruler, L2: PCR amplification product, L3: negative control.

2.3.7.3 Identification of ZF52

The 18S PCR amplicon was sequenced at Stellenbosch University, South Africa. Trimmed forward and reverse sequences were aligned and submitted to Genbank for comparison to other sequences. The result returned from Genbank showed ZF 52 has 99% identity to *Neofusicoccum luteum* strain CMW 10309 (Table 2.3).

Table 2.3: BLAST analysis of ZF 52

Description	Max score	Total score	Query cover	E value	Identity	Accession
<i>Neofusicoccum luteum</i> strain CMW 10309 18S ribosomal RNA gene, partial sequence: internal transcribed spacer 1.5 ribosomal	1070	1070	99%	0.0	99%	KF766202. 1

2.4 DISCUSSION

Resuscitation of the fungal endophytes from stock cultures was successful as morphology and pigmentation matched the original plates. Darkly pigmented medicinal plant extracts are reported in literature to possess strong bioactive activity; these include but are not limited to anti-HIV, antimalarial, antimicrobial, antioxidant and anticancer properties. The darkly pigmented endophytic extracts had no activity against *P. aeruginosa* as all three darkly pigmented extracts did not produce zones of inhibition. A study by Sharma *et al.* (2016) described a fungus with olive green pigmentation with extracts containing bioactive metabolites further suggesting that dark pigmented fungi that produce dark extracts are the most likely to contain bioactive metabolites.

In the current study, however, the darkly pigmented endophytic extracts had no activity against *P. aeruginosa* as all three darkly pigmented extracts did not produce zones of inhibition. However, ZF 52, ZF 91 and ZF 34, which were lightly pigmented had good activity against *P. aeruginosa* contrary to Sharma *et al.* (2016). No two extracts had the same colour. It is tempting to assume that they were produced by different fungal species or different strains of the same endophytic fungus as some of the fungi had the same pigmentation and colony morphology. This may be confirmed by identifying all the isolates.

In the antimicrobial activity testing, it was observed that most of the extracts had little to no activity against *P. aeruginosa*. In a previous study, it was observed that *K. africana* endophytic fungal extracts had antimicrobial activity mainly against fungi (Kuali, 2015, Shezi, 2014). This could be because within *K. africana*, beneficial and pathogenic fungi compete for nutrients and shelter thus resulting in fungal endophytes being able to kill most fungi. Out of the 45 extracts screened, only three namely ZF 52, ZF 91 and ZF 34 displayed activity against multi drug

resistant *P. aeruginosa* strain (with 40.33, 22 and 20 mm diameter zones of inhibition, respectively). A study by Ratnaweera and co-workers (2015) also reported variable zones of inhibition (8 to 35 mm) against three Gram-positive bacteria, *Bacillus subtilis* (UBC 344), *Staphylococcus aureus* (ATCC 43300) and MRSA (ATCC33591), two Gram-negative bacteria, *Escherichia coli* (UBC 8161), *P. aeruginosa* (ATCC 27853) and the pathogenic fungus *Candida albicans* (ATCC 90028). They screened eight endofungal extracts from the arid zone invasive plant *Opuntia dillenii* and only two produced zones of inhibition above 30 mm. However, none of these extracts were active against *P. aeruginosa*.

Phenolics, alkaloids and terpenes are the most encountered antibacterial compounds found in medicinal plants and it would be no surprise if the extracts from ZF 52, ZF 91 and ZF 34 also contain these compounds (Chandra *et al.*, 2017). Prabukumar *et al.* (2015) tested endophytic fungi CC1, CC2, CC3 and CC4 isolated from *Crescentia cujete* for antibacterial activity. These were evaluated against Gram-negative bacteria *Salmonella typhi* (ATCC 51812), *Shigella flexneri* (MTCC 1457), *Enterococcus faecalis* (ATCC 29212), *Klebsiella pneumoniae* (ATCC 432), *P. aeruginosa* (ATCC-27853), *E. coli* (ATCC-25922) and Gram-positive bacteria *B. subtilis* (ATCC 441), *S. aureus* (ATCC 25923). These extracts displayed good activity against bacterial human pathogens, in general. Strain CC1 and CC3 crude extracts displayed intermediate inhibition activity against all the human pathogens except *P. aeruginosa* and *S. aureus* while the crude extract of CC4 also inhibited all these human pathogens except for *S. aureus*. The extract of CC2 inhibited the growth of *S. typhi* and *Shigella* sp. The MeOH and EtOAc fungal crude extracts of endophytic fungus *Pestalotiopsis neglecta* BAB-5510 isolated from the leaves of *Cupressus torulosa* inhibited the growth of both Gram-negative and Gram-positive bacterial human pathogens (Sharma *et al.*, 2016). These had activity against *S. aureus*, *B. subtilis*, *S. typhimurium* and *E. coli*. However, they displayed no activity against *P. aeruginosa*.

Thin layer chromatography was conducted using several solvent systems before the one giving optimal separation was identified. The most efficient solvent system was hexane:EtOAc (60:40) and it resulted in six distinct spots with R_f values of (0.22, 0.30, 0.34, 0.43, 0.57 and 0.78). In a study conducted by Rashid *et al.* (2017), various solvent systems were utilised with the most effective one being toluene:EtOAc:acetic acid (36:12:5) which resulted in five spots which had R_f values of 0.4, 0.45, 0.46, 0.55, 0.82. Sharma *et al.* (2016) also used TLC to separate the different compounds from the crude extract of *P. niglecta* and the solvent system with optimal resolution was dichloromethane:MeOH (90:10). This yielded two distinct bands with the second band (R_f of 0.79) displaying antibacterial activity.

Antibacterial components were present in the EtOAc extract (Figure 2.9). This was consistent with a study conducted by Jesionek *et al.* (2017) where halos were observed on the bio-autogram against several bacterial test strains. The bio-autogram in the current study showed more than one spot of the developed TLC plate to have anti-*P. aeruginosa* activity. Live cells were seen close to the origin and on the fifth spot indicating that four out of five spots possessed anti-*Pseudomonas* activity. A study by Samrot *et al.* (2016) that utilised TLC and bio-autography to screen extracts from *Mangifera indica* observed a band (R_f of 0.82) that displayed anti-*P. aeruginosa* activity which is not frequently encountered, and which was contrary to the current study. However, in their study, they used a different dye, namely, the MTT dye instead of the 2% (w/v) 2,3,5-triphenyltetrazolium dye. Methanolic extracts of *Ricinus communis* were used to conduct bio-autography with *P. aeruginosa* (PC 002) and *K. pneumoniae* (MTCC 3384) as the test cultures (Sandam and Su, 2015). For *P. pneumoniae* four active bands were observed in total for the fractions with R_f values: 0.200, 0.2750, 0.8875 and 0.9125. One active band with R_f value 0.2750 was observed for *P. aeruginosa*. The methanolic extracts of *R. communis* displayed more activity against *K. pneumoniae* than *P. aeruginosa*.

Sequencing and BLAST analysis of the ITS2 amplicon of ZF 52 had 99% identity to *Neofusicoccum luteum* strain CMW 10309. This fungus was previously identified by Shezi in 2014, this therefore means that culture storage and maintenance, resuscitation and biomolecule production was successful for ZF 52 but was unsuccessful for ZF 91 and ZF 34. Sharma *et al.* (2016) studied the endophytic fungi associated with the *Cupressus torulosa*. Five fungi were isolated and identified as *Alternaria alternata*, *Penicillium oxalicum*, *Daldinia* sp. and *Pestalotiopsis* sp. Idris *et al.* (2013) isolated seven endophytic fungi and identified them as *Aspergillus flavus*, *Aspergillus* sp., *Cladosporium* sp., *Culvularia lunata* and three unknown fungi. A study by Maheswari and Rajagopal (2013) identified 28 endophytic fungi, none of which was *N. luteum*. In contrast Wicaksono *et al.* (2017) isolated *N. luteum* from plants as a pathogen which was inhibited by endophytic *Pseudomonas* sp. The *P. aeruginosa* endophyte was reported to produce diffusible and volatile compounds which inhibited the growth of six botryosphaeriaceous species including *N. luteum*, which is the opposite to the findings of the current study. These finding from these two studies clearly points out the shifting nature of plant-fungal relationships that depend on the balance of antagonism – the interplay of plant, fungal, other organisms and environmental factors (Kusari *et al.*, 2012).

2.5 CONCLUSION

Three extracts out of the 45 tested, displayed activity against *P. aeruginosa*. Although the proportion of active to inactive fungal extracts was low, the ones with activity had very significant activity. ZF 91 and ZF 34 were not tested further as resuscitation and storage difficulties were encountered. Separation of ZF 52 revealed the extract to contain more than one compound and the compounds present were shown to have antibiotic activity as 80% of the spots showed anti-*Pseudomonas* activity. The fungus, *N. luteum*, and the subsequent

extract that it produces are not well known, this therefore justifies this study. These findings promote the purification and further testing the of *N. luteum* extract.

2.6 REFERENCES

- Anderson IC, Campbell CD, Prosser JI. 2003. Potential bias of fungal 18S rDNA and internal transcribed spacer polymerase chain reaction primers for estimating fungal biodiversity in soil. *Environmental Microbiology*, 5: 36-47.
- Arkhipov A, Sindaarta J, Rayan P, McDonnell PA, Cook IE. 2014. An examination of antibacterial, antifungal, anti-Giardial and anticancer properties of *Kigelia africana* fruit extracts. *Pharmacognosy Communications*, 4: 62-76.
- Awouafack MD, McGaw LJ, Gottfried S, Mbouangouere R, Tane P, Spiteller M, Eloff JN. 2013. Antimicrobial activity and cytotoxicity of the ethanol extract, fractions and eight compounds isolated from *Eriosema robustum* (Fabaceae). *BMC Complementary and Alternative Medicine*, 13:1.
- Bello I, Shehu MW, Musa M, Asmawi MZ, Mahmud R. 2016. *Kigelia africana* (Lam.) Benth. (Sausage tree): Phytochemistry and pharmacological review of a quintessential African traditional medicinal plant. *Journal of Ethnopharmacology*, 253-276.
- Berendonk TU, Manaia CM, Merlin C, Fatta-Kassinos D, Cytryn E, Walsh F, Bürgmann H, Sørum H, Norström M, Pons M, Kreuzinger N, Huovinen P, Stefani S, Schwartz T, Kisand V, Baquero F, Martinez JL. 2015. Tackling antibiotic resistance: the environmental framework. *Nature Reviews Microbiology*, 13: 310–317.
- Chandra H, Bishnoi P, Yadav A, Patni B, Mishra AP, Anant Ram Nautiyal AR. 2017. Antimicrobial resistance and the alternative resources with special emphasis on plant-based antimicrobials—A Review. *Plants*, 6: 16.
- Chenia HY. 2013. Anti-quorum sensing potential of crude *Kigelia africana* fruit extracts. *Sensors*, 133: 2802–2817.
- Cook IE, van Vuuren SF. 2014. Anti-*Proteus* activity of some South African medicinal plants: their potential for prevention of rheumatoid arthritis. *Inflammopharmacology*, 22: 23-26.
- Das I, Panda MK, Rath CC, Tayung K. 2017. Bioactivities of bacterial endophytes isolated from leaf tissues of *Hyptis suaveolens* against some clinically significant pathogens. *Journal of Applied Pharmaceutical Science*, 7: 131-136.
- Das K, Tiwari RKS, Shrivastava DK. 2010. Techniques for evaluation of medicinal plant products as antimicrobial agents: current methods and future trends. *Journal of Medicinal Plants Research*, 4: 104–111.

- Dewanjee S, Gangopadhyay M, Bhattacharya N, Khanra R, Dua TK. 2015. Bioautography and its scope in the field of natural product chemistry. *Journal of Pharmaceutical Analysis*, 5: 75-84.
- Elisha IL, Botha SF, McGaw LJ, Eloff JN. 2017. The antibacterial activity of extracts of nine plant species with good activity against *Escherichia coli* against five other bacteria and cytotoxicity of extracts. *BMC Complementary and Alternative Medicine*, 17: 133.
- Fernebro J. 2011. Fighting bacterial infections - Future treatment options. *Drug Resistance Update*, 14: 125–39.
- Hancock RE, Speert DP. 2000. Antibiotic resistance in *Pseudomonas aeruginosa*: mechanisms and impact on treatment. *Drug Resistance Update*, 3: 247-255.
- Harris AD, Perencevich E, Roghmann MC, Morris G, Kaye KS. 2002. Risk factors for piperacillin-tazobactam-resistant *Pseudomonas aeruginosa* among hospitalized patients. *Antimicrobial Agents Chemotherapy*, 46: 854-858.
- Holmes AH, Moore LS, Sundsfjord A, Steinbakk M, Regmi S, Karkey A, Guerin PJ, Piddock LJV. 2016. Understanding the mechanisms and drivers of antimicrobial resistance-antimicrobials: access and sustainable effectiveness 2. *Lancet*, 387: 176-187.
- Hussain T, Fatima I, Rafay M, Shabir S, Akram M, Bano S. 2016. Evaluation of antibacterial and antioxidant activity of leaves, fruit and bark of *Kigelia africana*. *Pakistan Journal of Botany*, 48: 277-283.
- Idris A, Al-tahir I, Idris E. 2013. Antibacterial activity of endophytic fungi extracts from the medicinal plant *Kigelia africana*. *Egyptian Academic Journal of Biological Sciences*, 5: 1-9.
- Jesionek W, Majer-Dziedzic B, Horváth G, Móricz AM, Choma IM. 2017. Screening of antibacterial compounds in *Thymus vulgaris* L. Tincture using thin-layer chromatography direct-bioautography and liquid chromatography-tandem mass spectrometry techniques. *Journal of Planar Chromatography*, 30: 131-135.
- Joo EJ, Kang CI, Ha YE, Kim J, Kang SJ. 2011. Clinical predictors of *Pseudomonas aeruginosa* bacteraemia among Gram-negative bacterial infections in non-neutropenic patients with solid tumour. *Journal of Infection*, 63: 207-214.
- Kuali M. 2015. Screening for antimicrobial and antioxidant activities of *Kigelia africana* fungal endophytes. Honours Dissertation, 1-90.
- Kusari S, Pandley SP, Spiteller M. 2013. Untapped mutualistic paradigms linking host plant and endophytic fungal production of similar bioactive metabolites. *Phytochemistry*, 91: 81-87.

- Kwon HR, Son SW, Han HR, Choi GJ, Jang KS, Choi YH, Lee S, Sunog ND, Kim JC. 2007. Nematocidal activity of bikaverin and fusaric acid isolated from *Fusarium oxysporum* against pine wood nematode *Bursaphelenchus xylophilus*. *Plant Pathology Journal*, 23: 318-321.
- Maheswari S, Rajagopal K. 2013. Biodiversity of endophytic fungi in *Kigelia pinnata* during two different seasons. *Current Science*, 104: 515-518.
- Mudau M, Jacobson R, Minenza N, Kuonza L, Morris V, Engelbrecht H, Nicol MP, Bamford C. 2013. Outbreak of multi-drug resistant *Pseudomonas aeruginosa* bloodstream infection in the haematology unit of a South African Academic Hospital. *PLoS ONE*, 8: e55985
- Nyasulu P, Murray J, Perovic O, Koornhof H. 2012. Antimicrobial resistance surveillance among nosocomial pathogens in South Africa: systematic review of published literature. *Journal of Experimental and Clinical Medicine*, 4: 8-13.
- Nyasulu P, Murray J, Perovic O, Koornhof H. 2017. Laboratory information system for reporting antimicrobial resistant isolates from academic hospitals, South Africa. *The Journal of infection in Developing Countries*, 11: 705- 711.
- Prabavathy D, Nachiyar VC. 2014. Cytotoxicity of ethyl acetate extract of endophytic *Aspergillus fumigatus* on A549 Cell Lines. *Biosciences Biotechnology Research Asia*, 11: 797-802.
- Prabukumar S, Rajkuberan C, Ravindran K, Sivaramakrishnan S. 2015. Isolation and characterization of endophytic fungi from medicinal plant *Crescentia cujete* and their antibacterial, antioxidant and anticancer properties. *International Journal of Pharmacy and Pharmaceutical Sciences*, 7: 316-321.
- Rashid R, Hajam GN, Wani MH, Gulzar A. 2017. Thin layer chromatography profiling of the medicinal plant *Solanum nigrum* L. from the local Area of the district Anantnag of Jammu and Kashmir. *International Journal of Advance Research, Ideas and Innovations in Technology*, 3: 6-9.
- Ratnaweera PP, de Silva ED, Williams DE, Anderson RJ. 2015. Antimicrobial activities of endophytic fungi obtained from the arid zone invasive plant *Opuntia dillenii* and the isolation of equistatin from endophytic *Fusarium* sp. *BMC Complementary and Alternative Medicine*, 15: 220-227.
- Ristaino JB, Madritch M, Trout CL, Parra G. 1998. PCR amplification of ribosomal DNA for species identification in the plant pathogen genus *Phytophthora*. *Applied and Environmental Microbiology*, 64: 948 – 954.

- Saini S, Kauer H, Verma B, Sungh SK. 2009. *Kigelia africana* (Lam.) Benth- an overview. *Indian Journal of Natural Products and Resources*, 8: 190-197.
- Sandam N, Su P. 2015. TLC-Bioautography guided screening of the methanolic extract of *Ricinus communis*. *International Journal of Pharma and Bio Sciences*, 6: 427-432.
- Selvameenal L, Radhakrishnan M, Balagurunathan R. 2009. Antibiotic pigment from desert soil actinomycetes; biological activity, purification and chemical screening. *Indian journal of pharmaceutical sciences*, 71: 499-504.
- Sharma D, Pramanik A, Agrawal PK. 2016. Evaluation of bioactive secondary metabolites from endophytic fungus *Pestalotiopsis neglecta* BAB-5510 isolated from leaves of *Cupressus torulosa* D.Don. *Biotechnology*, 6: 210-214.
- Shezi S. 2014. Isolation and identification of fungal endophytes from K. Africana and determination of their antimicrobial properties. Honours Dissertation, 1-132.
- Srivastava J, Chandra H, Nautiyal AR, Kalra SJS. 2013. Antimicrobial resistance (AMR) and plant derived antimicrobials (PDAMs) as an alternative drug line to control infections. *Biotechnology*, 4: 451-460.
- Strobel G, Daisy B. 2003. Bioprospecting for microbial endophytes and their natural products. *Microbiology and Molecular Biology Reviews*, 67: 491-502.
- Talonsi FM, Facey P, Kongue Tatong MD, Islam TM, Fraudendoft H, Draeger S, von Tiedemann A, Laatsch H. 2012. Zoosporicidal metabolites from an endophytic fungus *Cryptosporiopsis* sp. of *Zanthoxylum leprieurii*. *Phytochemistry*, 83: 87-94.
- Theuretzbacher U, Mouton JW. 2012. Update on antibacterial and antifungal drugs - Can we master the resistance crisis? *Current Opinion Pharmacology*, 11: 429-432.
- Ventola CL. 2015. The antibiotic resistance crisis: part 1: causes and threats. *Pharmacy and Therapeutics*, 40: 277-283.
- White TJ, Bruns T, Lee S, Taylor J. 1990. Amplification and direct sequencing of fungal ribosomal RNA genes for phylogenetics. PCR protocols: a guide to methods and applications. Academic Press Incorporated. New York, N.Y. 315-322.
- Wicaksono WA, Jones EE, Monk J, Ridgway HJ. 2017. Using bacterial endophytes from a New Zealand native medicinal plant for control of grapevine trunk diseases. *Biological Control*, 114: 65-72.
- Yu H, Zhang L, Li L, Zheng C, Guo L, Li W, Sun P, Qin L. 2010. Recent developments and future prospects of antimicrobial metabolites produced by endophytes. *Microbiological Research*, 165: 437-449.

Zin NM, Sarmin NI, Ghadin N, Basri DF, Sidik NM, Hess WM, Strobel GA. 2007. Bioactive endophytic Streptomycetes from the Malay Peninsula. *FEMS Microbiology Letters*, 274: 83-88.

CHAPTER 3: PURIFICATION AND CHARACTERISATION OF THE *Neofusicoccum luteum* ANTI-*P. aeruginosa* COMPOUND FROM THE ETHYL ACETATE CRUDE EXTRACT

3.1 INTRODUCTION

Endophytic *Botryosphaeriaceae* species have been reported to be in high abundance and encountered very frequently and research has targeted their potential as producers of novel secondary metabolites with anticarcinogenic, antibiotic and fungicidal activity (Saikkonen, 2002; Garcia *et al.*, 2012; Dos Santos *et al.*, 2016). However, the extent to which some of these species might be considered true endophytes or pathogens undergoing a latent phase still remains in question (Reveglia *et al.*, 2018).

Neofusicoccum luteum host colonisation and infection happens mostly through horizontal transmission (individual infections via conidia or ascospores), although vertical transmission (infection through seeds) has been reported (Slippers *et al.*, 2013; Lopes *et al.*, 2016). Within the plant, species of this genus are able to exist without causing any symptoms and thus remain in the plant as endophytes. The endophytism of *Neofusicoccum* sp. could be the crucial feature aiding their wide distribution since they can be moved effortlessly around the world in cuttings, seeds and also in fruits, subsequently infecting both native and non-native trees in their new-found environments (Lopes *et al.*, 2016). *Neofusicoccum luteum* is a plant pathogen and causes dieback and canker in grapevines and tomato cuttings (Altermimi *et al.*, 2017; Rezgui *et al.*, 2018).

Isolation and purification of bioactive compounds is a technique that has undergone new developments in recent years (Altermimi *et al.*, 2015; Altermimi *et al.*, 2017; Kanagavalli and Sadiq, 2018). The technique provides concise separation, isolation and purification and offers an abundance of advanced bioassays (Poongunran *et al.*, 2016). When looking for bioactive compounds, the goal is to find an appropriate method to screen the extracts for antimicrobial, antioxidant and or cell toxicity in conjunction with simplicity, speed and specificity (Eruygur *et al.*, 2016; Altermimi *et al.*, 2017).

Numerous bioactive molecules have been separated and purified by thin-layer and column chromatographic methods (Devika and Koilpillai, 2015). These chromatographic methods are still the mostly used due to their affordability, convenience and availability. Alumina, cellulose, silica and polyamide are the most important materials when separating separating plant-based compounds (Kangavalli and Sadiq, 2018). Using multiple mobile phases to increase polarity is very important for high value separations. Heteronuclear Multiple Bond Correlation (HMBC) experiment correlates chemical shifts of two types of nuclei separated from each other with two or more chemical bonds while the Distortionless enhancement by polarization transfer (DEPT) experiment is able to fully separate the carbon signals. DEPT 45 yields CH, CH₂ and CH₃ signals positive, DEPT 90 yields only CH signals and DEPT 135 yields CH and CH₃ positive while CH₂ s negative (Kangavalli and Sadiq, 2018).

Due to the promising results obtained in Chapter 2 regarding the crude extract of *N. luteum*, the fungus *N. luteum* being relatively undocumented and the extract it produces being unknown, the aim herein was to purify and characterise the anti-*P. aeruginosa* compound.

3.2 MATERIALS AND METHODS

3.2.1 Activity-based purification by column chromatography

A glass column was prepared for silica gel gravity chromatography. The column was rinsed with hexane (reagent grade, Merck, India) and left to dry. A cotton plug was placed at the base of the column to prevent the silica from leaking. Activated silica gel (60 mesh, Sigma Aldrich, Switzerland) was then packed into the glass column (length: 53 cm and width: 15 cm) with hexane (Kaur *et al.*, 2015). Rotary evaporation was used to concentrate the *N. luteum* crude extract (2 g) which was then mixed with the silica gel in a ratio of 1:1 and loaded into the column.

Optimal separation of compounds was already obtained in 2.3.5. The EtOAc extract (2 g) was subjected to column chromatography with hexane:EtOAc as the mobile phase, starting with 100% hexane. The polarity of the solvent system was gradually increased by 5% for every 100 mL until 100% EtOAc was reached. The polarity of the mobile phase was further increased with 5 and 10% MeOH, sequentially. A total of 27 fractions were collected and combined into four fractions, namely, A (1 – 10, 230 mg), B (11-16, 310 mg), C (17-21, 150 mg) and D (22-27, 310 mg), based on similarities in the TLC profiles of the fractions. The four fractions were further processed by TLC, TLC-bioautography and MIC determinations as described in 2.2.5, 2.2.6 and 2.2.4.2, respectively.

3.2.2 Nuclear magnetic resonance (NMR)

From the MIC determinations conducted on the four fractions, it was observed that only fraction C displayed anti- *P. aeruginosa* activity, thus this fraction was subjected to further purification. Fraction C afforded compound 1 upon crystallization from ethanol. The isolate was dissolved in deuterated chloroform (CDCl₃) and subjected to 1 and 2D NMR spectroscopy.

3.3 RESULTS

3.3.1. Purification by activity-based fractionation of the anti-*P. aeruginosa* compound

Column chromatography, bioautographic detection and MIC assays were utilised to purify the anti-*P. aeruginosa* compound of interest. Fractions A-D were subjected to TLC and TLC-bioautography for detection. Smudged spots (no clear bands) were observed from TLC (Figure 3.2) and TLC-bioautography that yield inconclusive results. This was not repeated due to lack of sample; however, MIC determinations were conducted to determine if fractions contained anti-*P. aeruginosa* activity. The MIC results revealed fraction C to be the only fraction with activity against *P. aeruginosa* with an MIC of 2.441 $\mu\text{g/mL}$ (Figure 3.3). Further purification of Fraction C using column chromatography yielded compound 1 with an MIC of 0.6104 $\mu\text{g/mL}$ (Figure 3.4).

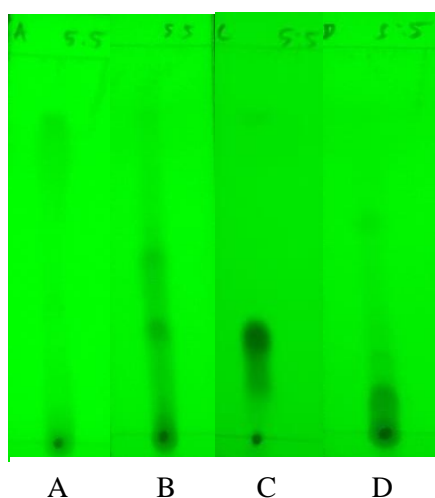


Figure 3. 1: Thin layer chromatography of fractions A, B, C and D.

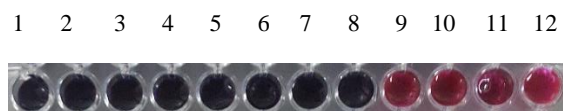


Figure 3. 2: Broth microtitre serial dilution assay ($\mu\text{g/mL}$) for MIC determination of partially purified pooled fractions. Wells 1-10 contain cells, Muller Hinton broth and sample; Well 11 contains 8% DMSO in water and Well 12 contains more media as a replacement for extract.

Table 3.1: Interpretation of the resazurin microtitre assay for Fraction C

Concentration ($\mu\text{g/mL}$)											
1	2	3	4	5	6	7	8	9	10	11	12
312.5	156.3	78.13	39.06	19.53	9.766	4.883	2.441	1.221	0.6103	0.3051	0.1521
-	-	-	-	-	-	-	-	+	+	+	+

Keys: +: growth -: no growth

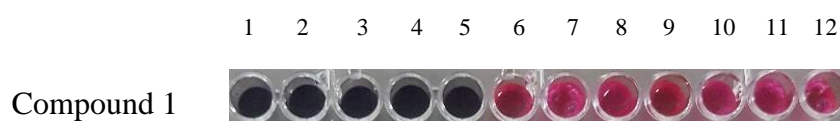


Figure 3. 3: Broth microtitre serial dilution assay ($\mu\text{g/mL}$) for MIC determination for purified compound 1. Wells 1-10 contain cells, Muller Hinton broth and sample; Well 11 contains 8% DMSO in water and Well 12 contains more media as a replacement for extract.

Table 3.2: Interpretation of the resazurin microtitre assay for compound 1

Concentration ($\mu\text{g/mL}$)											
1	2	3	4	5	6	7	8	9	10	11	12
9.766	4.883	2.441	1.221	0.6103	0.3051	0.1521	0.0761	0.0380	0.0190	0.010	0.0048
-	-	-	-	-	+	+	+	+	+	+	+

Key: +: growth; -: no growth

3.3.2 Nuclear magnetic resonance and structure elucidation

Compound 1: HR-ESI-MS: m/z 297.1109 $[\text{M}+\text{Na}]^+$, (calcd for $\text{C}_{16}\text{H}_{18}\text{O}_4\text{Na}$, 297.1103). IR (KBr) ν_{max} cm^{-1} : 2926, 2879, 1771, 1702, 1612, 1466, 1384, 1200, 1034, 878. ^1H NMR (CDCl_3 , 400 MHz): δ_{H} : 6.18 (1H, m, H-7), 5.73 (1H, d, $J = 1.52$ Hz, H-11), 5.00 (1H, brt, $J = 4.52$ Hz, H-6), 4.96 (1H, dt, $J = 13.57$ Hz, H-13a), 4.87 (1H, d, $J = 13.57$ Hz, H-13b), 2.24 (1H, ddd, $J = 13.71, 7.66, 5.64$ Hz, H-3a), 1.92 (1H, d, $J = 4.66$ Hz, H-5) (Figure 3.5 A and B), 1.72 – 1.58

(3H, overlapping multiplets, H-1a, 1b, 2b), 1.53 (1H, ddd, $J = 14.28, 7.45, 6.06$ Hz, H-3b), 1.30 (3H, s, H-15), 1.15 (3H, s, H-16) (Figure 3.6).

^{13}C NMR (CDCl_3 , 400 MHz): δ_{C} : 180.8 (C-14), 163.6 (C-12), 158.7 (C-9), 132.2 (C-8), 121.8 (C-7), 111.7 (C-11), 71.3 (C-6), 69.5 (C-13), 47.8 (C-5), 42.7 (C-4), 35.0 (C-10), 29.6 (C-1), 27.7 (C-3), 24.7 (C-16), 24.1 (C-15), 17.3 (C-2) (Figure 3.7).

A total of sixteen peaks, comprising two methyl, four methylene, four methine and six quaternary carbons were observed in the ^{13}C NMR spectrum (Figure 3.7) and the Distortionless enhancement by polarization transfer (DEPT) spectra (Figure 3.8) supported these findings. The HMBC spectrum showed 3J correlation between carbonyl at C-11 with methylene protons H-8, methine proton H-10 and methyl protons H-16; and carbonyl at C-2 with H-1b and H-3 (Figure 3.9). ^1H NMR was conducted on fraction 17 and compound 1 was isolated as a white solid from the extract of the fungus *N. luteum* with a molecular formula $\text{C}_{16}\text{H}_{18}\text{O}_4$ (Figure 3.10).

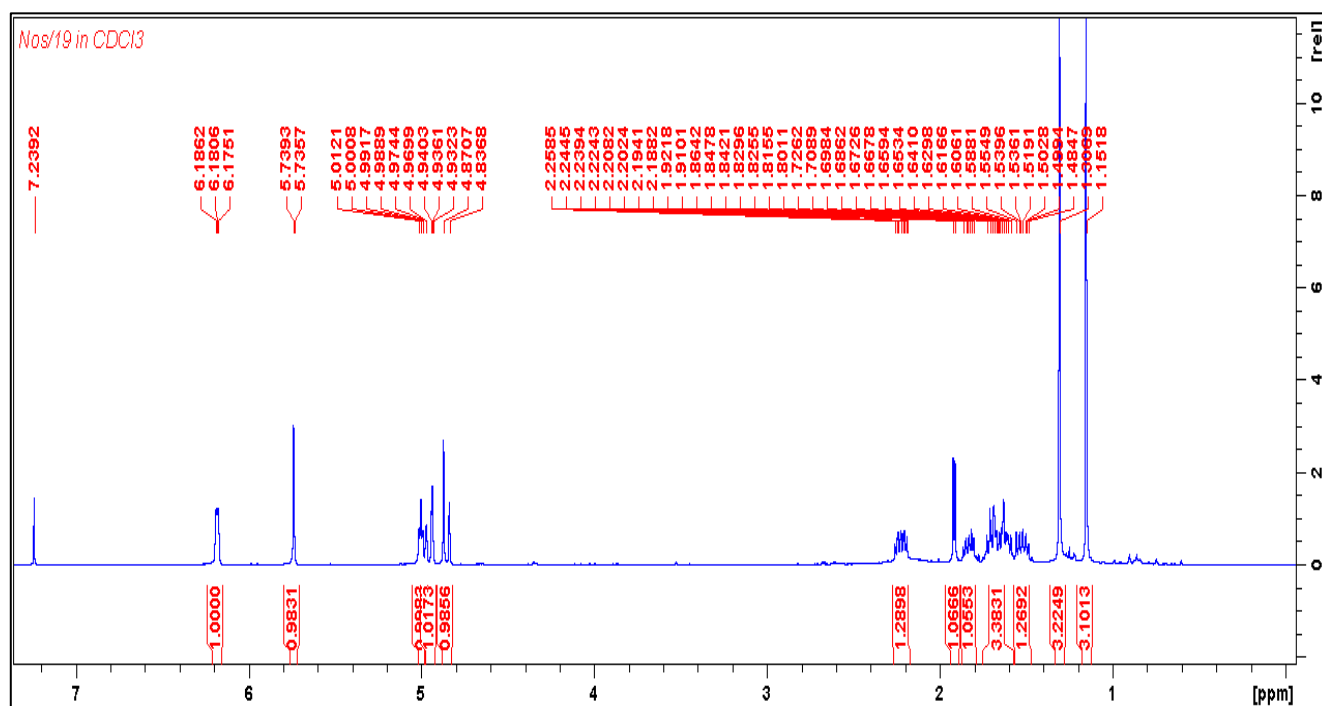


Figure 3.4: ^1H NMR spectrum of compound 1 in CDCl_3 .

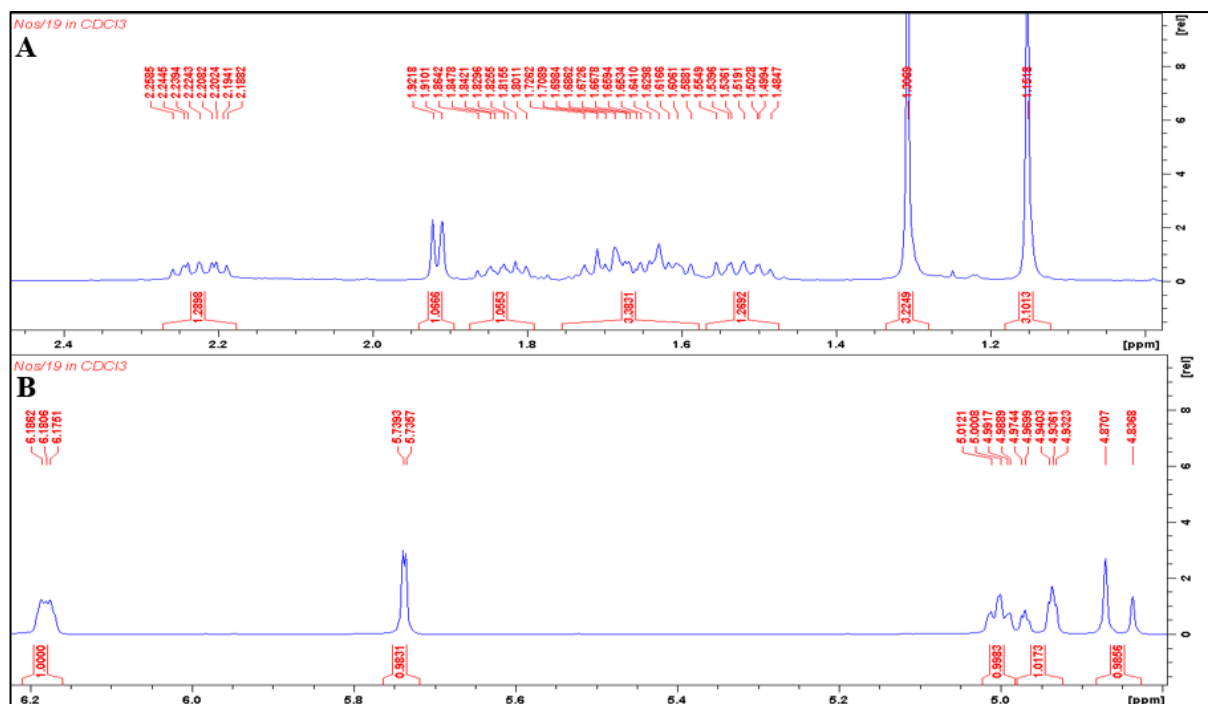


Figure 3.5: Expanded ¹H NMR spectrum of compound 1 in CDCl₃ (A and B).

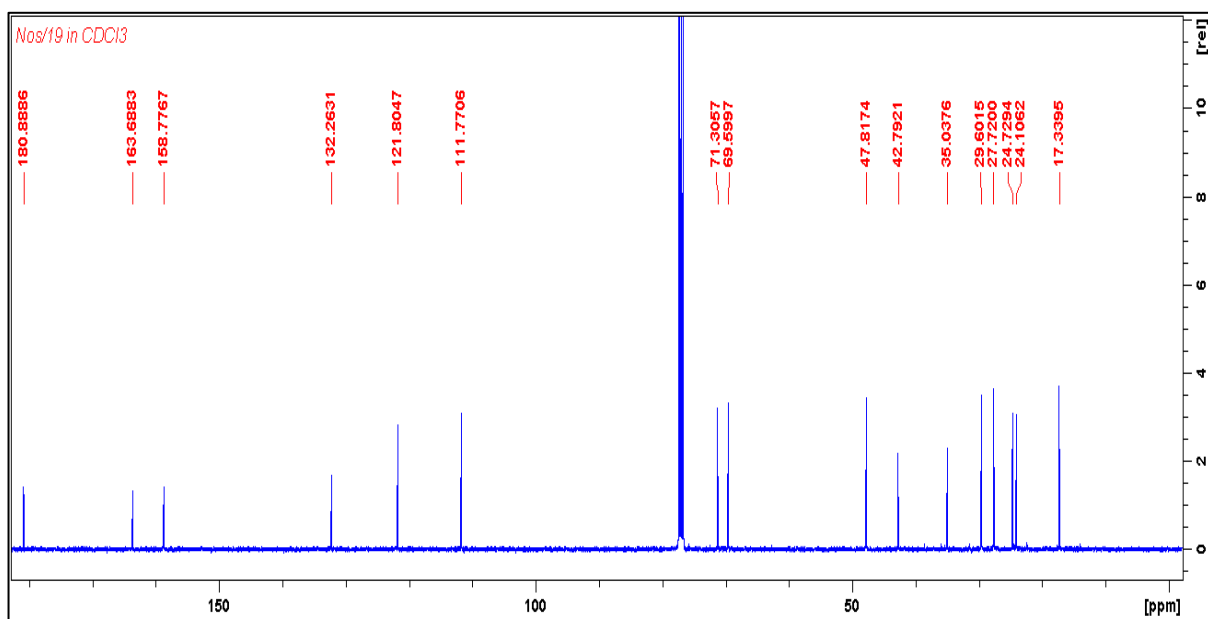


Figure 3.6: ¹³C NMR spectrum of compound 1 in CDCl₃.

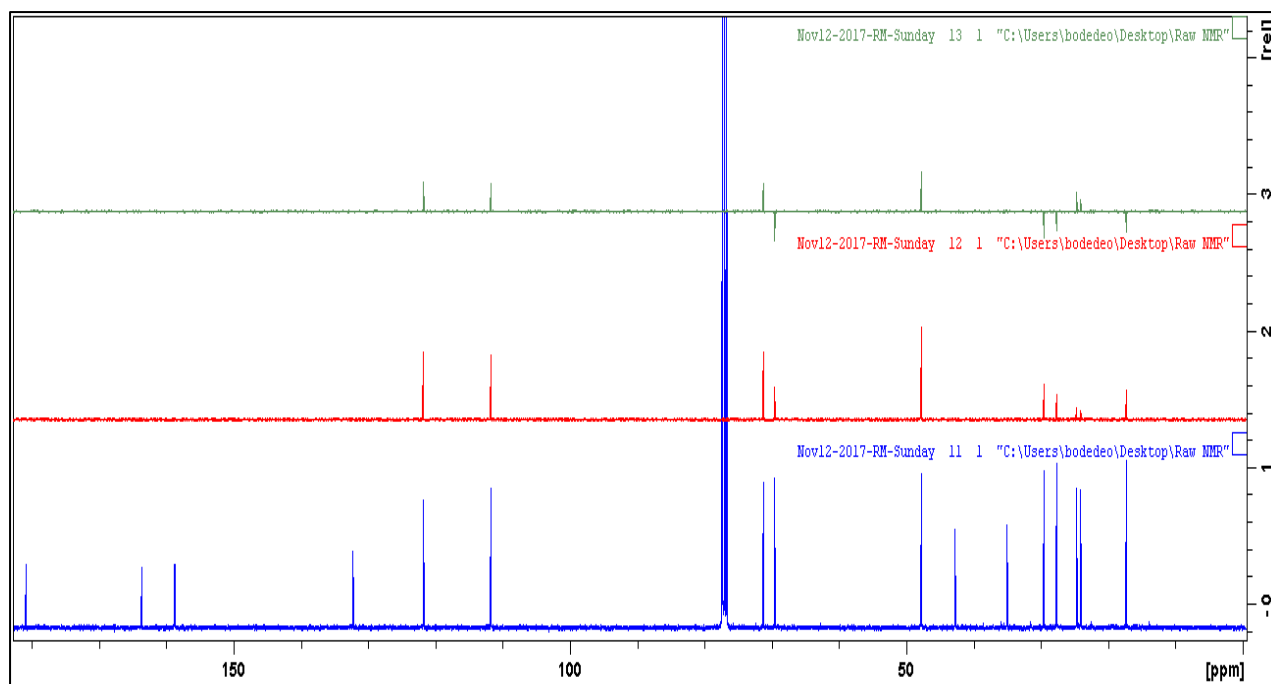


Figure 3.7: DEPT spectra of compound 1.

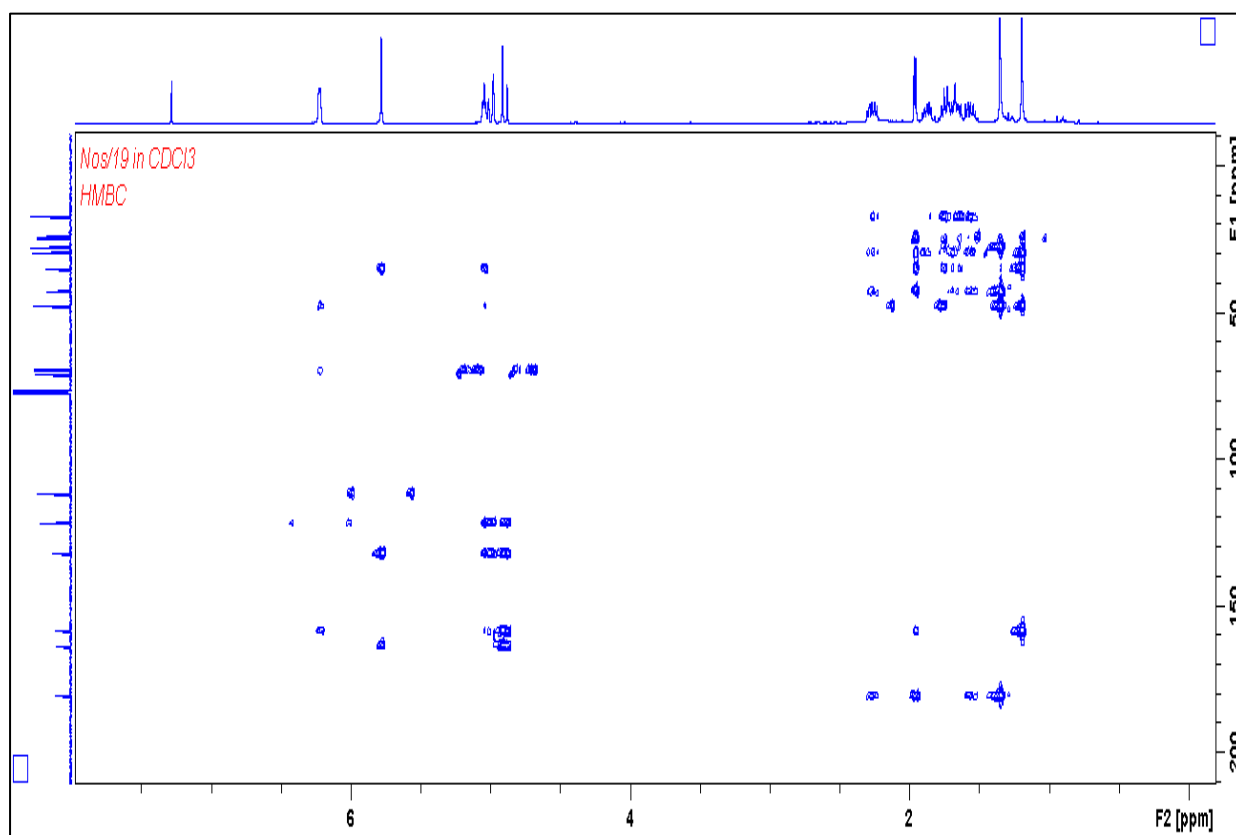


Figure 3.8: HMBC spectrum of compound 1.

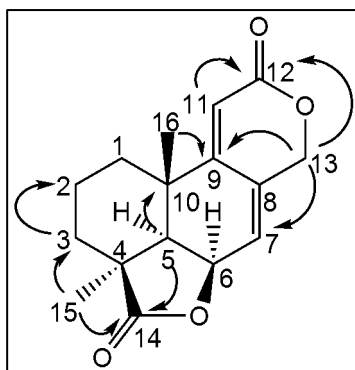


Figure 3.9: Major HMBC correlations observed in compound 1.

3.4 DISCUSSION

Analysis by TLC of these four fractions yielded inconclusive results and forced early MIC determination. The MIC determination showed only fraction C to possess bioactive metabolites which were able to kill *P. aeruginosa* (Figure 3.3). Fraction C was therefore purified and yielded a white crystalline substance, compound 1 (35 mg) which accounted for 1.75% of the crude extract (2 g).

The MIC obtained for compound 1 was exceptional at 0.6103 $\mu\text{g/mL}$ (Figure 3.4) indicating that the pure compound is more active than the partially purified extract (2.441 $\mu\text{g/mL}$ in Figure 3.3) and crude extracts (19.53 $\mu\text{g/mL}$ as seen in Figure 2.6) that contain a range of compounds. A similar study by Fall *et al.* (2017) using an ethanol extract of *Aphania senegalensis* resulted in antibacterial activity against *S. aureus*, *E. coli* and *E. faecalis* with MICs of 0.31 mg/mL, 0.16 mg/mL and 0.08 mg/mL respectively. However, the extract did not show growth inhibition against *P. aeruginosa*. In addition, a study by Malhadas *et al.* (2017) on the antibacterial activity of the EtOAc and MeOH extracts of *Alternaria alternata* fungus showed the extracts to have activity against several bacteria with MICs ranging between 0.095 and 25 mg/mL. The EtOAc extract of the fungus gave an MIC value of 3.125 mg/mL against *P. aeruginosa*, which was higher than the current study. These comparisons indicate that activity of the extracts of *N. luteum* against *P. aeruginosa* is encouraging.

The ^1H NMR spectrum (Figure 3.5) showed characteristic alkenyl resonances at δ_{H} 6.18 (H-7) and 5.73 (H-11) which were confirmed by the ^{13}C NMR chemical shifts at δ_{C} 121.8 and 111.7, respectively. Oxygenated methine (δ_{H} 5.00) and methylene (δ_{H} 4.96 & 4.87) protons were assigned to H-6 and H-13a&b, respectively, while the corresponding oxygenated methine and methylene carbons were observed at δ_{C} 71.3 (C-6) and 69.5 (C-13), respectively. The 16 peaks observed in Figure 3.7 were also observed by the DEPT spectra (Figure 3.8). Two of the quaternary carbons (δ_{C} 180.8 and 163.6) were ester carbonyl carbons which confirm the dilactone nature of compound 1 (Figure 3.10).

The locations of the angular methyl protons and the proximity of double bonds to rings B and C were confirmed using HMBC correlations (Figure 3.10) which were deduced from the HMBC spectrum presented in Figure 3.9. There was a correlation between H-11 and the ring C carbonyl. H-13 had correlations with C-12, C-9 and C-7 while the correlation of H-5 to C-14 carbonyl confirms the fusion of ring D with rings A and B. The NMR analysis, supported by the vibrational frequencies (cm^{-1}) of C=O (1771, 1702), C-O (1034), C=C (1612) and C-H (2926) using FTIR justify compound 1 as a dilactone. The dilactone was confirmed with an exact mass m/z 297.1109 for $\text{C}_{16}\text{H}_{18}\text{O}_4\text{Na}$. Thus, the molecular formula of compound 1 was deduced to be $\text{C}_{16}\text{H}_{18}\text{O}_4$.

Compound 1 ($\text{C}_{16}\text{H}_{18}\text{O}_4$) was identified as a dilactone (3a,10b-dimethyl-1,2,3,3a,5a,7,10b,10c-octahydro-5,8-dioxa-acephenanthrylene-4,9-dione) and it matched compound 3 in the study of antineoplastic agents conducted by Pettit *et al.* (2003). The same compound was synthesised from a Wieland-Miescher ketone and was similar to oidiolactone C ($\text{C}_{16}\text{H}_{18}\text{O}_5$) (Hanessian *et al.*, 2009). This compound occurs both naturally and synthetically. The compound was also tested for antibacterial and antifungal activity against *S. aureus*, *Shigella dysenteriae*, *Penicillium avellaneum*, *C. albicans* and *Saccharomyces cerevisiae*. It displayed anti-*C.*

albicans, anti-*S. cerevisiae* and anti-*P. avellaneum* activity but no antibacterial activity (Lin *et al.*, 2009). This suggests that existing compounds (synthetic and natural) need to be tested for new properties as none of the oidiolactones have displayed activity against resistant *P. aeruginosa* in the past.

Oidiolactones were first reported by John *et al.* (1999). The filamentous fungi represented by *Oidiodendron truncatum* and *Oidiodendron griseum* produced the tetranorditerpenoid dilactone, oidiolactones A-D. These were shown to display bioactive properties similar to those produced by cladosporin, a known antifungal, antibacterial and insecticide compound (Hanessian *et al.*, 2009).

3.5 CONCLUSION

The purification and characterisation of *N. luteum* ethyl acetate crude extract was successful and proved that the purer a crude extract is; the more antimicrobial activity it possesses. This could be due to antagonistic effects of inactive compounds present in the crude extract. The compound isolated from the ethyl acetate extract of *N. luteum* showed good anti-*P. aeruginosa* activity and this is a step in the right direction in treating infections caused by *P. aeruginosa*.

3.6 REFERENCES

- Altemimi A, Watson DG, Kinsel M, Lightfoot DA. 2015. Simultaneous extraction, optimization, and analysis of flavonoids and polyphenols from peach and pumpkin extracts using a TLC-densitometric method. *Chemistry Central Journal*, 9: 39-54.
- Altemimi A, Lakhssassi N, Baharlouei A, Watson DG, Lightfoot DA. 2017. Phytochemicals: Extraction, isolation, and identification of bioactive compounds from plant extracts. *Plants*, 6: 42-65.
- Devika R, Koilpillai J. 2015. Column chromatographic separation of bioactive compounds from *Tagetes erecta* linn. *International Journal of Pharmaceutical Sciences and Research*, 6: 762-766.
- Dos Santos TT, de Souza Leite T, de Queiroz CB, de Araújo EF, Pereira OL, de Queiroz MV. 2016. High genetic variability in endophytic fungi from the genus *Diaporthe* isolated from common bean (*Phaseolus vulgaris* L.) in Brazil. *Journal of Applied Microbiology*, 120: 388-401.
- Eruygur N, Yılmaz G, Kutsal O, Yücel, G, Üstün O. 2016. Bioassay-guided isolation of wound healing active compounds from *Echium* species growing in Turkey. *Journal of Ethnopharmacology*, 185: 370-379.
- Fall AD, Bagla VP, Bassene E, Eloff JN. 2017. Hytochemical screening, antimicrobial and cytotoxicity studies of ethanol leaf extract of *Aphania senegalensis* (sapindaceae). *African Journal of Traditional Complementary Alternative Medicine*, 14: 135- 139.
- García A, Rhoden SA, Filho CJ, Nakamura CV, Pamphile JA. 2012. Diversity of foliar endophytic fungi from the medicinal plant *Sapindus saponaria* L. and their localization by scanning electron microscopy. *Biological Research*, 45: 139-148.
- Hanessian S, Boyer N, Reddy GJ, Deschênes-Simard B. 2009. Total synthesis of oidiodendrolides and related norditerpene dilactones from a common precursor: metabolites CJ-14,445, LL-Z1271γ, Oidiolactones A, B, C, and D, and Nagilactone F. *Organic Letters*, 11: 4640-4643.
- John M, Krohn K, Flörke U, Aust H, Draeger S, Schulz B. 1999. Biologically active secondary metabolites from fungi. Oidiolactones A–F, Labdane diterpene derivatives isolated from *Oidiodendron truncate*. *Journal of Natural Products*, 62: 1218–1221.

- Kanagavalli U, Sadiq AM. 2018. Isolation and characterization of bioactive compound anthraquinone from methanolic extract of *Boerhavia diffusa* linn. *Journal of Drug Delivery and Therapeutics*, 8(5-s): 232-237.
- Kaur H, Onsare, JG, Sharma V, Singh AD. 2015. Isolation, purification, and characterization of novel antimicrobial species and its cytotoxicity studies. *Journal of Applied and Industrial Microbiology*, 5: 1-13.
- Lin Y, Pei-Ji Z, Juan M, Chun-Hua L, Yue-Mao S. 2009. Labdane and Tetranorlabdane Diterpenoids from *Botryosphaeria* sp. MHF, an Endophytic fungus of *Maytenus hookeri*. *Helvetica Chimica Acta*, 92: 1118-1125.
- Lopes A, Barradas C, Phillips AJL, Alves A. 2016. Diversity and phylogeny of *Neofusicoccum* species occurring in forest and urban environments in Portugal. *Mycosphere*, 7: 1-16.
- Malhadas C, Malheiro R, Pereira JA, de Pinho PG, Baptista P. 2017. Antimicrobial activity of endophytic fungi from olive tree leaves. *World Journal of Microbiology and Biotechnology*, 33: 46-58.
- Pettit GR, Tan R, Herald DL, Hamblin J, Pettit RK. 2003. Antineoplastic Agents. 488. Isolation and structure of Yukonin from a Yukon Territory fungus. *Journal of Natural Products*, 66: 276-278.
- Poongunran J, Perera HK, Jayasinghe L, Fernando IT, Sivakanesan R, Araya H, Fujimoto Y. 2016. Bioassay-guided fractionation and identification of α -amylase inhibitors from *Syzygium cumini* leaves. *Pharmaceutical Biology*, 55: 206-211.
- Reveglia P, Savocchia S, Billones-Baaijens R, Masi M, Cimmino A, Antonio EA. 2018. Phytotoxic metabolites by nine species of *Botryosphaeriaceae* involved in grapevine dieback in Australia and identification of those produced by *Diplodia mutila*, *Diplodia seriata*, *Neofusicoccum australe* and *Neofusicoccum luteum*. *Natural Product Research*, DOI: 10.1080/14786419.2018.1497631.
- Rezgui A, Vallance J, Ben Ghnaya-Chakroun A, Bruez E, Dridi M, Demasse RD, Sadfi-Zouaoui N. 2018. Study of *Lasiodiplodia pseudotheobromae*, *Neofusicoccum parvum* and *Schizophyllum commune*, three pathogenic fungi associated with the Grapevine Trunk Diseases in the North of Tunisia. *European Journal of Plant Pathology*, 152(1), 127-142.
- Saikkonen K, Ion D, Gyllenberg M. 2002. The persistence of vertically transmitted fungi in grass metapopulations. *Proceedings of the Royal Society B: Biological Sciences* 269: 1397-1403.

Slippers B, Boissin E, Phillips AJL, Groenewald JZ, Lombard L, Wingfield MJ, Postma A, Burgess T, Crous PW. 2013 – Phylogenetic lineages in the Botryosphaeriales: a systematic and evolutionary framework. *Studies in Mycology*, 76: 31-49.

CHAPTER 4: SUMMARY, CONCLUSIONS AND RECOMMENDATIONS FOR FUTURE WORK

4.1 SUMMARY OF FINDINGS

Plate stocks and mineral oil slants for endophytic storage are more efficient than glycerol stocks as plate stocks and mineral oil slants stocks resulted in fungal resuscitation with no contamination as opposed to glycerol stocks. Phenotypic traits of the endophytic fungi change slightly in response to being sub-cultured from different stocks over time. Due to fungal extracts being diverse and relatively untested for optimal time for the production of the bioactive compound, it was crucial to set up a time course in order to identify this for the anti-*P. aeruginosa* bioactive compound. Although the compound appears within one week of growth, maximal levels were produced at 4 weeks of growth. Over the various intervals of growth tested, the profiles of compounds varied.

It was important to assess the effect of purification on the anti-*P. aeruginosa* activity of the compound. Crude extracts contain a variety of compounds which either act together to have a combined effect, act against each other or each compound may have entirely different activities. Literature reports that bioactivity increases with purity due to the desired compound being present in higher concentrations and with no impurities. It needs to be noted that some studies have reported purification to have the opposite effect due to the compounds found in the crude extract acting synergistically. Thus, the purer the compound was, the more reduced its ability to inhibit a test organism was.

Isolation of the active metabolite from the crude extract and characterisation showed the compound to be a dilactone (3a,10b-dimethyl-1,2,3,3a,5a,7,10b,10c-octahydro-5,8-dioxacephenanthrylene-4,9-dione) which displayed anti-*P. aeruginosa* activity against a resistant strain. This has been a new approach in using this compound which was previously reported

to display antifungal activity and inhibit both lipopolysaccharide-induced interleukin-1 β and tumour necrosis factor- α production in human whole blood.

4.2 CONCLUSIONS

The aim of this study was to purify, identify and characterise ZF 52 and other *K. africana* endophytic fungi against *P. aeruginosa* which was a relatively new approach. When comparing the MIC of the crude, semi-purified and purified extract, the MIC of the purified extract had the most anti-*P. aeruginosa* activity. Characterisation and identification were successful and achieved by NMR spectroscopy. The isolated bioactive metabolite from the extract of *N. luteum* was identified as a dilactone (3a,10b-dimethyl-1,2,3,3a,5a,7,10b,10c-octahydro-5,8-dioxo-acephenanthrylene-4,9-dione). As purification of the *N. luteum* extract was successful, the hypotheses were accepted. Although the isolated compound is not novel and has previously been shown to have activity against some fungal species, its ability to inhibit the growth of *P. aeruginosa* to this degree is new. This suggests that known compounds need to be screened across a wide range of pathogens and organisms to determine potential activity.

4.3 RECOMMENDATIONS FOR FUTURE WORK

With the vast amount and rapid emergence of bacterial resistance to antibiotics, more testing of the anti-*P. aeruginosa* compound would help reduce the speed at which this pathogen gains resistance. Although the anti-*P. aeruginosa* activity was determined against one resistant strain of *P. aeruginosa*, in order to conclusively realise the activity of this compound it be tested against as many different resistant strains as possible as well as against any clinical strains with emerging resistance.

Column chromatography was used as a purification method, for future studies it may be beneficial to use prep-HPLC for purification as higher yields and greater purity of the purified product are reported to be obtained using this technique. The purified compound 1 isolated in this study is a known diterpene lactone that was first isolated from a marine sponge and demonstrated to have antifungal activity (John *et al.*, 1999). This finding highlights the fact that bioactive compounds need to be screened against a wide a panel as possible in order to properly determine their bioactive potential. A compound previously shown to have activity against one pathogen needs to be screened against a wide range of other pathogens, especially newly developing resistant strains, as a potential drug candidate may already be available, but its full spectrum not yet elucidated, and screening would provide a more rapid solution as the compound has already been purified and identified.

The determination of the mode of action (assessing membrane integrity) using a capturing confocal scanning laser microscope is also an important factor and next step in the process in deciding whether or not a compound will be taken to the next level of testing (pre-clinical screening and testing) and if the compound still looks promising, safety and efficacy clinical trials, as well as drug development, formulation and production.

Interdisciplinary research involving Microbiology, Animal biology and Chemistry is key in fast tracking future drug development. This is because different disciplines have access to different materials. It would be interesting to investigate anti-cancer and a- diabetic activities, however the Microbiology department does not have a tissue culture lab for anti-cancer determination, nor does it supply mice for anti-diabetic trails.

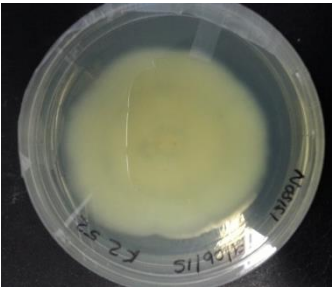


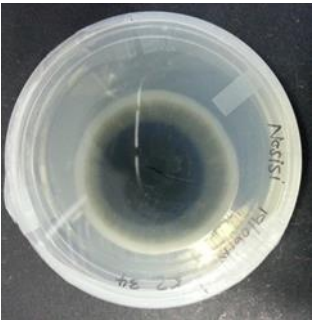
4.4 REFERENCES

John M, Krohn K, Flörke U, Aust H, Draeger S, Schulz B. 1999. Biologically active secondary metabolites from fungi. Oidiolactones A–F, Labdane diterpene derivatives isolated from *Oidiodendron truncate*. *Journal of Natural Products*, 62: 1218–1221.

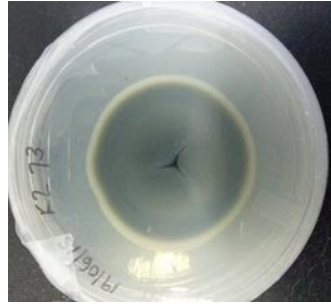
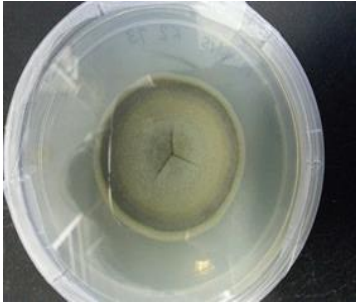
APPENDICES

APPENDIX A

Table A1: Growth of *K. africana* endophytic fungi on PDA.

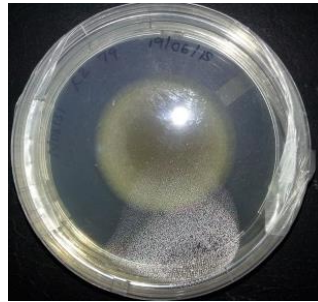
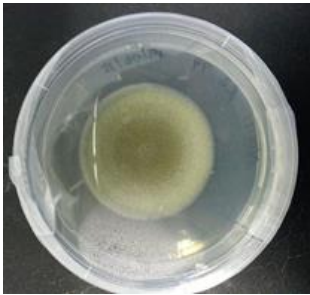
ISOLATE		Morphology
KZ 52		Top Brown centre with outward expansion. Green with a cream edge. Bottom Cream with light bottle green
		
KZ 34		Top Green of varying intensity as mycelia expand Bottom Navy centre, green expansion and white edge
		

KZ
73



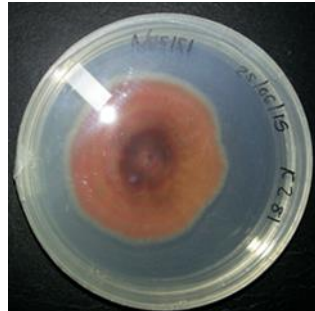
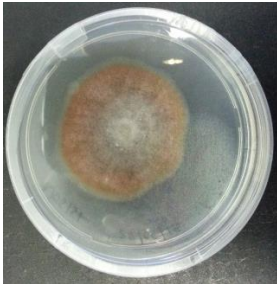
Top
Different shades of green and is lightest in the centre, with white edge
Bottom
Green with a white edge

KZ
79



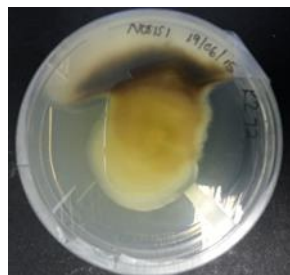
Top
Green, with the lightest shade at the centre
Bottom
Black with light green to white edge

KZ
81



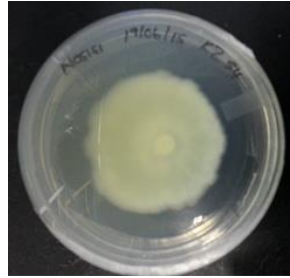
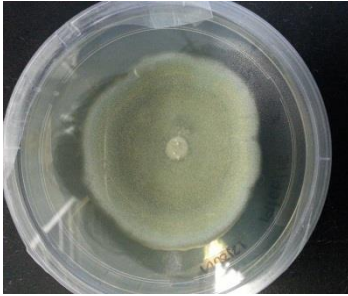
Top
Red with white woolly matter
Bottom
Brown centre with red carcadia

KZ
72



Top
Green with white edge
Bottom
Yellow, darkest at the centre, with black extremities

KZ
54



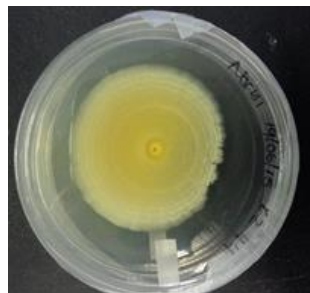
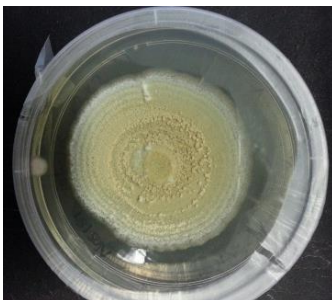
Top
Light green with faint green extremity
Bottom
White and snotty looking

KZ
49



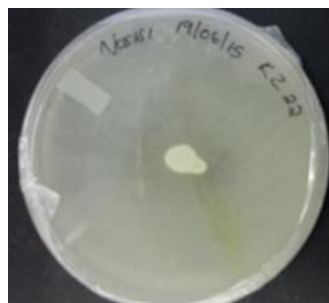
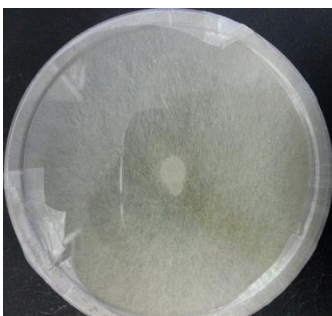
Top
Black, which changes to green as it spreads out
Bottom
Black at the centre and becomes lighter as fungi expands

KZ
44



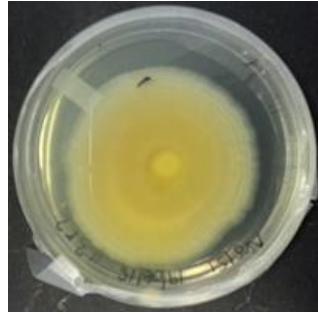
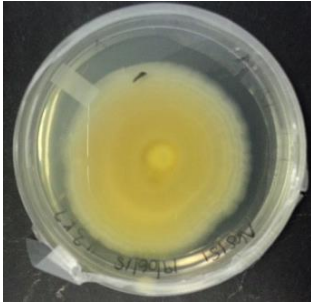
Top
Light green with white fluff
Bottom
Intense yellow and expands to be light yellow

KZ
22



Top
White fluff
Bottom
White centre, growing towards the ends with black dots/spores

KZ
43



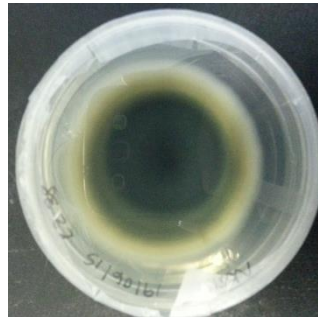
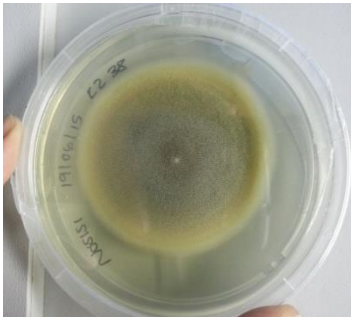
Top

Light brown with white fluff growing on the surface

Bottom

Yellow with circular yellow rings which become less intense

KZ
38



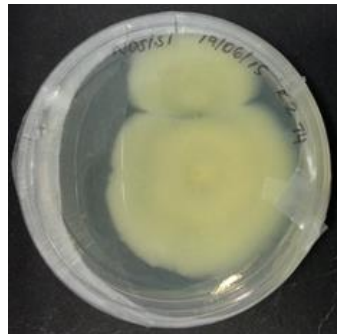
Top

Oldest part of the mycelia is bottle green and becomes faint green as it spreads out

Bottom

Pale green as it spreads to fresh medium, becomes intense green as it ages

KZ
74



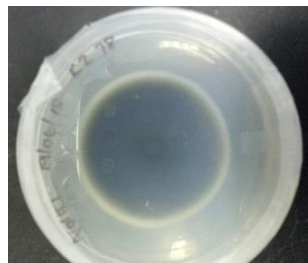
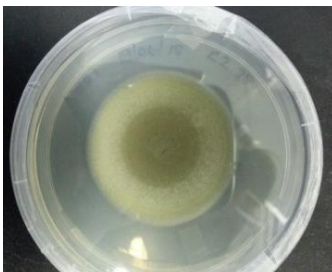
Top

Light green at the centre which becomes darker as it grows out

Bottom

White at the centre which becomes darker as it grows outward

KZ
78



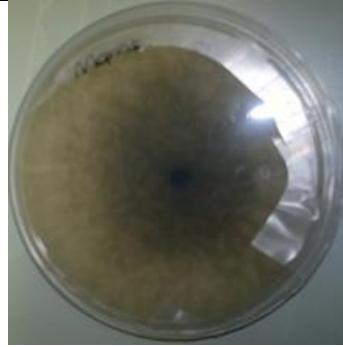
Top

Green centre with white fluff as it grows away from the centre

Bottom

Black with green and white colouration

**ZF
91**



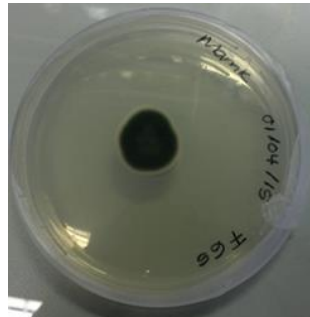
Top

Black inoculum plug which spreads to be white

Bottom

Becomes white as it spreads to fresh media. The oldest part is black

**ZF
65**



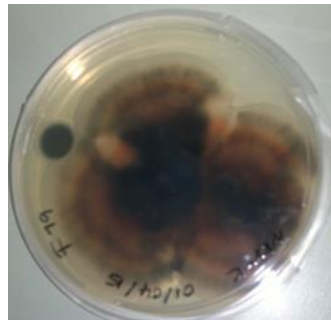
Top

Oldest part is black, spreads to be green. Has wholly fluff covering it

Bottom

Bottle green centre, with darker edges

**ZF
79**



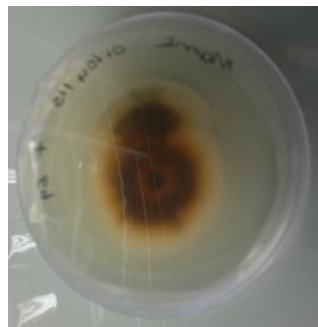
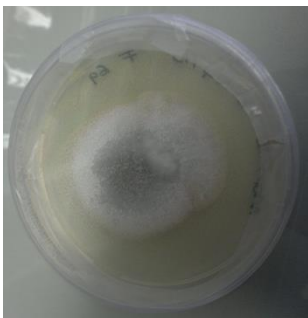
Top

Black with white fluff covering the surface

Bottom

Black centre, becomes orange as it spreads

**ZF
69**



Top

Green centre and grows to have fluff at the extremities

Bottom

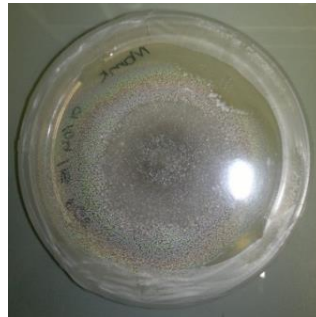
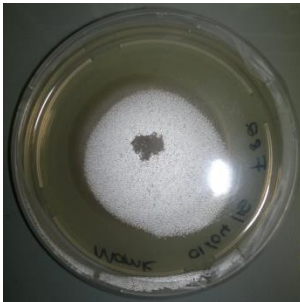
Intense orange centre and turns yellow as it grows in fresh media

**ZF
88**



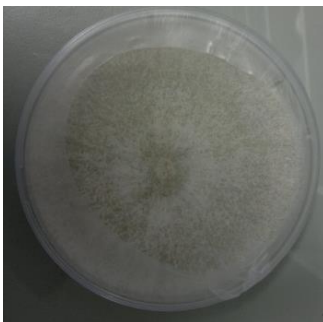
Top
White centre which
spreads to be ivory
Bottom
Pale brown centre which
Grows pale yellow

**ZF
68**



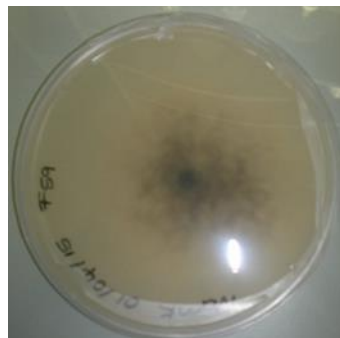
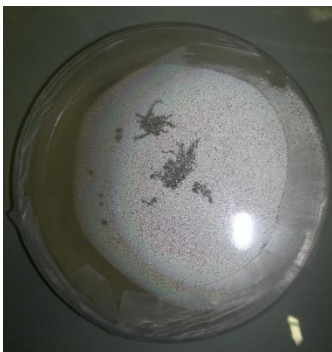
Top
Black centre which
spreads to be yellow
Bottom
Green and spreads

**ZF
84**



Top
Yellow at the centre and
spreads to have white
fluff
Bottom
Black initial growth at
the centre and spreads to
be pale yellow

**ZF
59**



Top
The centre has green
growth at the centre
Bottom
Black centre and grows
yellow as it spreads to
fresh media

**ZF
53**



Top

Orange at the centre, becomes white as it spreads to fresh media

Bottom

Intense orange centre and white edges

**ZF
96**



Top

Ivory centre with off-white extremities

Bottom

Ivory centre with

**ZF
66**



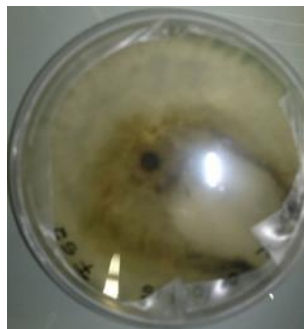
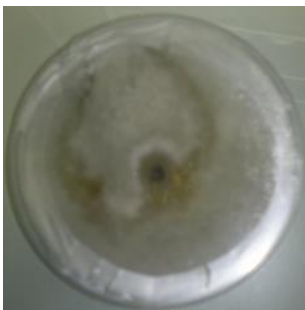
Top

Black centre, spreads white

Bottom

Brown centre, which spreads ivory

**ZF
52**



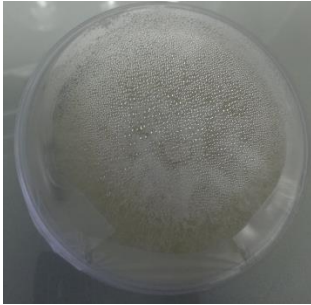
Top

Black centre, spreads yellow and white at the extremities

Bottom

Black with yellow edges

**ZF
58**



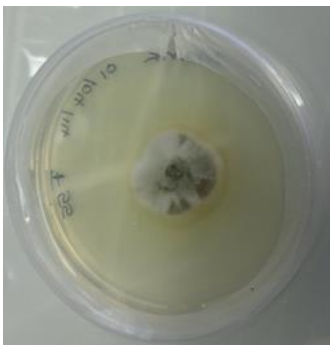
Top

Ivory centre, which spreads white

Bottom

Ivory and becomes white with fresh media

**ZF
55**



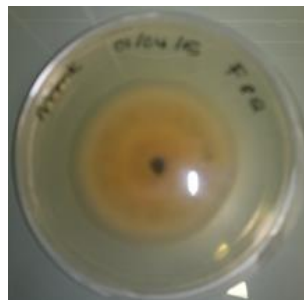
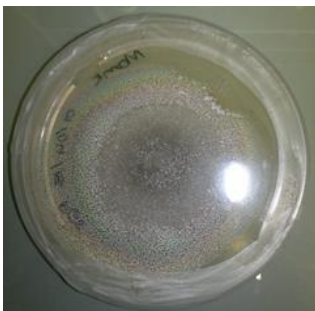
Top

Black centre, spreads green into fresh media

Bottom

Bottle green centre, becomes less intense green as it spreads to fresh media

**ZF
82**



Top

Green centre, becomes yellow as it grows on fresh media

Bottom

Black centre with new mycelia appearing yellow

ZF 5



Top

Mycelia looks green and turns black as it ages

Bottom

Black with ivory edges

P. aeruginosa

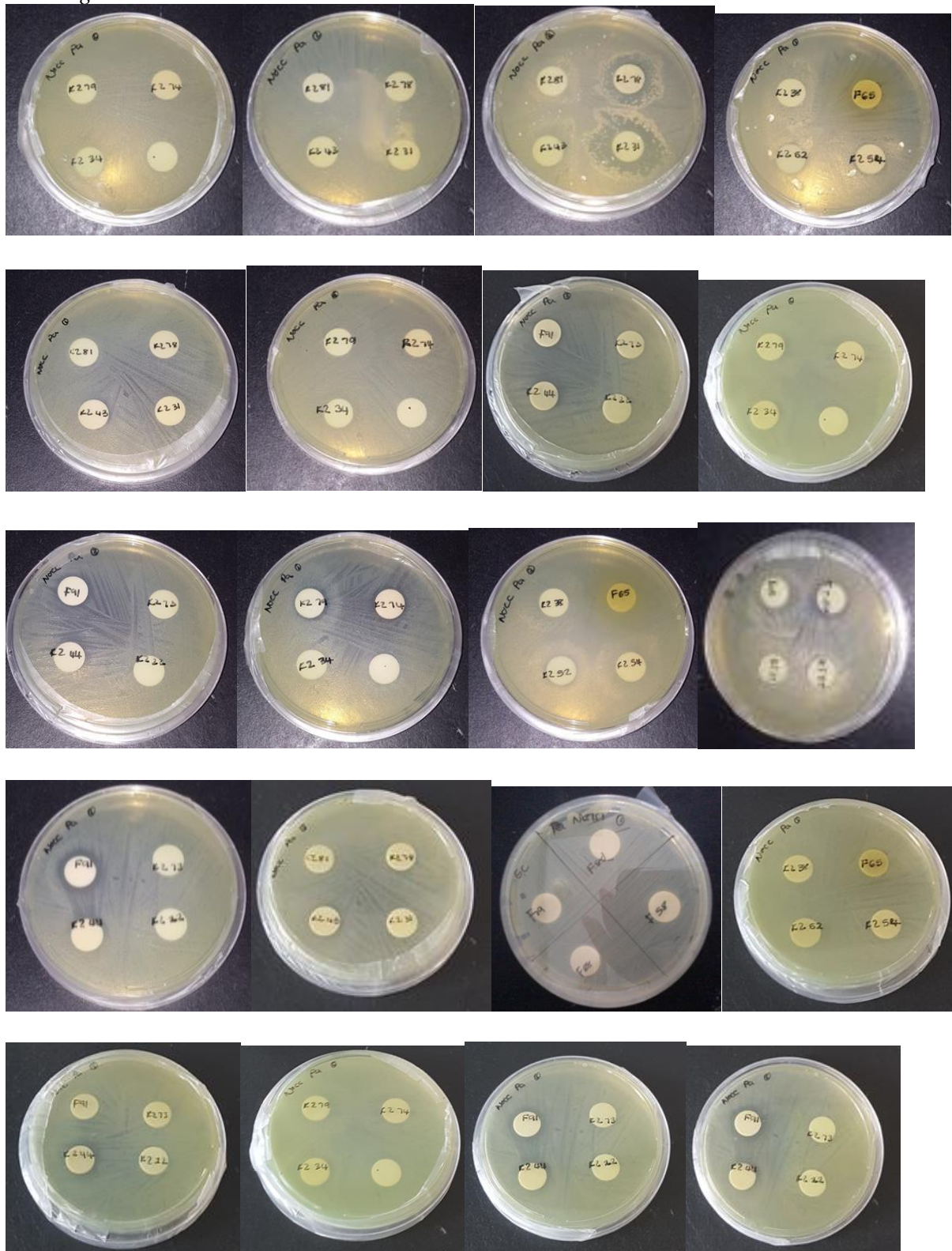
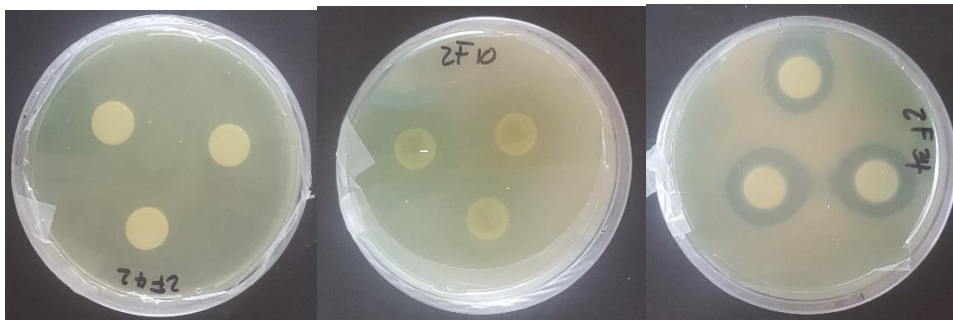
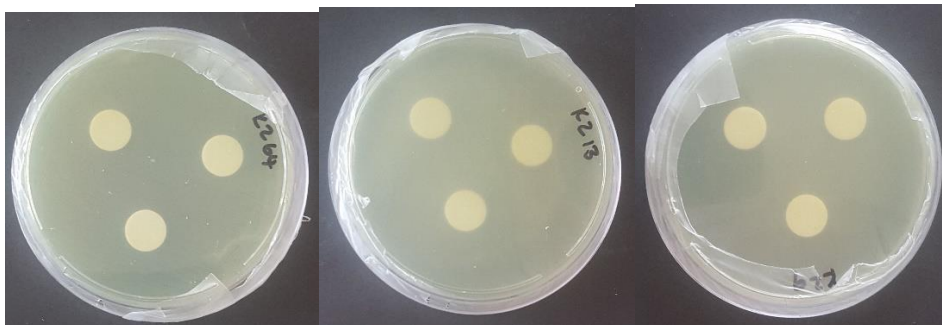
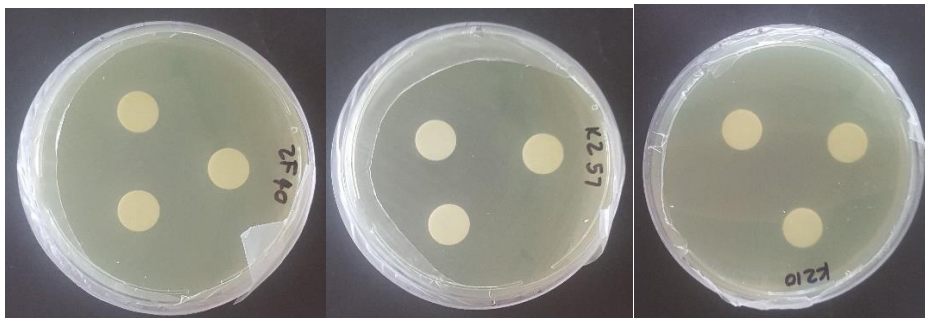
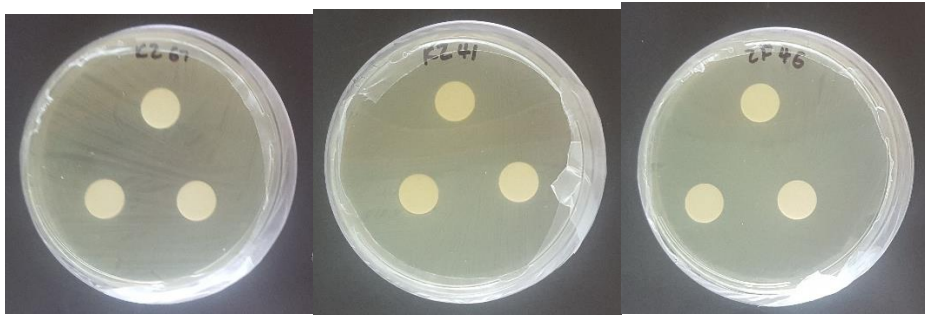


Figure B1.1: Kirby Bauer disc diffusion assay showing zones of inhibition by *K. africana* endofungal extracts



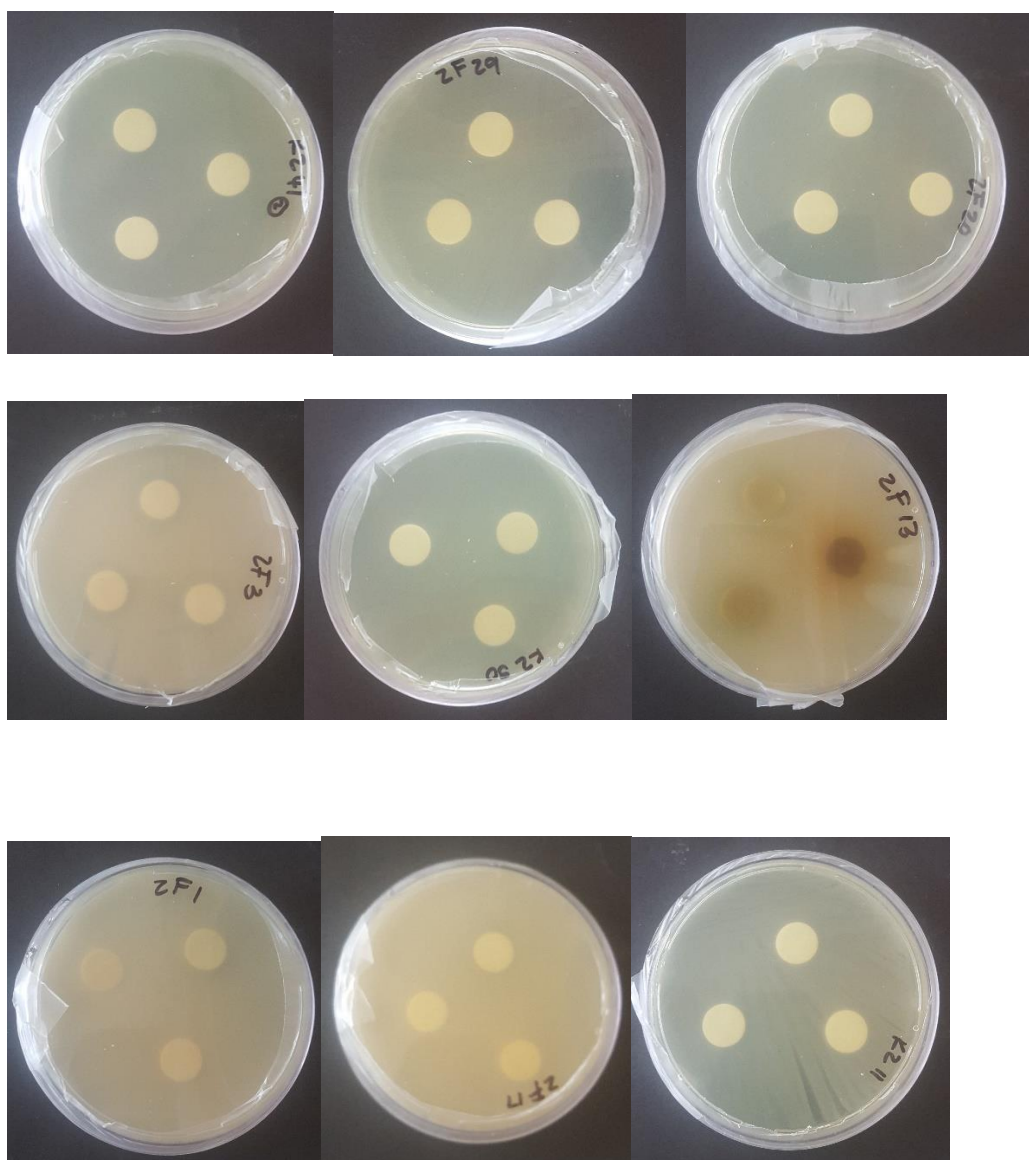


Figure B1.2: Kirby Bauer disc diffusion assay of Lab 2 extract stocks.

Table B1: Raw data from the Kirby Bauer disc diffusion assay for initial screening of extracts

	Zone of inhibition (mm)			Avg	STD
ZF52	42	40	39	40,33333	1,080123
ZF34	22	19	20	20,33333	1,080123
ZF91	20	25	20	22	2.357023

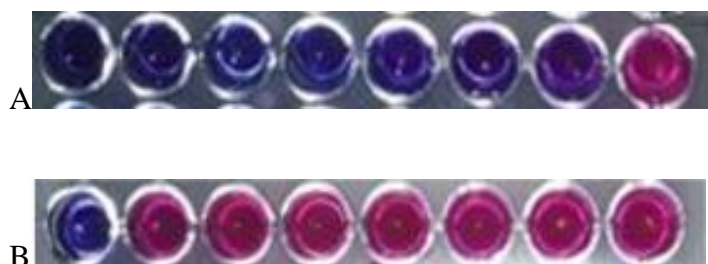
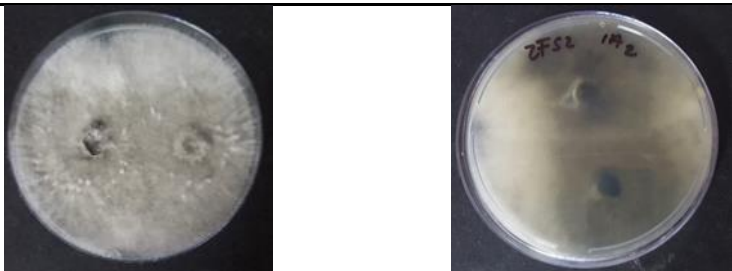


Figure B2: Resazurin colour reaction for MIC determination; A: ZF 52 and B: ZF 91.

Of the screened isolates ZF91, ZF52 and ZF 34 revealed anti-*P. aeruginosa* compounds of interest, however when ZF 91 was sub-cultured from stocks it did not grow and ZF34 was a lab isolate extract and the stock culture wasn't found. Therefore, ZF 52 was the only fungal isolate used for further testing.

APPENDIX C

Table C1: Growth of ZF 52 endophytic fungus on PDA.

Fungal isolate	Morphology
	<p>Top Older mycelia look black, as it grows on new media it turns cream/light yellow</p> <p>Bottom Black centre with new mycelia being yellow</p>

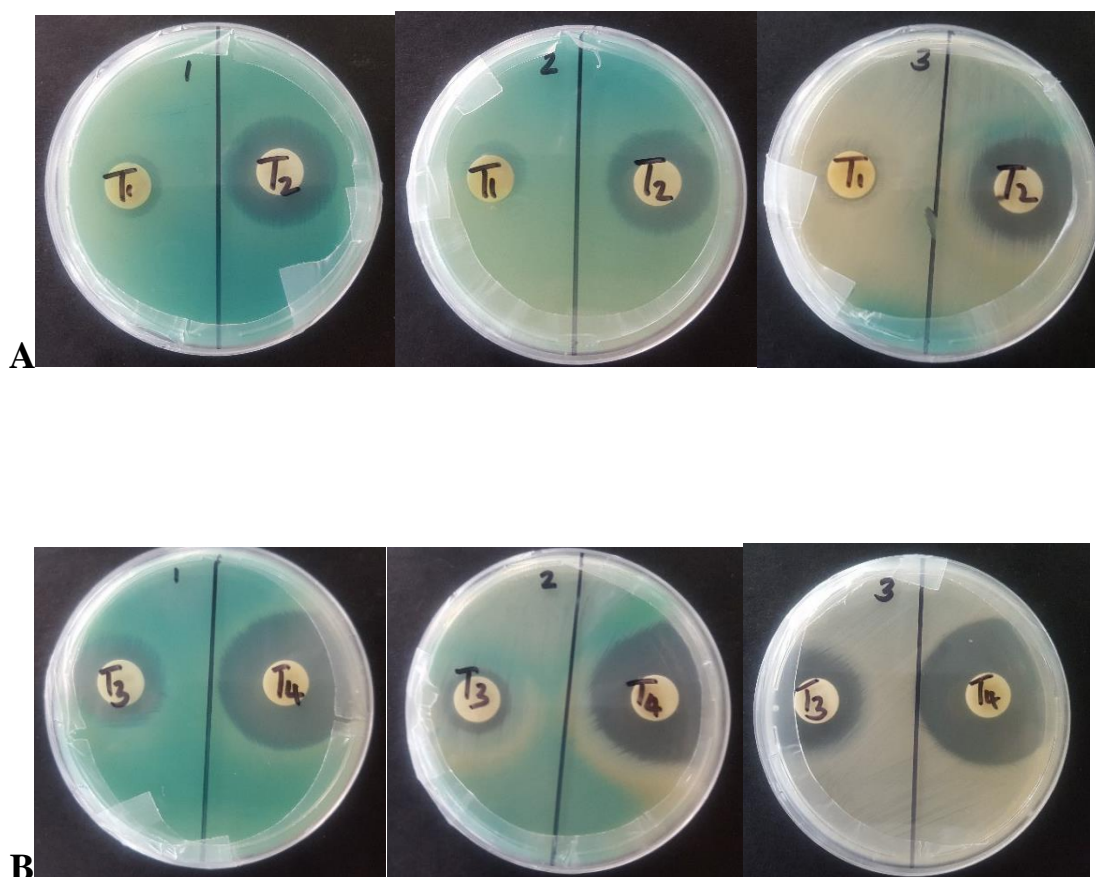


Figure C1: Kirby Bauer disc diffusion assay showing zones of inhibition produced by ZF 52 endofungal extracts against *P. aeruginosa*. A (T1 and T2) and B (T3 and T4).

Table C2: Raw data from the Kirby Bauer disc diffusion assay of the time course extracts.

Extract (days)	Triplicate 1	Triplicate 2	Triplicate 3	Average	Standard deviation
T1	14	17	15	15,33333	1,080123
T2	28	27	27	27,33333	0,408248
T3	25	18	28	23,66667	3,62859
T4	42	40	39	40,33333	1,080123

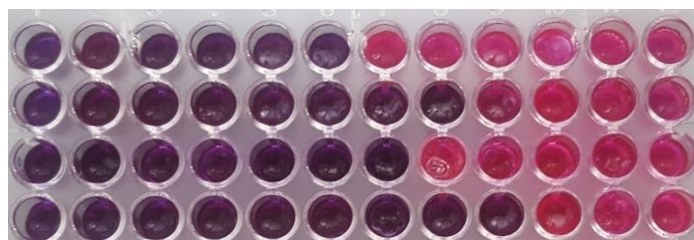


Figure C2: Resazurin colour reaction for MIC determination of extracts against *P. aeruginosa*.

Row A: 1 week ZF 52 extract (156.3 µg/mL); row B: 2 weeks ZF 52 extract (39.06 µg/mL); row C: 3 weeks old ZF 52 extract (78.13 µg/mL) and row D is 4 weeks old ZF 52 extract (19.53 µg/mL).

Table C3: Interpretation of the resazurin microtitre assay.

Extract age	Concentration (µg/mL)											
	5000	2500	1250	625	312.5	156.3	78.13	39.06	19.53	9.766	4.883	2.441
T1	-	-	-	-	-	-	+	+	+	+	+	+
T2	-	-	-	-	-	-	-	-	+	+	+	+
T3	-	-	-	-	-	-	-	+	+	+	+	+
T4	-	-	-	-	-	-	-	-	-	+	+	+

Identification of ZF 52

Sequencing data:

GGGKACTGCGGAGATCATTACCGAGTTGATTCGAGCTCCGGCTCGACTCTCCCAC
CCTATGTGTACCTACCTCTGTTGCTTTGGCGGGCCGCGGTCCTCCGCACCGGCGC
CCTTCGGGGGGCTGGCCAGCGCCCGCCAGAGGACCATAAACTCCAGTCAGTGA
ACTTCGCAGTCTGAAAAACAAGTTAATAAACTAAACTTTCAACAACGGATCTCT
TGGTTCTGGCATCGATGAAGAACGCAGCGAAATGCGATAAGTAATGTGAATTGC
AGAATTCAGTGAATCATCGAATC

Table C4: BLAST analysis of ZF 52.

Sequences producing significant alignments:

Select: [All](#) [None](#) Selected: 0

Alignments Download GenBank Graphics Distance tree of results							
	Description	Max score	Total score	Query cover	E value	Ident	Accession
<input type="checkbox"/>	Neofusicoccum luteum strain CMW 10309 18S ribosomal RNA gene, partial sequence; internal transcribed spacer 1, 5.8S ribosomal	1070	1070	99%	0.0	99%	KF766202.1

APPENDIX D

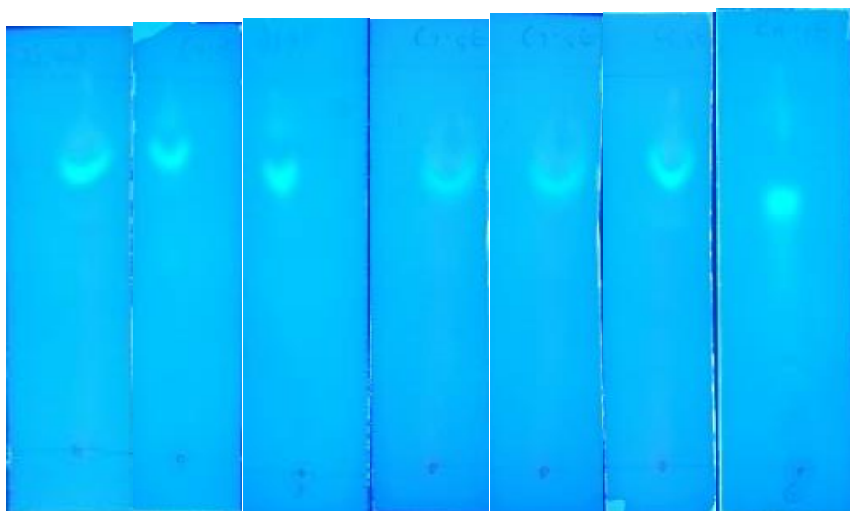


Figure D1.1: Thin layer chromatography of crude ethyl acetate extract chloroform:ethyl acetate.

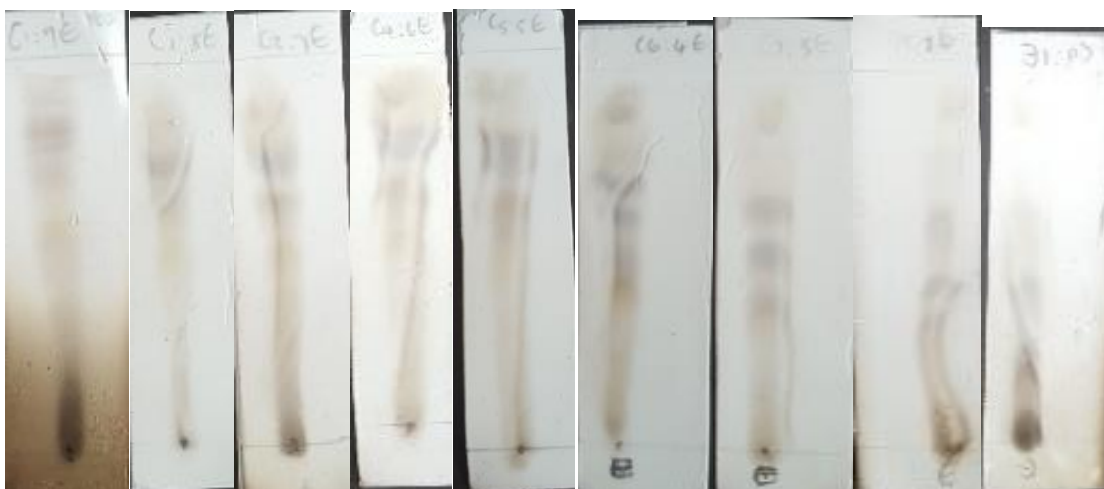


Figure D1.2: Thin layer chromatography of crude ethyl acetate extract chloroform:ethyl acetate stained with 5% methanol in sulphuric acid.



Figure D2: Thin layer chromatography of ethanol and methanol extracts using chloroform:Methanol.

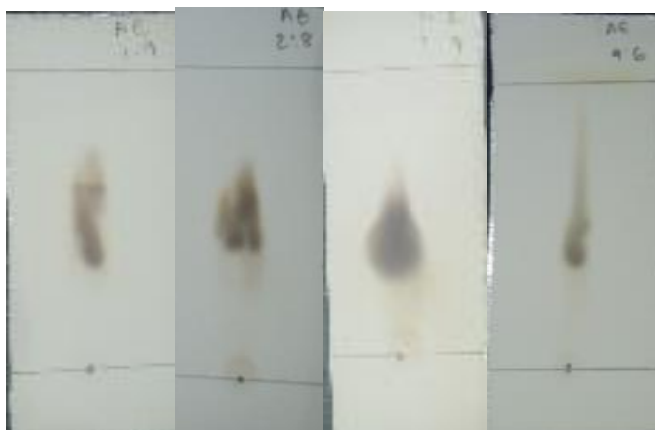


Figure D3: Thin layer chromatography of ZF 52 ethyl acetate extract using acetonitril:ethyl acetate

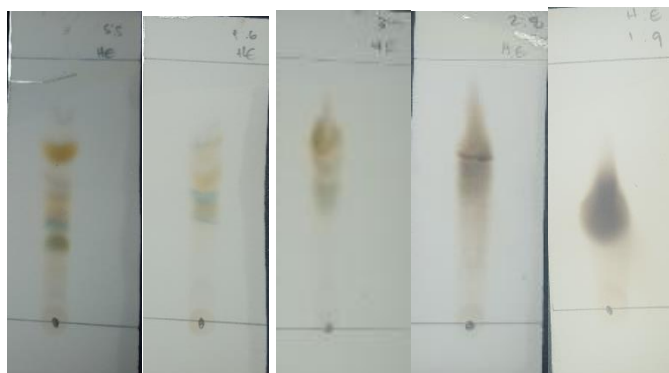


Figure D4: Thin layer chromatography of ZF 52 ethyl acetate extract using hexane:ethyl acetate

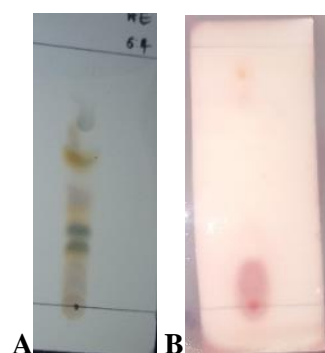


Figure D5: (A)Thin layer chromatography and (B) bioautography of the ZF 52 crude extract.

APPENDIX E

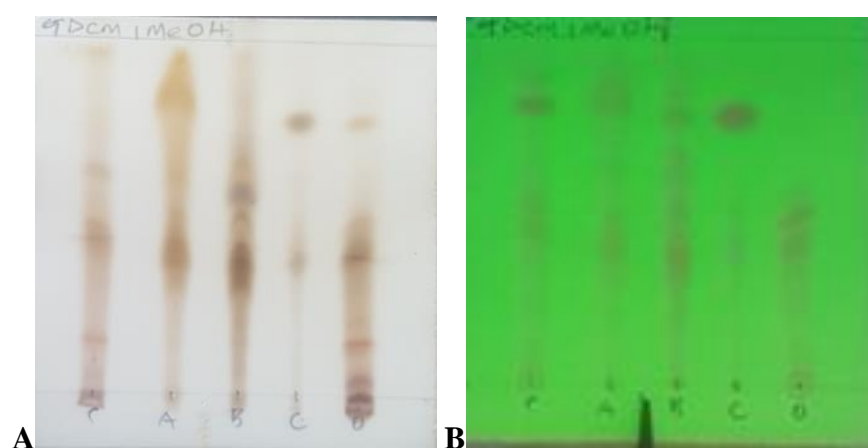


Figure E1: Thin layer chromatography of partially purified extract, with sub-fractions A, B, C and D.



Figure E2: Broth microtitre serial dilution assay for MIC determination of partially purified pooled fractions C



Figure E3: Broth microtitre serial dilution assay for MIC determination for purified compound 1.

APPENDIX F

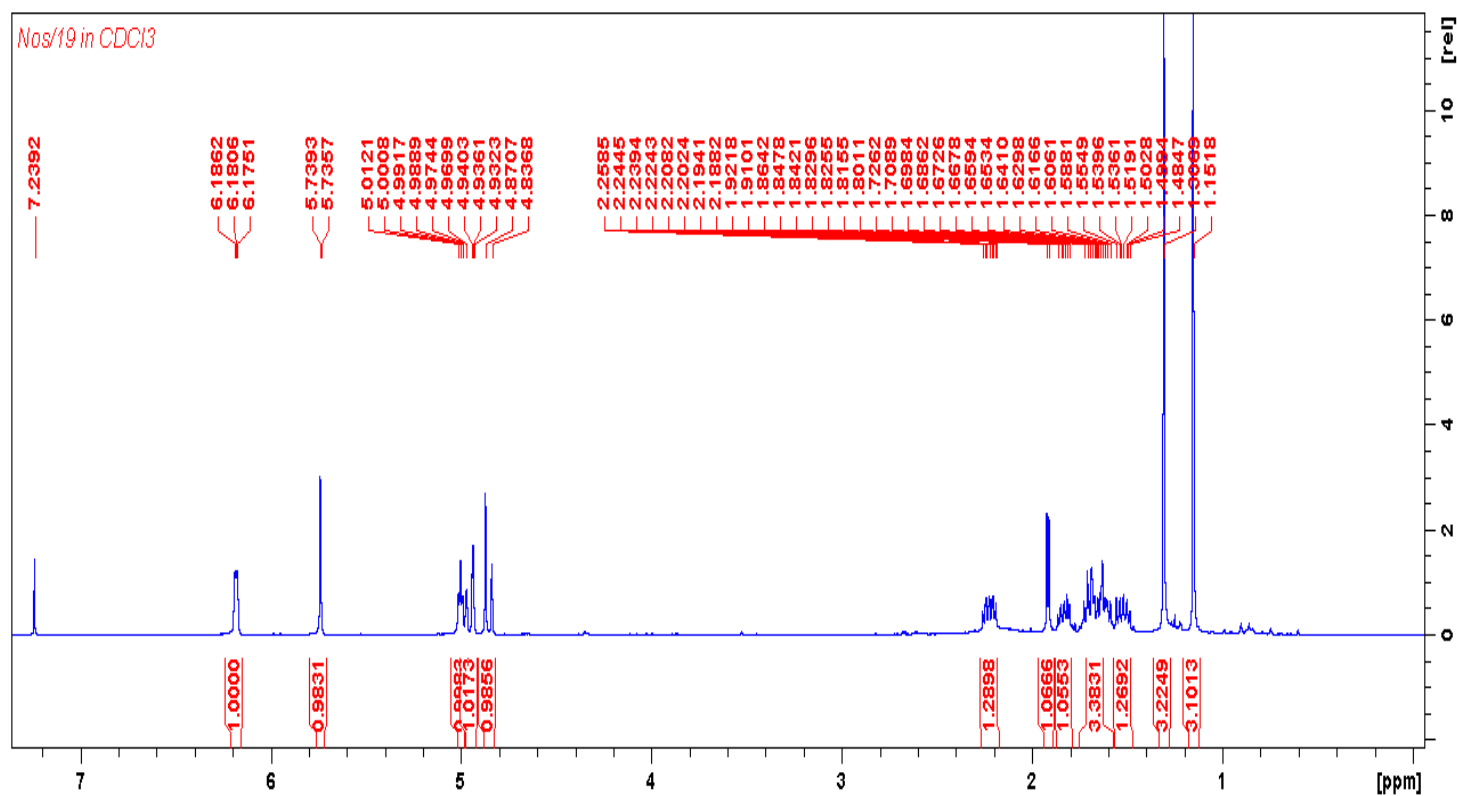


Figure F1: ¹H-NMR (chloroform d₁, MHz) of compound 1.

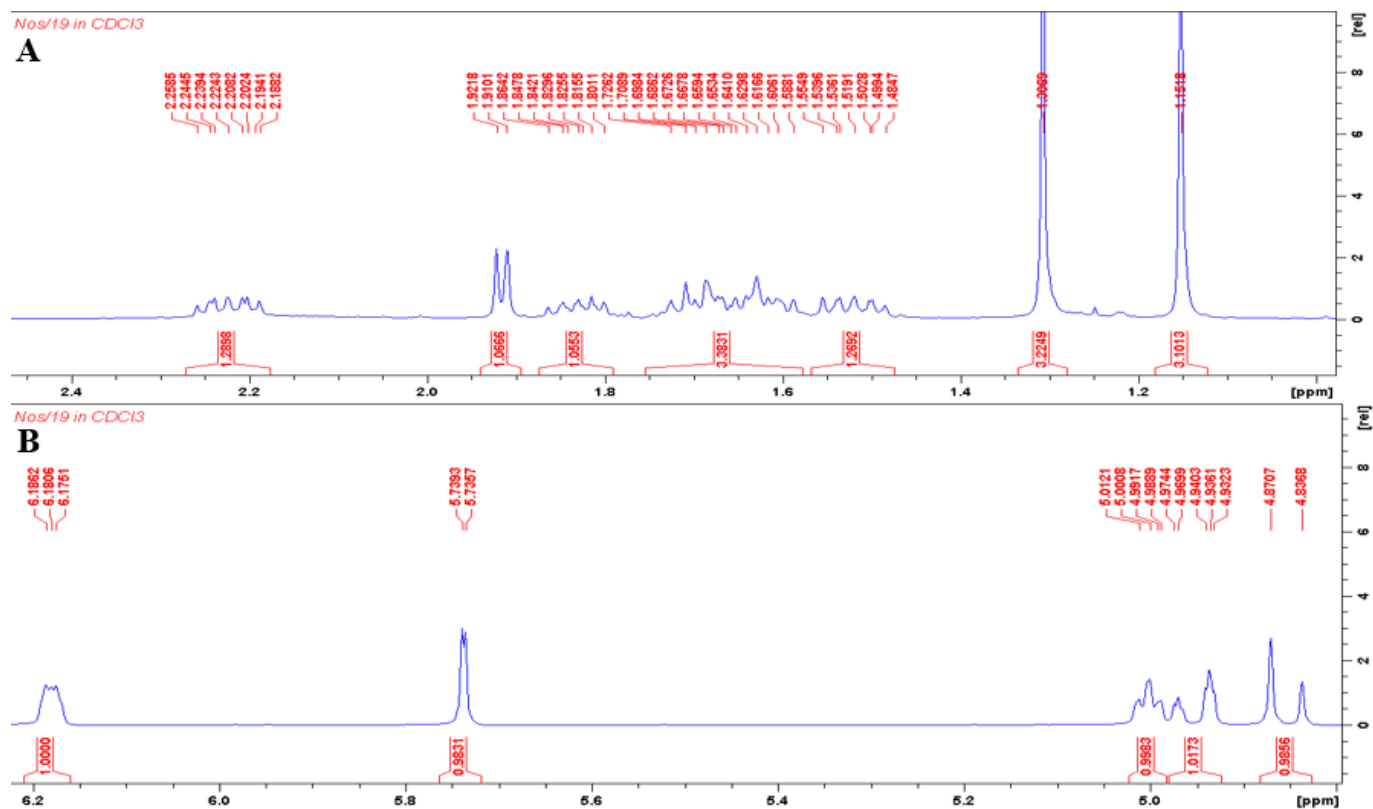


Figure F2: ¹H-NMR (chloroform d₁, MHz) of compound 1 (A and B).

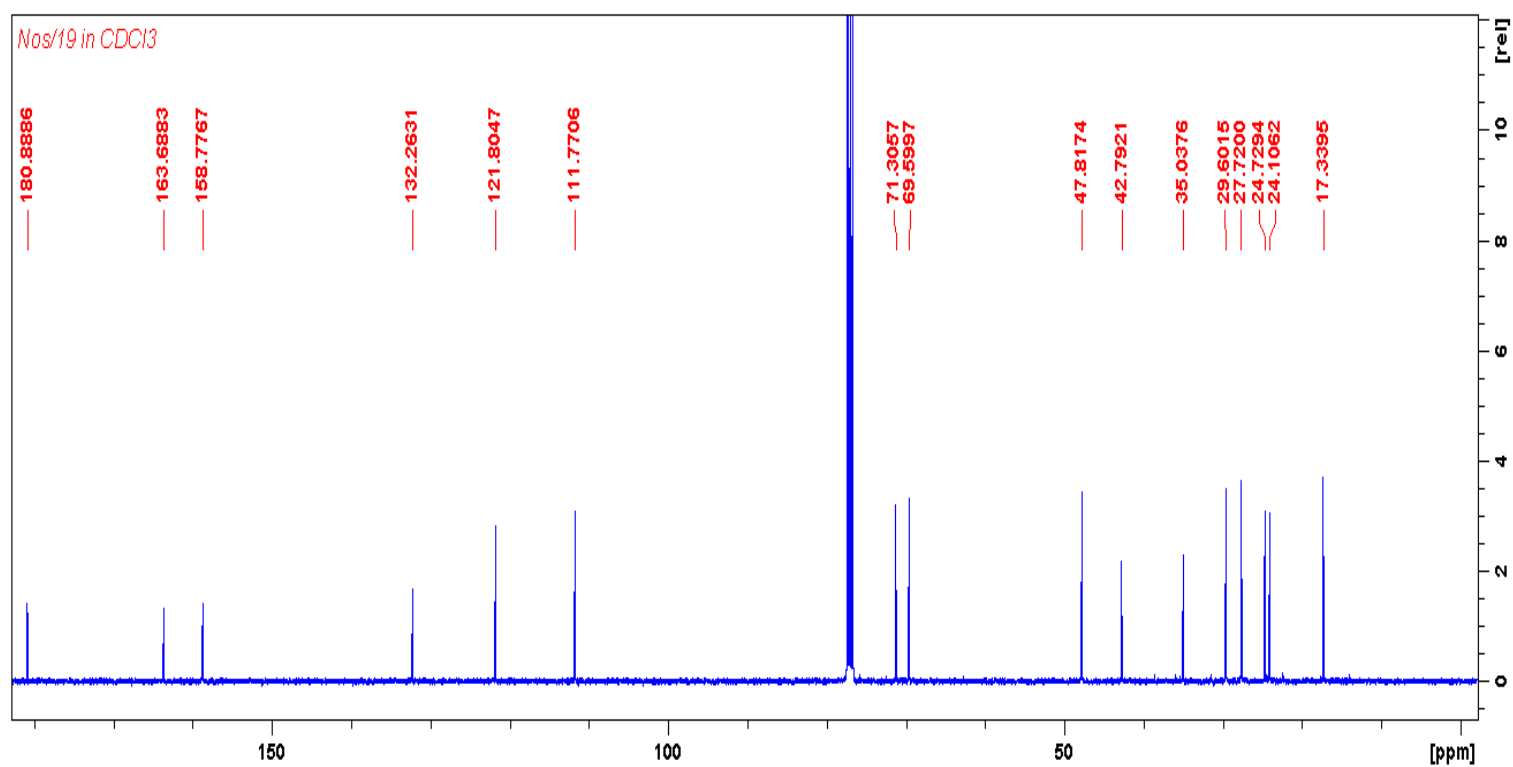


Figure F3: ¹³C-NMR of bioactive fraction compound 1.

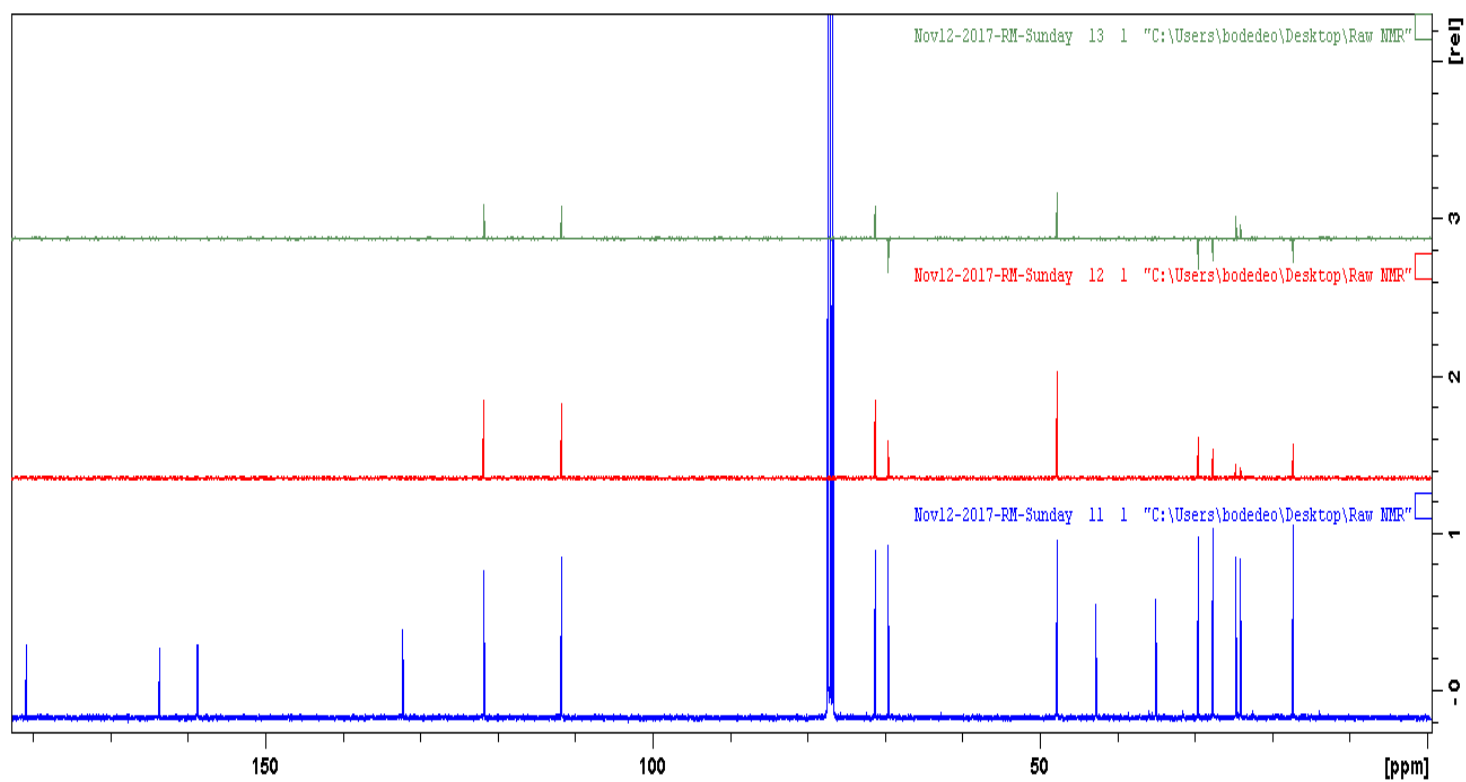


Figure F4: ^{13}C Dept 90 and Dept 135 of bioactive fraction superimposed.

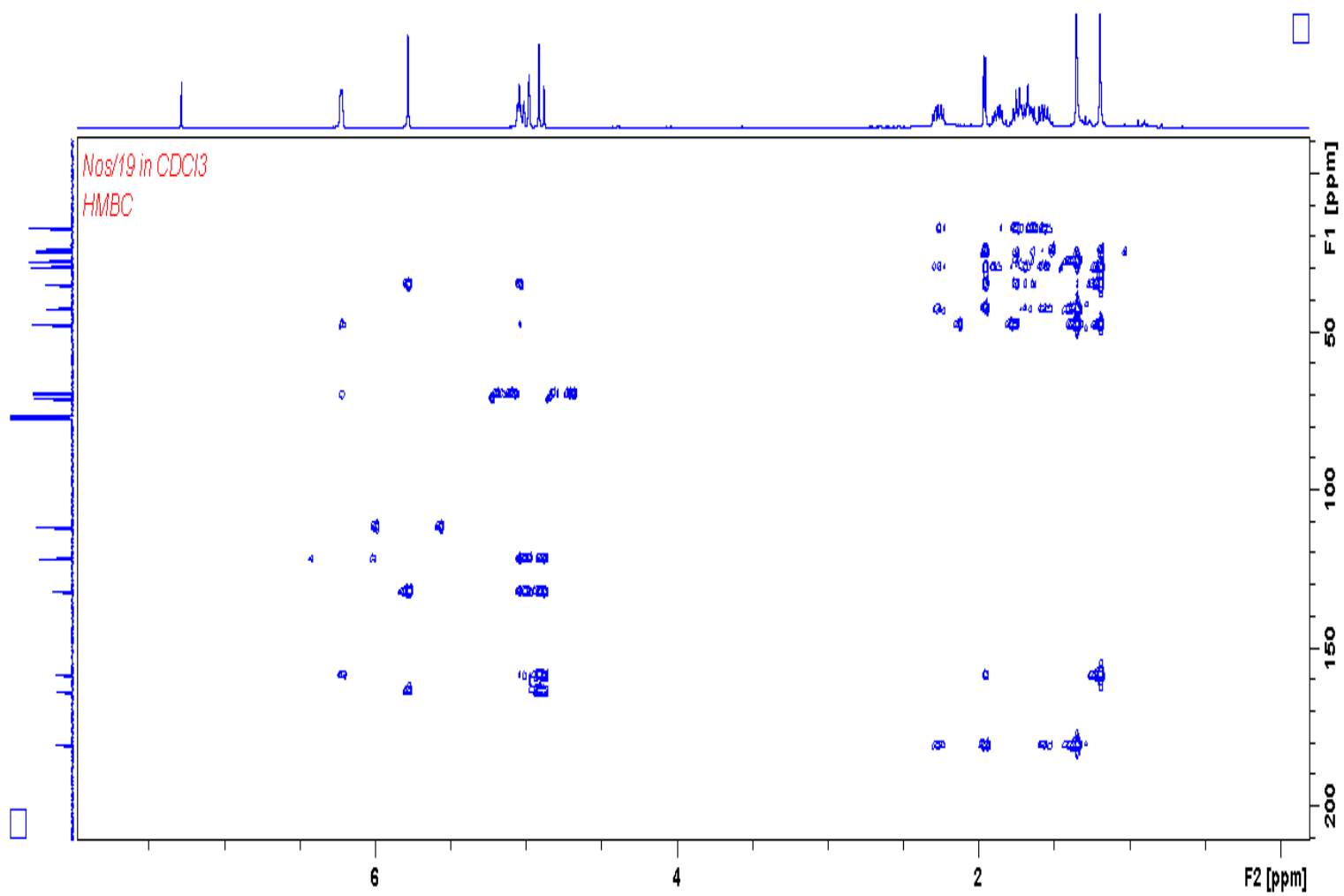


Figure F5: ^1H - ^{13}C HMBC NMR spectrum of compound 1.

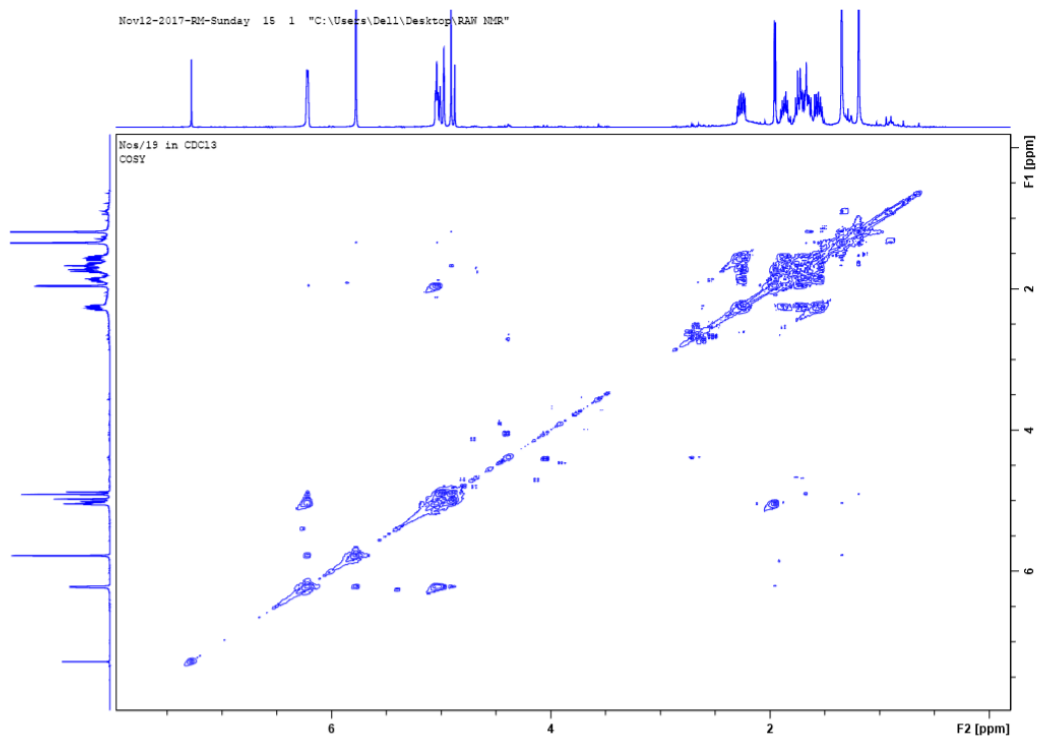


Figure F6: COSY ^1H -NMR spectrum of fraction compound 1.

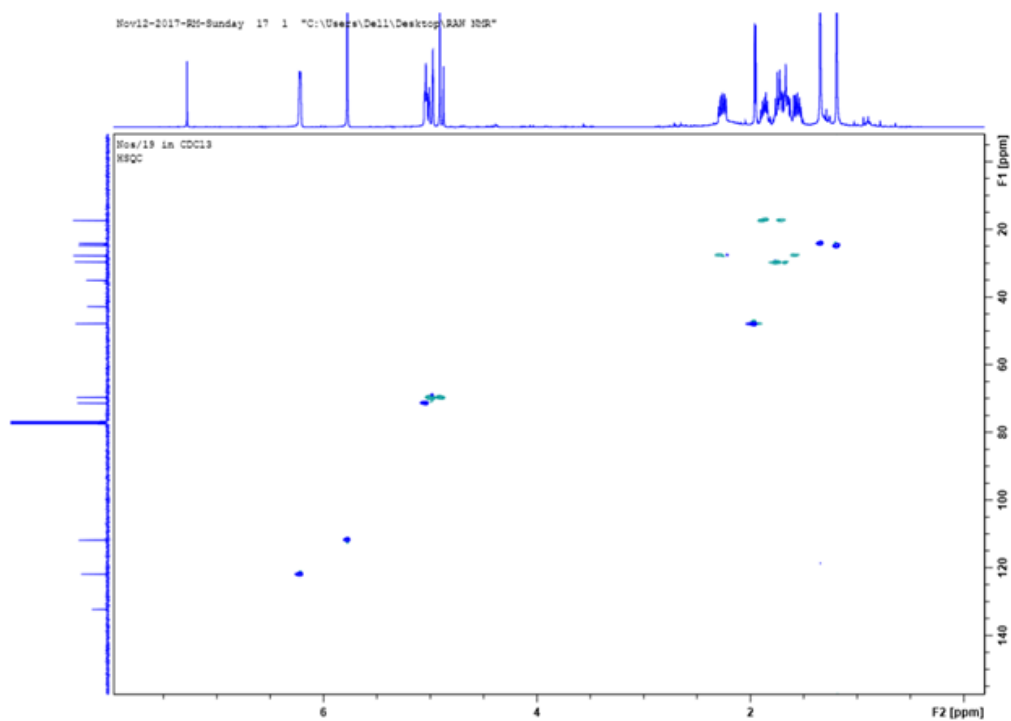


Figure F7: HSQC NMR spectrum of compound 1.

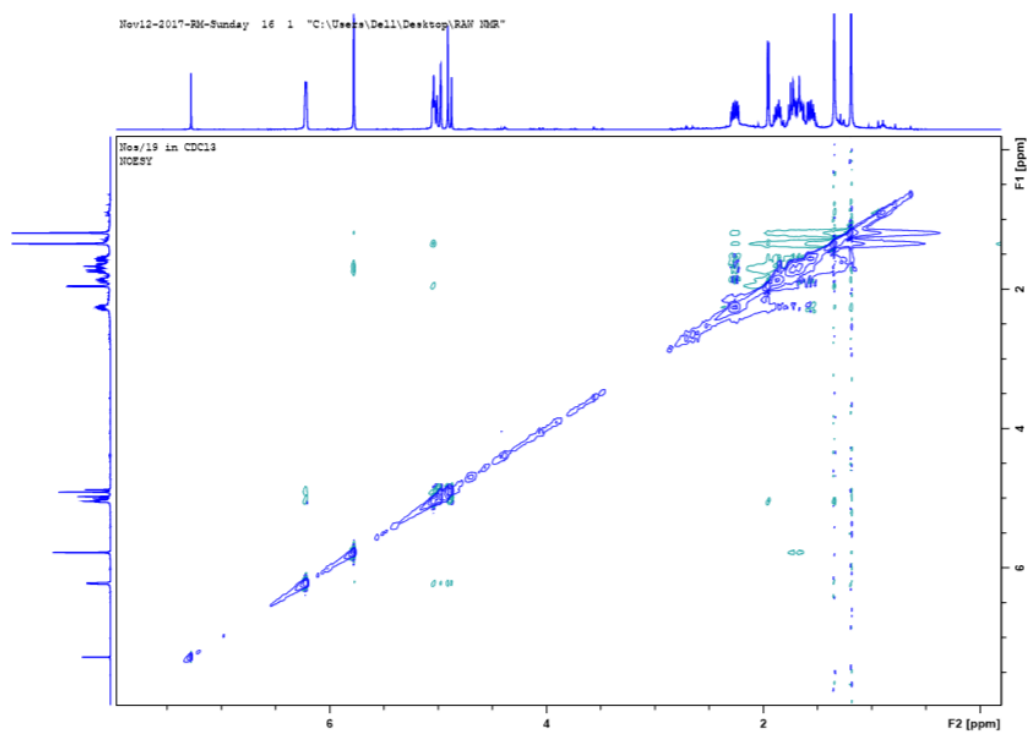


Figure F8: 2-D NOESY spectrum of compound 1.

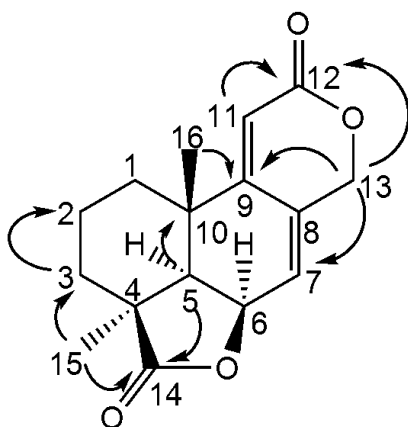


Figure F9: Major HMBC correlations observed in compound 1.

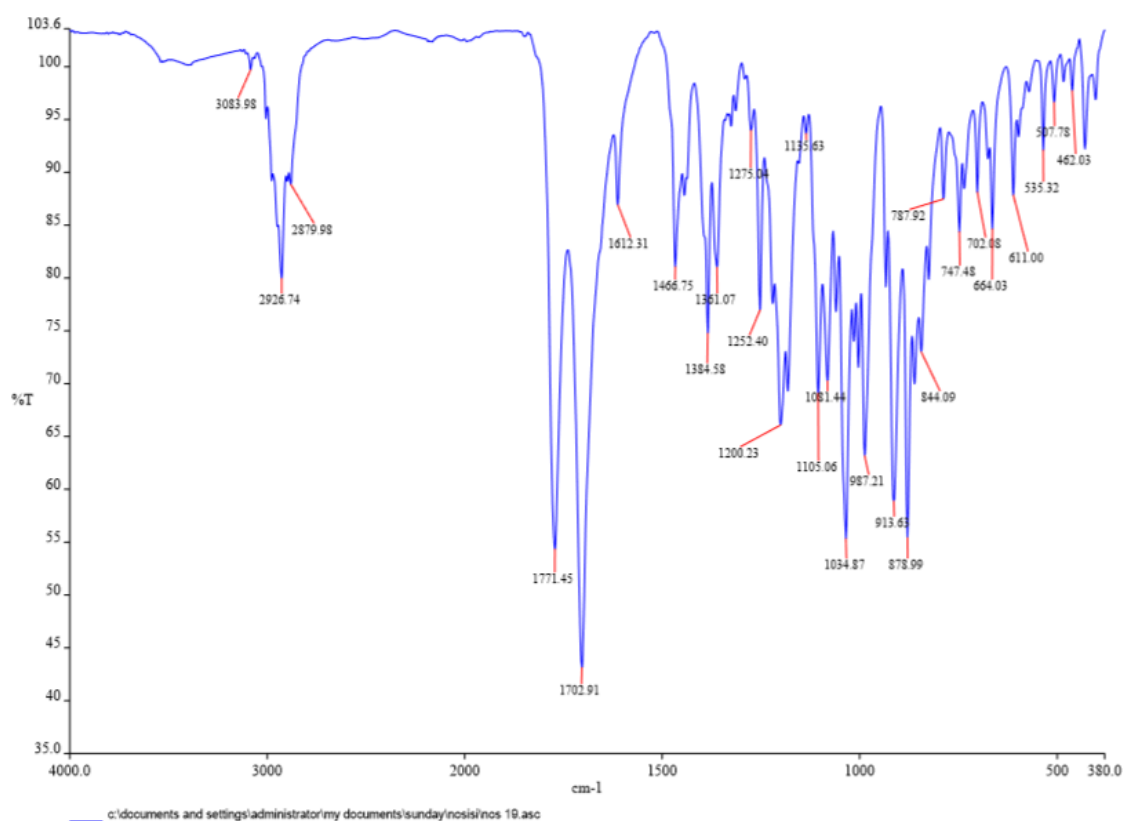


Figure F10: FTIR spectrum of compound 1.

APPENDIX G

Table G1: Crystal data and structure refinement for 18zs_bm_s1_0ma.

Table G1: Crystal data and structure refinement for 18zs_bm_s1_0ma.	
Identification code	18zs_bm_s1_0ma
Empirical formula	C ₁₆ H ₁₈ O ₄
Formula weight	274.30
Temperature/K	100
Crystal system	monoclinic
Space group	C2
a/Å	18.120(3)
b/Å	7.6922(13)
c/Å	12.393(4)
α/°	90
β/°	129.372(6)
γ/°	90
Volume/Å³	1335.3(5)

Z	4
$\rho_{\text{calc}}/\text{cm}^3$	1.364
μ/mm^{-1}	0.097
F(000)	584.0
Crystal size/mm^3	$0.29 \times 0.18 \times 0.11$
Radiation	MoK α ($\lambda = 0.71073$)
2θ range for data collection/$^\circ$	4.252 to 56.676
Index ranges	$-24 \leq h \leq 24, -10 \leq k \leq 10, -16 \leq l \leq 16$
Reflections collected	16326
Independent reflections	3281 [$R_{\text{int}} = 0.0458, R_{\text{sigma}} = 0.0296$]
Data/restraints/parameters	3281/1/183
Goodness-of-fit on F^2	1.061
Final R indexes [$I \geq 2\sigma(I)$]	$R_1 = 0.0387, wR_2 = 0.1015$
Final R indexes [all data]	$R_1 = 0.0407, wR_2 = 0.1032$
Largest diff. peak/hole / $e \text{ \AA}^{-3}$	0.40/-0.23
Flack parameter	0.2(3)

Table G2: Fractional Atomic Coordinates ($\times 10^4$) and Equivalent Isotropic Displacement Parameters.

Fractional Atomic Coordinates ($\times 10^4$) and Equivalent Isotropic Displacement Parameters ($\text{\AA}^2 \times 10^3$) for 18zs_bm_s1_0ma. U_{eq} is defined as 1/3 of the trace of the orthogonalised U_{IJ} tensor.				
Atom	x	y	z	$U(\text{eq})$
O4	6223.6(11)	-2781(2)	6527.3(17)	27.5(4)
O3	7745.1(10)	-2460.1(18)	8450.4(15)	21.4(3)
O2	10496.6(10)	2835.2(19)	12525.0(15)	21.4(3)
O1	10445.4(11)	5510(2)	11854.1(16)	26.3(3)
C11	6970.5(14)	-2024(3)	7120(2)	20.0(4)
C9	7233.6(13)	-609(3)	6558(2)	18.6(4)
C10	8087.3(13)	215(2)	7927.9(19)	15.8(4)
C5	7797.6(13)	1635(3)	8484.6(19)	17.1(4)
C4	8730.7(13)	2177(3)	9861(2)	17.3(4)
C3	9070.0(14)	3800(2)	10260(2)	19.0(4)
C2	10033.9(14)	4140(3)	11588(2)	20.1(4)
C12	8553.2(14)	-1345(2)	8899(2)	18.5(4)
C8	6433.4(14)	659(3)	5494(2)	22.2(4)
C7	6323.6(14)	2332(3)	6060(2)	24.1(4)
C6	7271.0(14)	3051(3)	7367(2)	22.1(4)
C15	7155.5(14)	993(3)	8826(2)	20.9(4)
C14	9293.6(13)	745(2)	10840.0(19)	17.5(4)
C13	9174.9(13)	-904(3)	10421(2)	18.3(4)
C1	9957.9(14)	1298(3)	12341(2)	20.5(4)
C16	7562.4(15)	-1609(3)	5847(2)	24.7(4)

Table G3: Anisotropic Displacement Parameters ($\text{\AA}^2 \times 10^3$) for 18zs_bm_s1_0ma. The Anisotropic displacement factor exponent takes the form: $-2\pi^2[h^2a^{*2}U_{11}+2hka^*b^*U_{12}+\dots]$.

Anisotropic Displacement Parameters ($\text{\AA}^2 \times 10^3$) for 18zs_bm_s1_0ma. The Anisotropic displacement factor exponent takes the form: $-2\pi^2[h^2a^{*2}U_{11}+2hka^*b^*U_{12}+\dots]$.						
Atom	U ₁₁	U ₂₂	U ₃₃	U ₂₃	U ₁₃	U ₁₂
O4	22.4(7)	29.3(8)	33.1(8)	-2.6(6)	18.8(7)	-7.2(6)
O3	20.6(7)	20.2(7)	25.9(7)	0.5(6)	15.9(6)	-2.2(5)
O2	18.0(7)	21.7(7)	22.6(6)	-1.4(5)	12.0(6)	-1.6(5)
O1	23.5(7)	22.6(7)	30.5(7)	-2.6(6)	16.1(6)	-3.7(6)
C11	21.2(9)	18.8(8)	26.5(9)	-2.0(7)	18.1(8)	-1.0(7)
C9	16.7(9)	22.7(10)	20.9(9)	-1.4(7)	14.1(8)	-1.6(7)
C10	14.5(8)	18.6(8)	19.5(8)	-0.3(7)	13.2(7)	-0.6(7)
C5	15.0(8)	17.9(8)	21.4(9)	1.2(7)	12.9(8)	0.9(7)
C4	16.4(8)	20.8(9)	21.1(8)	0.3(7)	15.0(7)	1.4(7)
C3	18.0(9)	19.1(9)	23.6(9)	0.4(7)	14.9(8)	1.7(7)
C2	20.6(9)	21.7(9)	24.3(10)	-2.5(8)	17.2(8)	0.0(8)
C12	17.1(8)	18.5(8)	24.2(9)	0.0(7)	15.1(8)	-0.1(7)
C8	19.5(9)	26(1)	21.5(9)	2.7(8)	13.2(8)	1.6(8)
C7	18.0(9)	24.5(9)	24.6(9)	2.8(8)	11.1(8)	2.3(8)
C6	20.4(9)	19.4(9)	25.0(9)	3.3(8)	13.6(8)	2.5(7)
C15	17.2(9)	26(1)	25.2(9)	-1.1(8)	16.0(8)	-0.3(7)
C14	14.8(8)	21.6(9)	21.0(8)	1.3(7)	13.7(7)	0.3(7)
C13	16.3(8)	20.3(9)	22.6(9)	3.4(7)	14.4(8)	1.8(7)
C1	19.6(9)	22.9(9)	21.3(8)	0.5(8)	14.1(8)	-1.1(7)
C16	22.5(10)	32.5(11)	25.1(9)	-5.8(8)	18.0(8)	-1.0(8)

Table G4: Bond Lengths for 18zs_bm_s1_0ma.

Bond Lengths for 18zs_bm_s1_0ma.					
Atom	Atom	Length/ \AA	Atom	Atom	Length/ \AA
O4	C11	1.204(3)	C5	C4	1.511(3)
O3	C11	1.366(2)	C5	C6	1.529(3)
O3	C12	1.469(2)	C5	C15	1.550(3)
O2	C2	1.350(2)	C4	C3	1.340(3)
O2	C1	1.456(2)	C4	C14	1.468(3)
O1	C2	1.210(3)	C3	C2	1.477(3)
C11	C9	1.523(3)	C12	C13	1.499(3)
C9	C10	1.531(3)	C8	C7	1.538(3)
C9	C8	1.539(3)	C7	C6	1.533(3)
C9	C16	1.546(3)	C14	C13	1.336(3)
C10	C5	1.550(3)	C14	C1	1.500(3)
C10	C12	1.520(3)			

Table G5: Bond Angles for 18zs_bm_s1_0ma.

Bond Angles for 18zs_bm_s1_0ma.							
Atom	Atom	Atom	Angle/°	Atom	Atom	Atom	Angle/°
C11	O3	C12	109.14(15)	C15	C5	C10	114.98(16)
C2	O2	C1	118.69(15)	C3	C4	C5	126.65(18)
O4	C11	O3	120.98(19)	C3	C4	C14	118.57(17)
O4	C11	C9	128.6(2)	C14	C4	C5	114.77(17)
O3	C11	C9	110.33(16)	C4	C3	C2	121.19(18)
C11	C9	C10	100.26(15)	O2	C2	C3	118.48(18)
C11	C9	C8	116.55(16)	O1	C2	O2	118.31(17)
C11	C9	C16	104.52(17)	O1	C2	C3	123.13(19)
C10	C9	C8	115.32(16)	O3	C12	C10	103.99(15)
C10	C9	C16	110.76(15)	O3	C12	C13	112.41(16)
C8	C9	C16	108.75(16)	C13	C12	C10	114.46(16)
C9	C10	C5	113.32(15)	C7	C8	C9	117.64(16)
C12	C10	C9	102.35(15)	C6	C7	C8	113.69(17)
C12	C10	C5	112.25(15)	C5	C6	C7	109.69(16)
C4	C5	C10	104.15(14)	C4	C14	C1	113.75(17)
C4	C5	C6	115.72(17)	C13	C14	C4	122.34(18)
C4	C5	C15	106.03(15)	C13	C14	C1	123.80(18)
C6	C5	C10	106.96(15)	C14	C13	C12	120.76(18)
C6	C5	C15	109.20(16)	O2	C1	C14	110.82(16)

Table G6: Torsion Angles for 18zs_bm_s1_0ma.

Torsion Angles for 18zs_bm_s1_0ma.									
A	B	C	D	Angle/°	A	B	C	D	Angle/°
O4	C11	C9	C10	159.3(2)	C4	C3	C2	O2	-12.9(3)
O4	C11	C9	C8	34.1(3)	C4	C3	C2	O1	163.9(2)
O4	C11	C9	C16	-85.9(3)	C4	C14	C13	C12	8.7(3)
O3	C11	C9	C10	-24.4(2)	C4	C14	C1	O2	-47.5(2)
O3	C11	C9	C8	-149.55(17)	C3	C4	C14	C13	-159.64(19)
O3	C11	C9	C16	90.41(18)	C3	C4	C14	C1	24.1(2)
O3	C12	C13	C14	-118.8(2)	C2	O2	C1	C14	43.1(2)
C11	O3	C12	C10	20.64(19)	C12	O3	C11	O4	179.32(18)
C11	O3	C12	C13	145.00(17)	C12	O3	C11	C9	2.7(2)
C11	C9	C10	C5	-86.00(18)	C12	C10	C5	C4	61.39(19)
C11	C9	C10	C12	35.10(17)	C12	C10	C5	C6	-175.61(15)
C11	C9	C8	C7	91.0(2)	C12	C10	C5	C15	-54.2(2)
C9	C10	C5	C4	176.73(15)	C8	C9	C10	C5	40.0(2)
C9	C10	C5	C6	-60.3(2)	C8	C9	C10	C12	161.13(16)
C9	C10	C5	C15	61.2(2)	C8	C7	C6	C5	-54.1(2)
C9	C10	C12	O3	-35.00(17)	C6	C5	C4	C3	10.0(3)
C9	C10	C12	C13	-158.03(16)	C6	C5	C4	C14	-171.15(16)
C9	C8	C7	C6	33.3(2)	C15	C5	C4	C3	-111.2(2)

C10	C9	C8	C7	-26.2(2)	C15	C5	C4	C14	67.6(2)
C10	C5	C4	C3	127.1(2)	C15	C5	C6	C7	-58.2(2)
C10	C5	C4	C14	-54.1(2)	C14	C4	C3	C2	6.6(3)
C10	C5	C6	C7	66.8(2)	C13	C14	C1	O2	136.24(19)
C10	C12	C13	C14	-0.4(3)	C1	O2	C2	O1	169.16(18)
C5	C10	C12	O3	86.82(17)	C1	O2	C2	C3	-13.9(2)
C5	C10	C12	C13	-36.2(2)	C1	C14	C13	C12	-175.40(17)
C5	C4	C3	C2	-174.61(17)	C16	C9	C10	C5	164.06(16)
C5	C4	C14	C13	21.4(3)	C16	C9	C10	C12	-74.84(19)
C5	C4	C14	C1	-154.89(16)	C16	C9	C8	C7	-151.27(18)
C4	C5	C6	C7	-177.67(17)					

Table G7: Hydrogen Atom Coordinates ($\text{\AA}\times 10^4$) and Isotropic Displacement Parameters ($\text{\AA}^2\times 10^3$) for 18zs_bm_s1_0ma.

Hydrogen Atom Coordinates ($\text{\AA}\times 10^4$) and Isotropic Displacement Parameters ($\text{\AA}^2\times 10^3$) for 18zs_bm_s1_0ma.				
Atom	<i>x</i>	<i>y</i>	<i>z</i>	U(eq)
H10	8534.62	721.69	7798.21	19
H3	8683.59	4749.02	9677.96	23
H12	8948.36	-1970.02	8716.33	22
H8A	6537.25	998.96	4828.79	27
H8B	5820.34	21.03	4956.59	27
H7A	6014.79	3230.62	5320.78	29
H7B	5895.88	2093.87	6282.03	29
H6A	7670.96	3450.62	7127.97	27
H6B	7147.19	4058.29	7729.51	27
H15A	6580.78	445.15	7997.27	31
H15B	6972.35	1983.45	9108.79	31
H15C	7507.41	145.45	9588.83	31
H13	9488.3	-1808.37	11095.01	22
H1A	9585.47	1553.5	12655.52	25
H1B	10405.25	337.9	12921.88	25
H16A	8042.21	-2476.07	6495.48	37
H16B	7840.3	-791.1	5585.95	37
H16C	7013.12	-2193.22	5008.32	37
Experimental				

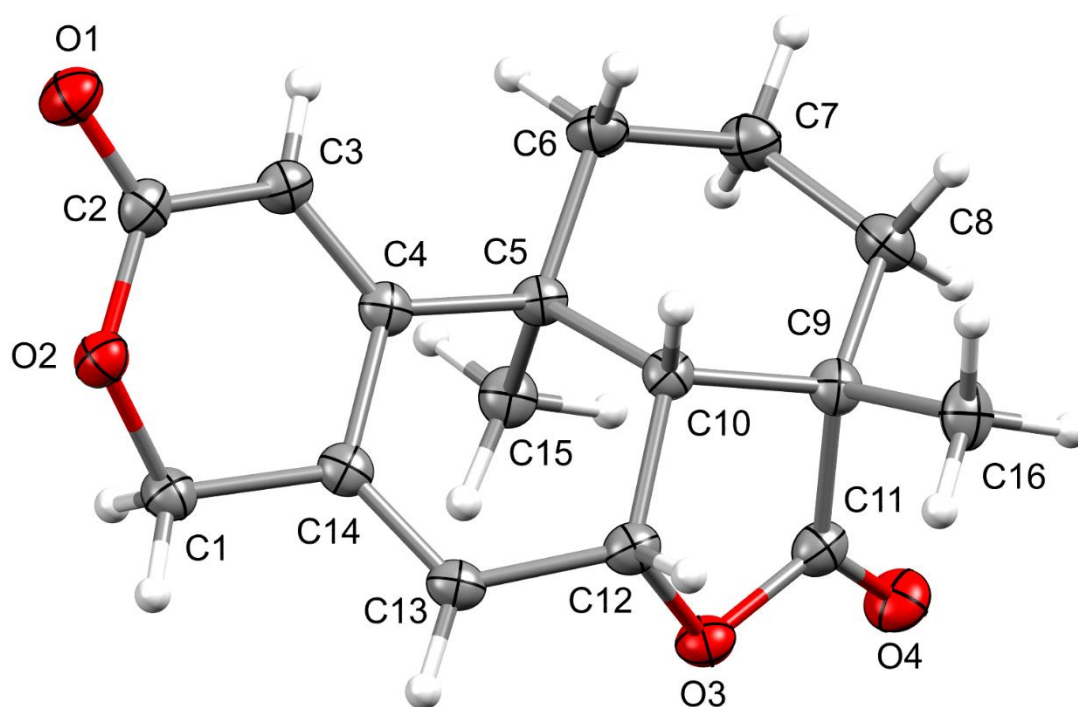


Figure G1: Single-crystal X-ray structure and numbering scheme of compound 1.

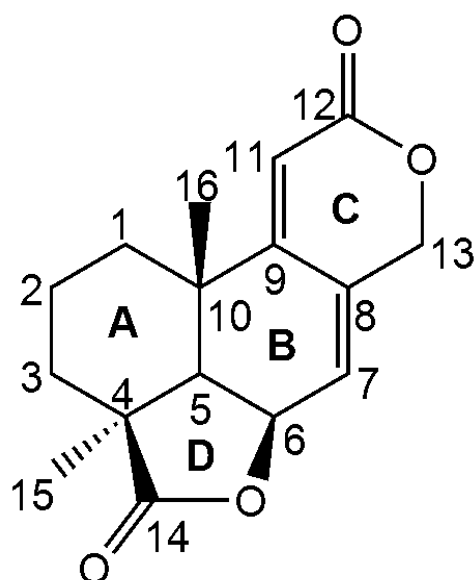


Figure G2: Structure of CJ-14445.